WATER SOLUBLE DISTYRYL-BORADIAZAINDACENES AS EFFICIENT PHOTOSENSITIZERS FOR PHOTODYNAMIC THERAPY

A THESIS SUBMITTED TO
THE GRADUATE SCHOOL OF NATURAL AND APPLIED SCIENCES
OF
MIDDLE EAST TECHNICAL UNIVERSITY

BY

SERDAR ATILGAN

IN PARTIAL FULFILLMENT OF THE REQUIREMENTS
FOR
THE DEGREE OF MASTER OF SCIENCE
IN
CHEMISTRY

SEPTEMBER 2006

Approval of the Graduate School of Natural and Applied Sciences

Prof. Dr. Canan Özgen
Director

I certify that this thesis satisfies all requirements as a thesis for the degree of Master of Science.

Prof. Dr. Hüseyin İşçi
Chairman of the Department

This is to certify that we have read this thesis and in our opinion, it is fully adequate, in scope and quality, as a thesis for the degree of Master of Science.

Prof. Dr. Engin U. Akkaya
Supervisor

Examining Committee Members

Prof. Dr. İdris M. Akhmedov (METU, CHEM) _____

Prof. Dr. Engin U. Akkaya (METU, CHEM) _____

Prof. Dr. Ahmet Önal (METU, CHEM) _____

Prof. Dr. Dönüş Tuncel (BILKENT, CHEM) _____

Asst. Prof. Dr.Neslihan Şaki (Kocaeli Univ., BIOCHEM) _____

I hereby declare that all information in this document has been obtained and presented in accordance with academic rules and ethical conduct. I also declare that, as required by these rules and conduct, I have fully cited and referenced all material and results that are not original to this work.

Name, Last name : SERDAR ATILGAN

Signature :

ABSTRACT

WATER SOLUBLE DISTYRYL-BORADIAZAINDACENES AS EFFICIENT

PHOTOSENSITIZERS FOR PHOTODYNAMIC THERAPY

ATILGAN, SERDAR

M. S. , Department of Chemistry

Supervisor: Prof.Dr. Engin U. AKKAYA

September 2006, 90 pages

Photodynamic therapy (PDT) is an emerging treatment modality for a range of disease classes, both cancerous and noncancerous. This has brought about an active pursiut of new PDT agents that can be optimized for the unique set of photophysical characteristics that are required for a succesful clinical agent. There are many reported or commercially available photosensitizers, but most have limitations, such as low photostability, or a limited usable range of solvent conditions.

In this study, we introduced a novel class of extended conjugation water soluble boradiazaindacene dyes which are efficient singlet oxygen generators. These sensitizers have strong absorptions in the therapeutic window and have spectacular photoinduced cytotoxicity. In addition, they display no dark toxicity at the active concentrations. With these remarkable properties, they are likely to find applications as promising new reagents for photodynamic therapy.

Keywords: Photodynamic Therapy, boradiazaindacence dyes, photosensitizer, singlet oxygen.

ÖZ

FOTODİNAMİK TERAPİ İÇİN ETKİLİ FOTOSENSİTİZER OLAN SUDA ÇÖZÜNÜR Dİ-STYRL-BORADİAZAİNDACENE

ATILGAN, SERDAR
M. S. , Kimya Bölümü
Tez Yöneticisi: Engin U. AKKAYA

Eylül, 2006, 90 sayfa

Fotodinamik terapi, kanserli ve kanserli olmayan bir sınıf hastalık alanı için ortaya çıkan model bir tedavidir. Bu bir klinik agent için gereken bir unit set fotofiziksel karakterleri ile en iyi şekilde kullanılabilecek yeni fotodinamik terapi agentların aktive takibine sebep olmuştur. Yayınlanmış ve ticari olarak bulunan birçok fotosensitizer var, fakat çoğunun düşük fotodayanıklığı ya da sınırlı kullanılabilir çözücü alanları gibi sınırlamaları var.

Bu çalışmada, biz, verimli bir singlet oksijen üreticisi olan yeni bir sınıf genişletilmiş birleşimli suda çözünür bir boya sunduk. Bu sensitizerler tedavi verici pencerede yüksek absorbansı ve görülmeye değer ikna edici sitototoksitiseye sahiptir. Bununla birlikte, aktif konsantrasyonda hiçbir karanlık toksite göstermemektedir. Bu dikkate değer özellikleri ile, bunlar fotodinamik terapi için ümit verilen yeni reagentlar gibi uygulamasını bulabileceklerdir.

Anahtar kelimeler: Fotodinamik terapi, boradiazaindacence boyalar, fotosensitizer, singlet oksijen

To my family and grandmother

ACKNOWLEDGEMENTS

I would like to express my sincere appreciation to my supervisor Prof. Dr. Engin U. Akkaya for his guidance, continuous support, patience and directing me to this productive study during the course of this research, as well as his endless faith in me which was a strong motivation for me in this project.

1 would like to thank Prof. Dr. Dicle Güç, Dr. Lale Dogan, and Dr. Hande Canpınar for their guidance and support during our collaboration in this study.

I also would like to express my gratitude to the NMR specialist Fatos Doganel Polat.

I wish to thank to our lab members, Erhan, Deniz, Altan, Zeynep, Ali, Burcak, Ceyda, Çağlar, Tuğba and Tamer.

My special thanks go to my family and especially to my sister Nurdan for their continuous support, patience and encouragement, and also to Ebru Kaya for her giving positive energy.

TABLE OF CONTENTS

LIST OF FIGURES

FIGURES

LIST OF ABBREVIATIONS

BODIPY	Boradiazaindacene
PDT	Photo Dynamic Therapy
ARMD	Age-related macular degeneration
PDI	Perylenediimide dyes
TFA	Trifluoro acetic acid
LED	Light-emitting diode

CHAPTER 1

INTRODUCTION

1.1 What is Supramolecular Chemistry?

Supramolecular chemistry has been defined by one of its leading proponenets, Jean-Marie Lehn who won the Nobel prize for his work in the area in 1987, as the 'chemistry of molecular assemblies and of the intermolecular bond'. More colloquially this may be expressed as 'chemistry beyond the molecule'. Other definitions include phrases such as 'the chemistry of the non-covalent bond ' and 'nonmolecular chemistry'.This kind of definiton is highlighted in Fig.1.1, which illustrates the relationship between molecular and supramolecular chemistry in terms of both structures and function [1].

By the appropriate manipulation of noncovalent interactions, supramolecular chemistry became the chemistry of molecular information, involving the storage of information at the molecular level, in the strucural features, and its retrieval, transfer, processing at the supramolecular level, through molecular recognition processes operating via specific interactional algorithms. A further step consisted of the design of systems undergoing self-organization, i.e systems capable of spontaneously generating well-defined supramolecular architectures by self-assembly from their components under the control of the molecular information stored in the covalent framework of the components and read out at the supramolecular level through specific interactions [2].

Supramolecular chemistry is a highly interdisciplinary field of science. A major feature is the range of perspectives offered by the cross-fertilization of supramolecular chemical research due to its location at the intersection of chemistry, biology, and physics. Drawing on the physics of organized condensed matter and

extending to the complex entities and processes of biology, supramolecular chemistry expands into a supramolecular science. It has penetrated such diverse areas

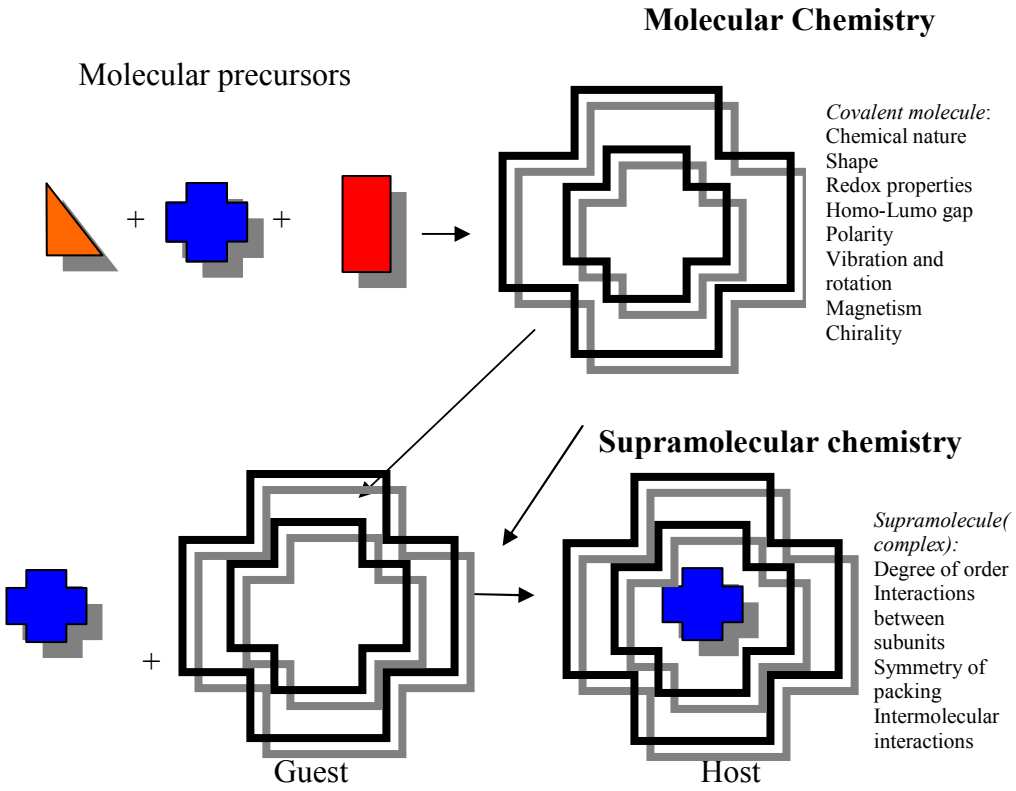

Figure 1. Comparison between the scope of molecular and supramolecular chemistry according to Lehn [1]

as for instance polymer chemistry and material science, solid-state chemistry and crystal engineering, species for nonlinear optics, biological interactions and drug design, sensor and diagnostic procedures, nanoscience and nanotechnology, etc [2].

1.2 Photodynamic therapy

Photodynamic therapy (PDT) is a noninvasive technique for the treatment of a variety of cancer tumor types by the combined use of visible or near-visible light with a photosensitizing drug [3].

Over the past 30 years, clinical protocols for numerous cancers have been developed including cancers of the lung, gastrointestinal tract, the head and neck region, bladder, prostate, and nonmelanoma skin cancers and actinic keratosis. Photodynamic therapy produces a complete response in a very high percentage of patients, and the frequency of follow-up treatments for recurrences is no greater than found with other treatment modalities. Ex vivo procedures have also been examined for treating leukemia patients' bone marrow and hematopoietic stem cell grafts [4].

PDT is employed as a treatment for noncancerous conditions such as psoriasis and age-related macular degeneration (ARMD). Until recently, laser photocoagulation was the only viable treatment to reduce the risk of vision loss from ARMD but was suitable for only about 15% of patients. PDT has been found to be a well tolerated treatment that stabilizes or slows visual activity loss in adult patients and is a suitable treatment for 30-40% of all cases. Successful treatment of atherosclerosis or arterial plaque with PDT has been reported. The combination of the photosensitizer and a blood vessel catheter to deliver the light gives photoangioplasty that appears to be safe and well tolerated with minimal damage to the blood vessel walls in treated regions. PDT has also been shown to have some efficiency against local viral diseases such as herpes. PDT has also been used to purge blood and blood products of viral and bacterial pathogens [4].

1.3 Photosensitizer

A photosensitizer is a molecule that is activated to an excited singlet state when it absorbs a photon of an appropriate wavelength; it can react with biological targets. In photodynamic therapy, either a photosensitizer or the metabolic precursor of one is administered to the patient [5].

In designing improved photosensitizers, a number of factors need to be considered in addition to their ease of synthesis. A photosensitizer should have:

- little or no toxicity in the dark

- good pharmacokinetic behaviour, i.e. high selectivity for tumor tissue and easy elimination from the body (amphiphilic character seems to be advantageous);

- a constant composition (preferably a single achiral substance)

- a high triplet quantum yield and a triplet energy >94 kJ mol^{-1} with efficient energy transfer to produce singlet oxygen;

- red absorption to take advantage to deep light penetration

The first generation photosensitizers, however, possess three-major drawbacks: their selectivity is low and, consequently, skin photosensitivity is a major side effect; absorption in the red region is weak, and so deep tumours are diffucult to treat; and the photosensitizers are complex mixtures of active components [6].

The investigation of non-porphyrin photosensitizers predate the development of second-generation photosensitizers, none have been approved for use in vivo [7].

1.3.1 Porphyrin –Related Photosensitizers

1.3.1.1 Haematoporphyrin and related photosensitizers (HpD, Photofrin)

Haematoporphyrin and related compounds which include Photofrin, has been extensively studied in kinetic terms [6].

Photofrin was the first and at the present time remains the most common, clinically used PDT agent. Although it has been approved for use in the United States, Canada, Japan, and Europe or the treatment of esophageal, endobroncheal, bladder, lung, stomach, cervical, and skin cancers, [8] it is widely recognized that it is far from being an ideal drug for use in PDT. It is an undefined mixture of dimerism and oligomeric compounds derived from the acidic treatment of hematoporphyrin **1** followed by semi purification [9].

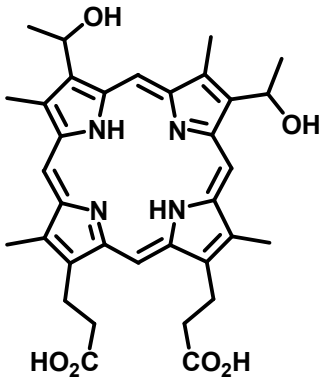

1

Figure 2. Structure of hematoporphyrin, **1**.

Photofrin and other porphyrin-related sensitizers have weak absorbance in the red region of the spectrum (>600 nm where penetration of light in tissue is optimal) and induce long-lasting skin photosensitivity (4-6 weeks) through retention in cutaneous tissue [9]. Absorption maximum of Photofrin is at 630 nm with a weak molar extinction coefficient, ε , of 1170 M^{-1} cm^{-1}. The tetraarylporphyrins were the first easily prepared, easily purified porphyrins to be evaluated as photosensitizers. Tetraphenylporphyrin, **2**, (TPP) has an absorption maximum of 630 nm and is an efficient generator of $^1O_2$ but has limited solubility. Sulfonation of TPP gives the tetrasulfonate $TPPS_4$, **3**, which remains an excellent producer of $^1O_2$, [10] has excellent water solubility, and was once viewed as a promising photosensitizer for PDT [11]. $TPPS_4$ is membranepermeable, displays lysosomal accumulation in cells, accumulates in tumors, and is effective both in vitro and in vivo. However, clinical ambitions for $TPPS_4$, **3,** ended after reported neurotoxicity in mice exposed to high doses of $TPPS_4$ [12].

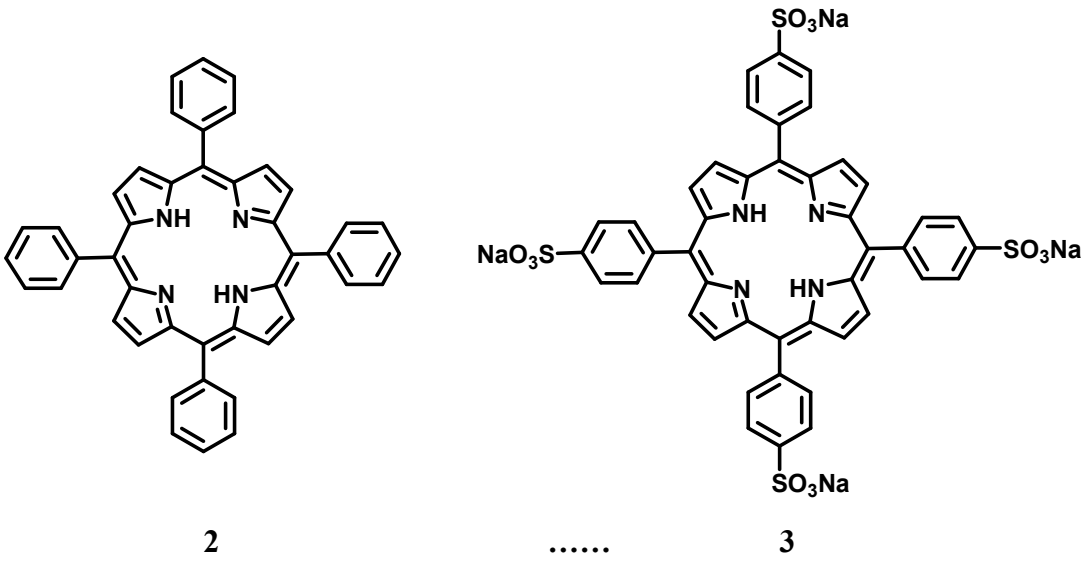

2 …… **3**

Figure 3. Structure of Tetraphenylporphyrin, **2**, (TPP), tetrasulfonate $TPPS_4$**, 3**.

1.3.1.2 Core-Modified Porphyrins

Substituent changes in the meso positions of the porphyrins have little impact on the wavelengths of absorption of the porphyrin chromophore. While this allows tailoring of biological properties without a major change in absorption maximum, it limits the absorption maxima of porphyrin molecules to the shorter wavelength region of the biological window for PDT. Longer-wavelength-absorbing porphyrins (absorption maxima of 665 nm) have been prepared by substituting a chalcogen atom (S, **4**, or Se, **5**) for an NH at the 21-position of the porphyrin ring [13]. Such molecules are called core-modified porphyrins, and sulfonated analogues of the 21-thia- and 21-selenaporphyrins have been evaluated as photosensitizers for PDT [14] [15].

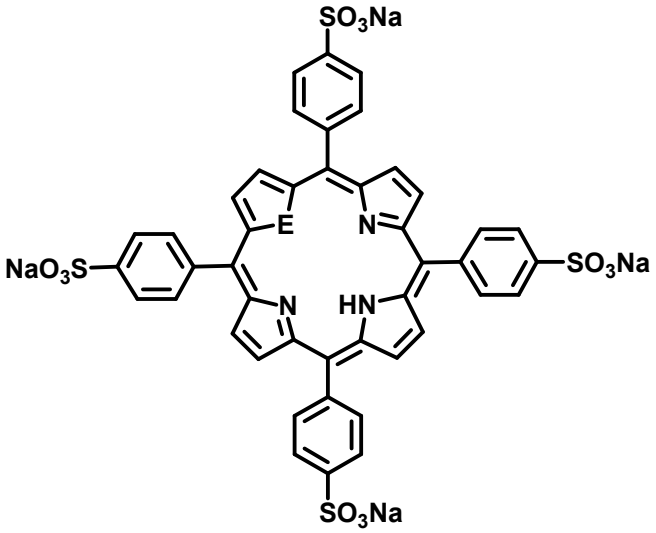

Figure 4. Structure of core-modified Porphyrin, **4, 5.**

1.3.2. Phthalocyanines and Related Compounds

Phthalocyanines**,** **6**, absorb very strongly in the red region of the spectrum with absorption maxima in the 670-780 nm window and values of*, ε,* greater than 100 000 M^{-1} cm^{-1}. These molecules are easily prepared, and water-soluble derivatives are prepared by sulfonation of the phthalocyanine core [16]. The zinc, **6**, aluminum, **7-9**, and silicon, **10**, phthalocyanines are efficient generators of singlet oxygen with long-lived triplet states and have been found to be useful photosensitizers for PDT [17-20]. The silicon phthalocyanine Pc 4, **10**, (λ_{max} = 670 nm) is in various stages of clinical evaluation for cutaneous and subcutaneous lesions from diverse solid tumor origins. The phthalocyanines, porphyrins, and core-modified porphyrins share a common SAR. Uptake and efficacy are directly related to the number of hydrophilic groups. In the aluminum phthalocyanine series, AlPcS2, **7**, with two sulfonate groups shows greater uptake and phototoxicity than AlPcS3, **8**, with three sulfonate groups, which in turn shows greater uptake and efficiency than AlPcS4, **9**, with four sulfonate groups [20].

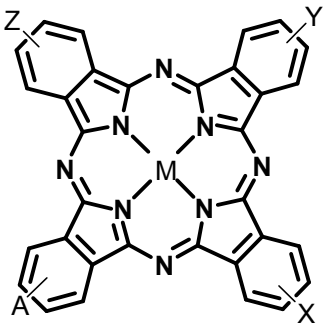

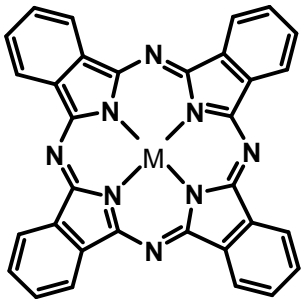

6, ZnPc, M= Zn
7, $AlPcS_2$,M= Al, A=X=SO_3^-
8, $AlPcS_2$,M= Al, A=X=Y=SO_3^-
9, $AlPcS_2$,M= Al, A=X=Y=Z=SO_3^-

10,Pc 4
M=$Si(OH)OSi(CH_3)_2CH_2CH_2CH_2NMe_2$

Figure 5. Structure of Phthalocyanines and Phthalocyanines derivatives

1.3.3. Synthetic Chlorins

The synthetic chlorine 5,10,15,20-tetra(3-hydroxyphenyl)-2,3-dihydroporphyrin, **11**, (*m*THPC), is perhaps the most useful photosensitizer of the synthetic chlorins. *m*THPC (Foscan, Biolitec Pharma, Scotland, U.K.), figure 11, has been approved in Europe for use against head and neck cancer, and additional indications have been filed for prostate and pancreatic tumors. *m*THPC has also been used effectively in recurrent breast cancer for chest wall lesions with patients receiving 0.10 mg kg^{-1} and 5 J cm^{-2} of 652 nm light [21]. However, *m*THPC shows long-term skin photosensitization of up to 6 weeks, which is one drawback to its use. *m*THPC has an absorption maximum of 652 nm with , ε, of 30 000 M^{-1} cm^{-1}. *m*THPC has four phenolic hydroxyl groups with p*K*a values higher than that of the carboxylic acid functionality on other chlorin photosensitizers. However, the cellular uptake of *m*THPC and its porphyrin analogues are unaffected by pH in the range 6.5- 8.0 [22].

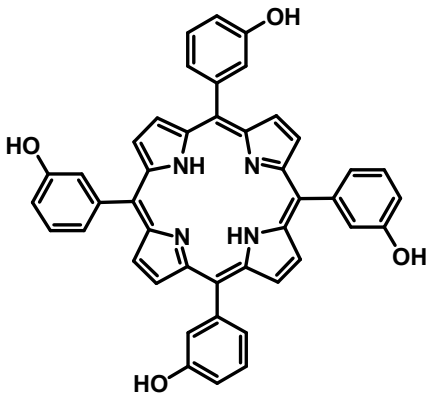

11, *m*THPC

Figure 6. Structure of 5, 10, 15, 20-tetra(3-hydroxyphenyl)-2,3-dihydroporphyrin, **11**, (*m*THPC)

1.3.4 Other photosensitizers

1.3.4.1 Cyanine Dyes

Cyanine dyes were originally developed another part of applied photosensitization that of photographic sensitizers: any critical application may be regarded as a bonus [23].

1.3.4.2 Hypericin

Hypericin is a naturally extended quienone. This substance has PDT activity against mammary carcinoma implants in athymic mice. In a single case (mesothelioma) where it was applied superficially, it was not effective by itself, but appeared to act synergistically with HpD given subcutaneously [23].

1.3.4.3 Squaraines

The squarine dyes derived from squaric acid by condensation with π excessive aromatic compounds. Squaric acid and two molecule of phloroglucinol (1,

3, 5-trihydroxybenzene) give condensation product. Iodination of the product gives the tetraiodosquaraine derivative [23].

1.3.4.4 Texaphyrins

Texaphyrins have an extended coordination with five nitrogen atoms, and it is metal complexes rather than the free base which appear to be making the running. They readily form complexes with metal ions, including those with larger ionic radii can be readily accommodated by porphyries. These complexes have a strong absorption band in the 600- 900 nm regions, the position of which can be varied by suitable cohice of substituent [23].

1.3.4.5 Xanthane

The xanthane dyes, for example, fluorescein, eosin, and rose bengal are excellent photosensitizers for singlet oxygen formation and are perhaps the most commonly used compounds where singlet oxygen is required in organic synthesis. The earliest clinical experiments in this field was carried out by Jesionek and von Tappenier with eosin(in 1903 and 1905) and in 1974 Dougherty started his PDT studies with fluorescein. However, he quickly moves on to HpD because it was much more effective [25].

1.3.4.6 Perylenediimide dyes (PDIs)

PDIs are reddish dyes with very high quantum yields. As such they are not long-wavelength dyes. But, by single or double amine substitution on the perylene core, the absorption maxima at these dyes can be shifted up to 750 nm with further appropriate modifications; solubility can be improved [23].

1.3.4.7 BF_2 chelated Azadipyromethene dyes

These dyes are studied by O'Shea. He has reported the synthesis, photo physical properties and in vitro cellular uptake evaluation of a totally new class of PDT agent [24] of azadipyromethene dyes. A study of the spectroscopic properties of **13** and **14** in chloroform demonstrated that they have a sharp absorption band at 650 nm [24].

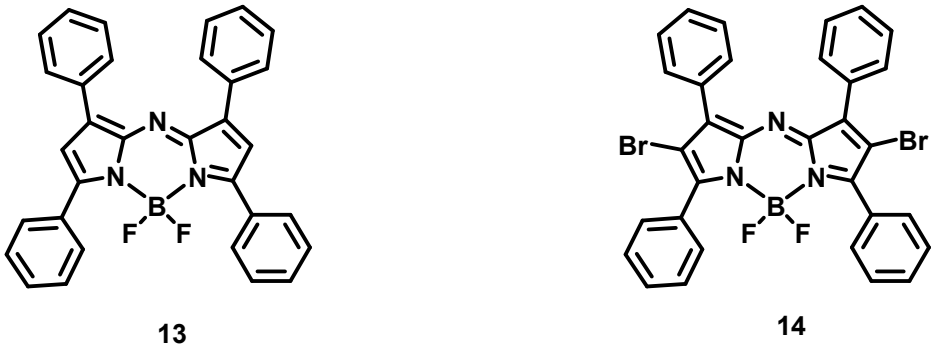

Figure 7. Structure of azadipyromethene dyes

1.3.4.8 Borondipyrromethene (BODIPY) dyes

Nagono et all report a novel photosensitizer, which is highly efficient, photostable, and usable in both lipophilic and aqueous environments. To develop this photosensitizer, they focused on the boron dipyrromethene (BODIPY) fluorophore since BODIPYs generally have high extinction coefficients (ε) and high quantum efficiencies of fluorescence (Φ), which are relatively insensitive to environment [25] (i.e., solvent polarity or pH), and they are also resistant to PDT [26].Thus, they hypothesized that the BODIPY fluorophore can be transformed into a general photosensitizing chromophore without loss of its unique characteristics. A novel photosensitizer, 2I-BDP, **15**, was developed without loss of the unique characteristics of the BODIPY fluorophore by Nagano et all. They have already shown that

BODIPY can be easily modified chemically for the preparation of various derivatives and is available for the development of potentially useful bioimaging fluorescence probes [27].

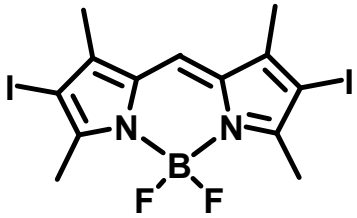

15

Figure 8 Structure of 2I- boron dipyrromethene

1.4 Oxygen in PDT

1.4.1 Singlet Oxygen

Singlet oxygen, the predominant cytotoxic agent produced during PDT [28] is a highly reactive form of oxygen that is produced by inverting the spin of one of the outermost electrons. Normally, ground state oxygen has two unpaired electrons residing separately in the outermost antibonding orbitals. In the absence of a magnetic field the electronic configuration is indistinguishable, however in a magnetic field (fluorescence) the spins of the electrons can be revealed to be in one of three possible configurations, both spins aligned up, both spins aligned down, or one up and down [29]. When the spins are both aligned up the oxygen molecule will deflect down in a magnetic field, when both spins are aligned down they will deflect the molecule upwards in a magnetic field, and when the spins are anti-parallel the molecule will pass unperturbed through the magnetic field. Because of these three possible states the ground state of oxygen is called a triplet state. Any molecule with such a valance electron configuration is considered to be in a triplet state [29, 30].

In figure 8, The extreme reactivity of singlet oxygen arises from the pairing of two electrons into one of the π_{2P}* antibonding orbitals. In the ground state the outermost electrons are distributed, according to Hund's rule, in the P_x and P_y

antibonding orbitals [29]. Since the orbitals are degenerate and the electrons have aligned spins, the quantum numbers of each electron are identical and thus are forced to occupy separate orbitals to comply with the Pauli exclusion principle [31]. During an interaction with the excited photosensitizer the spin of one electron inverts, making its quantum numbers unique, allowing them to pair together into the antibonding orbital which destabilizes the molecule. Although singlet oxygen is often depicted as diradical, it is actually a highly polarized zwitterions (Figure 8) [31].

Singlet oxygen is so reactive that it has a lifetime that ranges from 10-l00μs in organic solvents. In an aqueous environment singlet oxygen's lifetime is reduced to approximately 2μs because the energy of oxygen-hydrogen (O-H) stretching in water molecules nearly equals the excited-state energies of singlet oxygen. The energy is dissipated as heat by the stretching and vibrational motions of water molecules. Because singlet oxygen reacts so rapidly, PDT-induced oxidative damaged is highly localized to regions no larger in diameter than the thickness of a cell membrane. Photodynamic damage is probably confined to targets near to or within hydrophobic regions of the cell due to the hydrophobic character of most photosensitizers [31].

In tissue oxygenation, the importance of tissue oxygenation in PDT was demonstrated by several researchers [32, 33]. Hypoxic cells, those with less than 5% oxygenation, were found to be resistant to PDT. Henderson et al have reported that oxygen consumption depends on the fluence rate of the light [34], and that tissue destruction might be enhanced by using lower fluence rates. Lower fluence rates do not deplete the tissue's oxygen supply as rapidly and as a result the tissue is exposed to singlet oxygen for a longer time during treatment [32, 35].

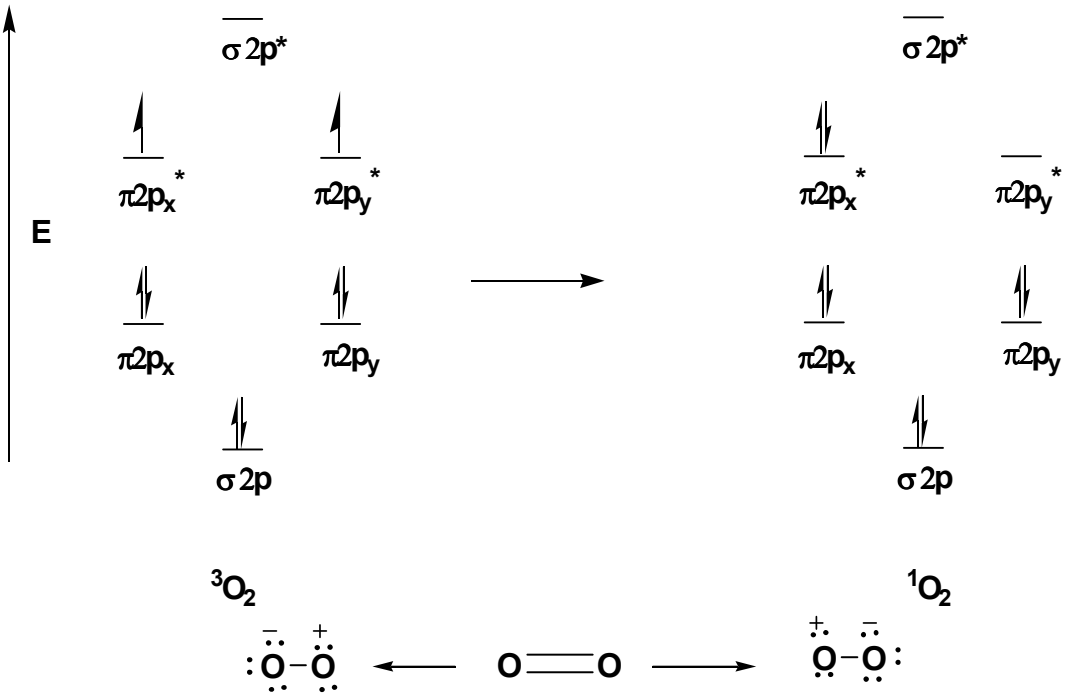

Figure 9. Molecular Orbital Diagrams showing the electron distribution in triplet and singlet oxygen (top). Lewis structure depicting the zwitterionic character of singlet oxygen (bottom).

In general, the efficacy of PDT depends on the yield of $^1O_2$ produced in the tumor, which in turn depends on the concentration of molecular oxygen in the tissue [36, 37, 38]. Therefore, hypoxic cells are generally more resistant to PDT, and attempts to improve tumor oxygenation may be necessary to make this treatment efficient [5]

1.4.2 Heavy Atom effect

An electronic transition from a singlet to a triplet excited state within a molecule is a spin-forbidden process and as such occurs inefficiently for many compounds. In order for a transition between states of different spin multiplicities to

occur effectively, a spin-orbit perturbation is generally required [39]. Enhanced spin-orbit perturbations can be achieved by the attachment of a heavy atom directly onto the molecule [40] (internal heavy-atom effect) or placing the molecule in a surrounding environment containing heavy atoms [41] (external heavy-atom effect).

As singlet oxygen is the key cytotoxic agent in the PDT therapeutic process, it is essential that control can be exerted over this component of the therapy. The quantity of singlet oxygen generated by a photosensitizer is regulated by the efficiency of a spin-forbidden electronic transition from a singlet to a triplet state (ISC). The introduction of a heavy atom into a molecule is known to have an influence over the rates of the ISC and is termed the heavy-atom effect [42].

O'Shea et al. has studied heavy atom effect on their work for singlet oxygen generation. They chose the internal heavy-atom approach, but in attempt to effect varying degrees of spin-orbit coupling, they placed the heavy atoms at two different positions in the molecule. This would allow them to modulate the degree of spin-orbit coupling and hence the efficiency of singlet oxygen production by three modes: (i) no heavy atom within the sensitizer, thereby relying on the inherent spin-orbit coupling of the molecule; (ii) positioning of bromines on the aryl rings (not directly on the sensitizer), which could give rise to an intermediate singlet-oxygen generation level (termed an intramolecular external heavy-atom effect); [43] and (iii) positioning of the bromine directly onto the sensitizer, thereby fully exploiting the internal heavy-atom effect and providing the most efficient singlet-oxygen producers [7] (figure 9).

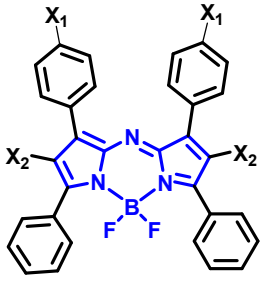

15

(i) X^1,X^2= H:inherent spin-orbit coupling
(ii) X^1= Br, X^2=H: itramolecular external heavy atom effect
(iii) X^1=H, X^2=Br: internal heavy atom effect

Figure 10. Positioning of the bromine heavy atom around the core sensitizer (blue)

However, the heavy atom effect can be small for some aromatic hydrocarbons if:

(i) The fluorescence quantum yield is large so-that de-activation by fluorescence emission dominates all other de-activation processes;

(ii) The fluorescence quantum yield is very low so that the increase in efficiency of intersystem crossing is relatively small;

(iii) There is no triplet state energetically close to the lurescing state [7].

1.5 Photodynamic Action

Photodynamic action, which is the expression of the photodynamic effect, refers to the damage or destruction of living tissue by visible light in the presence of a photosensitizer and oxygen.

In principal, light in the very near infrared region could be employed, but sensitizers absorbing there are rather uncommon, and in most cases irradiation is with visible light. The light source may be incoherent (e.g. a tungsten lamp) or coherent (e.g. a laser): the sensitizer must absorb the light and the excited sensitizer then activates oxygen in some way. Molecular oxygen is essential for the process to occur, and in most examples is derived from the atmosphere.

1.5.1 Light

In order to come to an appreciation of the nature electromagnetic radiation, of which visible light is a small part, it is necessary to be able to think of it as a form of energy which can be expressed both as a wave and as a particle (quantum, photon). The wave approach allows a treatment of light propagation, refraction, diffraction and polarization, whereas the particle approach is suited for an understanding of absorption and emission phenomena.

The place of visible light in the electromagnetic spectrum is shown in Figure 10. Electromagnetic radiation can be interpreted in terms of a transverse plane wave of wavelength associated with electric and magnetic fields, the vectors of

which are in planes perpendicular to one another and to the direction of propagation. The wavelength of visible light falls in the range 400-750 nm: 400 nm we see as indigo, and 750 nm we see as red

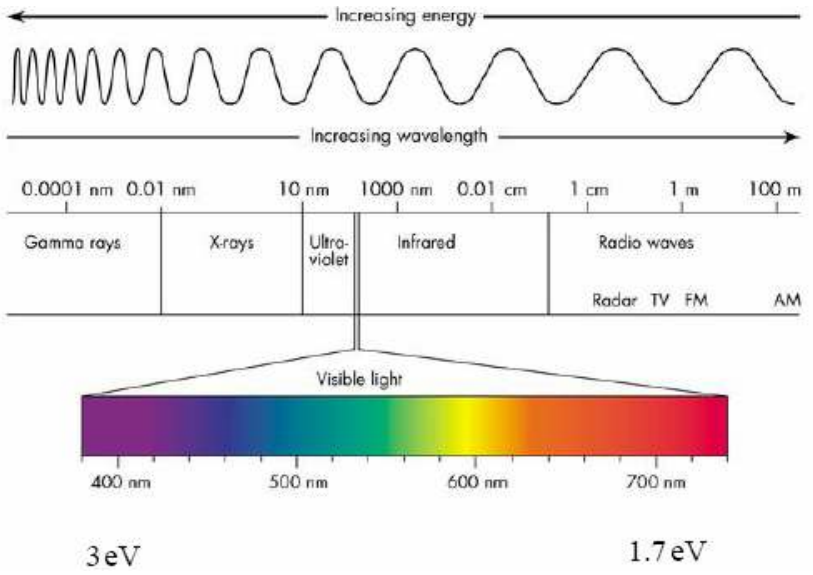

Figure 11. The Electromagnetic Spectrum, showing particularly the Near-UV, Visible, and Near-IR Regions in which occur The Principal Electronic Transitions of Interest in Phototherapy

1.5.2 Light Sources

The light source may be incoherent (e.g. a tungsten lamp) or coherent (e.g. a laser): the sensitizer must absorb the light and the excited sensitizer then activates oxygen in some way. Molecular oxygen is essential for the process to occur. Actually there are five light sources which are,

1.5.2.1. Sunlight

It is evident from everyday observation that solar energy maintains life on Earth, and it is commonly thought to have been a key factor in the generation of that life. Being so important and so widespread, photosynthesis is the most obvious sunlight-dependant process in the biosphere, but is by no means the only one: in the plant world we have phototropism and photoperiodism; in the animal world, vision and seasonal affective disorder. Photobiology is a rich subject, and much of it is related to sunlight.

1.5.2.2. Incandescent lamps

These depend on a filament (e.g. tungsten) which is heated in an evacuated glass envelope by an electric current. Such lamps are inexpensive and have been used in PDT. For example, in the treatment of basal cell carcinoma using δ-aminolaevulinic acid as a pro-drug, Kennedy and Pettier employed a projector lamp as the light source. In the phototherapy of neonatal hyperbilirubinemia fluorescent tubes have commonly been used but Ohmeda have recently developed a woven fiber optic pad which wraps around the infant and which is supplied with light from a l00 w halogen bulb. Infrared and ultraviolet light are filtered out with filters and a dichroic reflector to give illumination in the required 400-550 nm region (bilirubin λ_{max} 450 nm).

1.5.2.3. Arc lamps

The mercury arc lamp is the workhorse of organic photochemistry, and has some applications in photomedicine. There are three main types. The low-pressure mercury arc operates at room temperature and about 10^{-3} mm pressure: the main emission is a single line at 253.7 nm. This is well into the UV-C region, and germicidal lamps are of this type. Medium-pressure mercury lamps operate at about 1 atmosphere: the emission contains a number of lines, of which 366 nm and

546 nm are the principal ones. When such a source is filtered by Wood's glass, the 366 nm line remains, and it is filtered ultraviolet light which is commonly used to observe the red fluorescence of porphyrins and other dyestuffs. The high-pressure mercury arc operates at ~100 atmospheres and is an intense source: the emission is practically a continuum. Such lamps must be cooled and even then have a short life. More convenient to use are point-source arcs using xenon or xenon-mercury: these are also intense sources, operating at about 20 atmospheres, but do not require cooling. Thus the Paterson lamp is a low-cost portable xenon short arc lamp (300 W) which plugs into the mains and which has no special cooling demands. It is provided with rapidly interchangeable wavelength filters, and the output can be effectively coupled with a liquid light guide.

Where it is desired to generate a narrow wavelength band from lamps (such as the xenon lamp just referred to, or the incandescent lamp), this can be done by using, a monochromator or by using commercial filters. Water cuts out much of the infrared: 2 mm of Pyrex glass effectively removes ultraviolet below ~300 nm. In those cases where light has to be delivered to an internal site, the light is earned through a guide such as a fiber optic or a plastic tube full of liquid. (Laser beam is carried most efficiently in this way). The fiber tip is specially shaped to deliver the light as required, for example, to send it in one direction, or to diffuse it generally.

1.5.2.4 Light-emitting diodes (LEDs)

They are III, IV semiconductor based devices driven by an electric current. The emission is not coherent (this is not a laser source), and is low power, so not much heat is produced. Wavelength can be adjusted by changing the semiconductor, and the devices are small, but they can be bunched together to fit a particular structure. They are finding increasing application. Thus, the LED system recently announced by Diomed consists of a close-packed array of LEDs in a water-cooled head which is designed to be kept in contact with the area of treatment. The irradiation wavelength is 635 nm or 652 nm, with a fluence rate of up 200 $mWcm^{-2}$ [23].

1.5.2.5 Lasers

A **laser** (from the acronym ***L**ight **A**mplification by **S**timulated **E**mission of **R**adiation*) is an optical source that emits photons in a coherent beam. The back-formed verb *to **lase*** means "to produce laser light" or possibly "to apply laser light to". Laser light is typically near-monochromatic, i.e. consisting of a single wavelength or color, and emitted in a narrow beam. This is in contrast to common light sources, such as the incandescent light bulb, which emit incoherent photons in almost all directions, usually over a wide spectrum of wavelengths.[44]

1.5.3 Photophysical Processes of an excited molecule

Once a molecule is excited by an absorption of a photon, it can return to the ground state with photon absorption, emission of fluorescence, internal conversion, intersystem crossing, phosphorescence, delayed fluorescence and triplet-triplet transitions. The Perin-Jablonski diagram is convenient for visualizing in a simple way these possible processes [23].

1.5.3.1 Internal conversion

Internal conversion is a non-radiative transition between two electronic states of the same spin multiplicity. In solution, this process is followed by a vibrational relaxation towards the lowest virational level of the final electronic state. The excess vibrational energy can be indeed transferred to the solvent during collisions of the excited molecule with the surrounding solvent molecules.

When a molecule is excited to an energy level higher than the lowest vibrational level of the first electronic state, vibrational relaxation (and internal conversion if the singlet excited state is higher than S_1) leads the excited molecule towards the 0 vibrational level of the S_1 singlet state with a time-scale of 10^{-13}-10^{-11} s [44].

From S_1, internal conversion to S_0 is possible but is less efficient than conversion from S_2 to S_1, because of the much larger energy gap between S_1 and S_0. Therefore, internal conversion from S_1 to S_0 compete with emission of photons

(fluorescence) and intersystem crossing to the triplet state from which emission of photons (phosphorescence) can possibly be observed [44].

1.5.3.2 Fluorescence

Emission of photons accompanying the S_1 to S_0 relaxation is called *fluorescence.* It should be emphasized that, apart from a few exceptions, fluorescence emission occurs from S_1 and therefore its characteristics (except polarization) do not depend on the excitation wavelength.

The fluorescence spectrum is located at higher wavelengths (lower energy) than the absorption spectrum because of the energy loss in the excited state due to the vibrational relaxation [44].

1.5.3.2.1 Quantum yield

The fluorescence quantum yield Φ_f is the fraction of excited molecules that return to the ground state S_0 with emission of fluorescence photons.

In other words, the fluorescence quantum yield is the ratio of the number of emitted photons (over the whole duration of the decay) to the number of absorbed photons [44].

1.5.3.3 Intersystem crossing and subsequent processes

A third possible de-activation process from S_1 is intersystem crossing toward the T_1 triplet state followed by the other processes according to the Figure12.

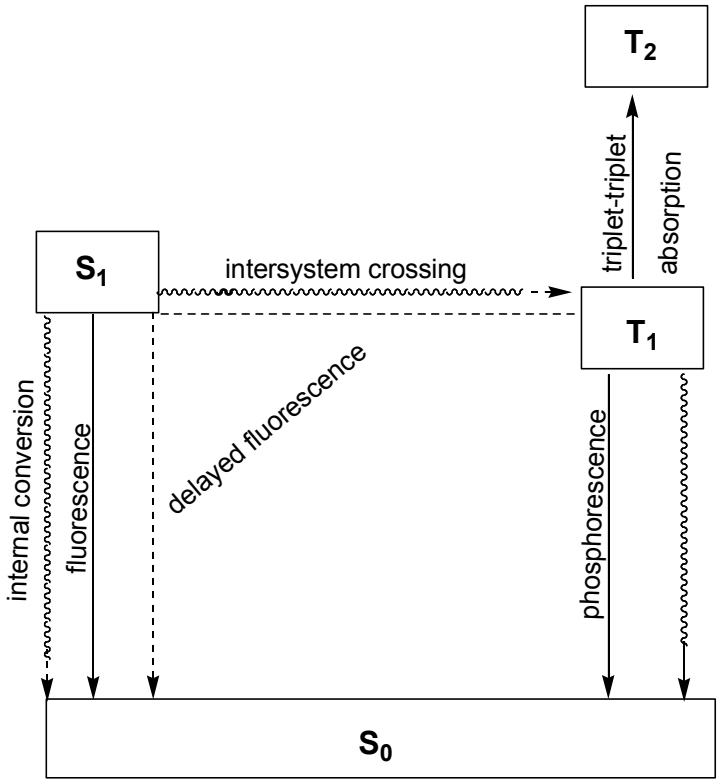

Figure 12. Inter-system crossing and possible processes on triplet state

1.5.3.3.1 Intersystem crossing

Intersystem crossing is a non-radiative transition between two isoenergetic vibrational levels belonging to electronic states of different multiplicities. For example, an excited molecule in the 0 vibrational level of the T_n triplet state; then vibrational relaxation brings it into the lowest vibrational level of T_1. Intersystem crossing may be fast enough (10^{-7}-10^{-9}) to compete with other pathways of de-activation from S_1 (fluorescence and internal conversion S_1 to S_0) [44].

Crossing between states of different multiplicity is in principle forbidden, but spin-orbit coupling (i.e. coupling between the orbital magnetic moment and the spin magnetic moment) can be large enough to make it possible. The probability of intersystem crossing depends on the singlet and triplet states involved. If the transition S_0 to S_1 is of n to π^* type for instance, intersystem crossing is often efficient. It should also be noted that the presence of heavy atoms (i.e. whose atomic

number is large, for example Br, Pb) increases spin-orbit coupling and thus favors intersystem crossing [44].

1.5.3.3.2 Phosphorescence

In solution at room temperature, non-radiative de-activation from the triplet state T_1, is predominant over radiative de-activation called *phosphorescence*. In fact, the transition T_1 to S_0 is forbidden (but it can be observed because of spin-orbit coupling), and the radiative rate constant is thus very low. During such a slow process, the numerous collisions with solvent molecules favor intersystem crossing and vibrational relaxation in S_0 [44].

On the contrary, at low temperatures and/or in a rigid medium, phosphorescence can be observed. The life time of the triplet state, may under these conditions, is long enough to observe phosphorescence on a time-scale up to seconds, even minutes or more [44].

1.5.3.3.3 Delayed fluorescence

Reverse intersystem crossing T_1 to S_0 can occur when the energy differences between S_1 and T_1 is large enough. This results in emission with the same spectral distribution as normal fluorescence but with a much longer decay time constant because the molecules stay in the triplet state before emitting from S_1. This fluorescence emission is thermally activated; consequently, its efficiency increases with increasing temperature. It is also called delayed-fluorescence of E-type because it was observed for the first time with eosin [44].

1.5.3.3.4 Triplet-Triplet transitions

Once a molecule is excited and reaches triplet state T_1, it can absorb another photon at a different wavelength because triplet-triplet transitions are spin allowed. These transitions can be observed provided that the population of molecules in the

triplet state is large enough, which can be achieved by illumination with an intense pulse of light [44].

1.5.4 Mechanism for Photodynamic action

The photo physics associated with photosensitization involve [45] excitation of the photosensitizer ground state by photon energy in the 600- 800 nm range to give the excited singlet state of the photosensitizer and [46] intersystem crossing from the excited-state singlet to the triplet state [3]. The interactions of the photosensitizer excited states with endogenous oxygen in the target cells or the surrounding target tissues provide the cytotoxic effects. Electron transfer from the photosensitizer excited state to ground-state oxygen produces a superoxide radical anion (O_2^-), while a spin-allowed interaction of the triplet-state photosensitizer with ground-state oxygen, which is also a triplet, produces $^1O_2$. Nearly all of the photodynamic action described in this perspective involves the production of either $^1O_2$ or O_2^-. However, phototherapy of severely hypoxic tissues would necessitate different mechanisms of action such as direct photoinduced charge transfer from photosensitizer to biological tissue or photochemical bond formation such as [2 + 2] cycloaddition reactions. Molecular oxygen must be present at sufficient levels throughout irradiation of target tissues or cells to produce $^1O_2$ continuously [45, 3]. Depletion of molecular oxygen in tissue during high-fluence-rate irradiation has been reported to counteract the effectiveness of PDT. Light delivered at high fluence rates generates $^1O_2$ at a rate that depletes molecular oxygen more quickly than it can be resupplied, which limits the cellular and tissue damage derived from $^1O_2$. This complication has gained much attention, and numerous methods have been developed to circumvent this problem. Addition of oxygen enhancers such as fluosol DA prior to irradiation have met with minimal success, while fractionation of the exciting light to allow for resupply of oxygen during dark periods has been shown to increase the effectiveness of PDT under some conditions [47]. Thus, a combination of photosensitizer at optimal concentration, abundant molecular oxygen, and delivery of light at a fluence rate that

allows for resupply of molecular oxygen within the target tissue are necessary for successful application of PDT.

Therefore, the cellular effects of PDA depend on at least 4 factors: the concentration of the dye, the concentration of O_2 and the appropriate wavelength and intensity of the light [5].

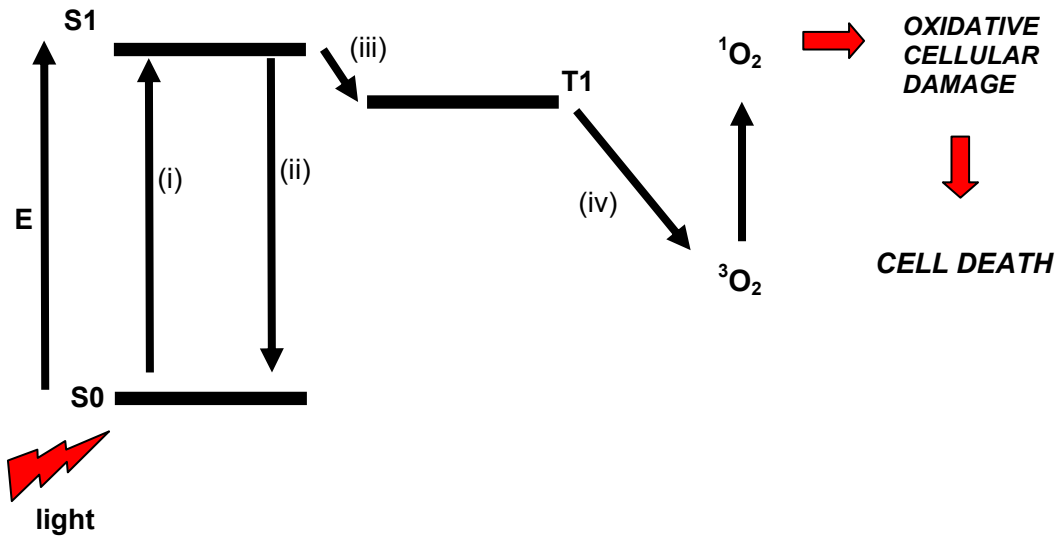

Figure 13. Simplified Jablonski diagram for the PDT process i) absorption, ii) fluorescence, iii) Intersystem crossing, iv) Energy transfer

1.5.5 Advantages and Limitations of PDT

PDT has several advantages. First, it works on virtually all types of cancers, lacking the specificity of chemotherapeutic and radiation. The procedure can be repeated several times, if needed, because there are no cumulative toxic effects, and it is usually an outpatient procedure. Moreover, because of its lower risk profile, it can be used even in the elderly or in people who are too sick for surgery. The main side effect is sensitization to light, and because of this, patients undergoing PDT need to avoid direct sunlight and bright indoor light for at least 6 weeks [5].

Notwithstanding the benefits described above, there are some important limitations to PDT. The photosensitizer is injected into the bloodstream, and depending on the type of dye, absorbed by the dye, absorbed by cells all over the

body. It is known that photosensitizers remain in tumor cells for a long time than normal cells, although the mechanisms of this retention are not well understood. The light exposure is then carefully timed so that it occurs when nearly all of the photosensitizing agent has left normal cells but is still present in cancer cells. Subsequently, when these cells are exposed to light, the photodynamic reactions occur [5].

The mechanisms of PDA were elucidated using cells in culture. However, the tumor response to PDT is more complex and is not completely understood at present. Nevertheless, it is well documented that the effectiveness of PDT depends on events occurring in the malignant cells themselves and in the tumor vasculature. Those events may result in blood flow states, vascular collapse and\ or vascular leakage [38, 48] and cell death occurs by necrosis or apoptosis [49, 50].

When a biological tissue is exposed to light, absorption and scattering processes by the macromolecules that comprise the tissue may occur, which is an important limitation of PDT. In the blood, the most important protein that absorbs light is hemoglobin. This molecule absorbs light particularly between 400 and 600 nm. Thus, the illumination must contain wavelengths greater than 600 nm to ensure significant penetration into the target tissue. On the other hand, photons of wavelengths greater than 850 nm do not have sufficient energy to participate in photochemical reactions. Therefore, therapeutic wavelengths vary from 600 to 800 nm, and only dyes with absorption peaks in this range are clinically relevant [5].

Although common light bulb lamps may be used to produce PDA, the Standard light sources for PDT are lasers, due to their monochromatic nature, high power output and ease of coupling to fiber optics for endoscopic light delivery within a body cavity of for interstitial implants. Thus, due to light depth limitations, photodynamic treatment is more effective for small tumors and for tumors situated in cavities, although bulky tumors may be treated, often requiring repeated light exposure. Finally as PDT is a local treatment, it cannot be applied systemically, which makes it inefficient for treating widespread metastases [5].

1.6 Cancer

The phototherapy of cancer is essentially photodynamic therapy, requiring visible light, a photosensitizer and oxygen [23].

The activated oxygen (principally singlet oxygen) then causes damage to the living system, e.g. photodynamic therapy of cancer is the treatment of disease by the use of visible or near infrared light together with an administered photosensitizer and in the presence of molecular oxygen at ambient levels. Light is absorbed by the photosensitizer, which then serves to activate oxygen (principally singlet oxygen): then causes damage to the living system, e.g. PDT of cancer; photodynamic destruction of microbes. Phototherapy is thus a general term used to describe all cases where light is used therapeutically: Photo chemotherapy is a subset of it, and photodynamic therapy is a division of that, as shown in the following Venn diagram in Figure 14

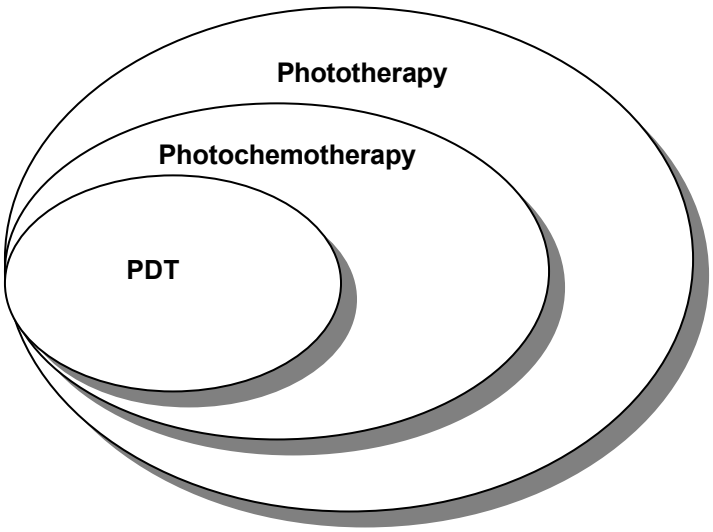

Figure 14. Photopheresis

Phototherapy is the use of ultraviolet, visible, or near infrared light in the treatment of disease. In cases where no photosensitizer is administered the light is absorbed by

photosensitizers present in the tissue, e.g. phototherapy of neonatal hyperbilirubinemia; photogeneration of vitamin D_3 [23].

Photochemoterapy is the use of ultraviolet, visible or near infrared light together with an administered photosensitizer (the photochemotherapeutic agent) in the treatment of disease. Light is absorbed by the photosensitizer, e.g. PUVA therapy of psoriasis and other skin diseases [23].

Photopresis is the refers to extracorporeal photochemotherapy. Thus the blood (or blood components) are removed from the body, treated by photochemotherapy *in vitro,* and then put back again. This procedure has been used to treat cutaneous T cell lymphoma (following oral 8-MOP) with beneficial effect [23].

1.6.1 Mechanism of Tumor Destruction

1.6.1.1 Apoptosis and Necrosis

For every cell, there is a time to live and a time to die. The primary role of PDT is to kill unwanted eukaryotic cells. Macroscopic damage to the tumor in PDT appears to occur by at least three pathways: (i) Direct damage to tumor cells; (ii) Damage to endothelial cells of the vascular system of, and around, the tumor, so shutting off its blood supply; and (iii) Macrophage-mediated infiltration of the tumor. For example, according to studies by Moan and his colleagues [51], meta isomer 5, 10,15,20-tetrakis(hydroxyphenyl)porphyrin (m-THPP) is mainly localized in the stroma of tumors, and destroys the microvasculature; whereas m-THPC, **11**, is distributed in the vascular interstitium and neoplastic cells of tumors, and destroys vascular walls and tumor cells. The death of the tumor cells seems to occur by two distinct processes, the balance between depending both on the cell line and the photosensitizer structure [52]. They are apoptosis and necrosis. Since the term "apoptosis' was introduced in 1972, cell killing mechanisms are generally classified as occurring through apoptosis or necrosis. Apoptosis is a normal physiological process essential for the control of tissue development and involution and for tissue

homeostasis. Apoptosis is a tightly regulated process of cell suicide, controlled by both intracellular and extracellular signals, terminating in a characteristic sequence of morphological and biochemical changes for the systematic dismantling of the cell and preparation of the residual cell components, known as apoptotic bodies, for engulfment by tissue macrophages or other neighboring cells. The loss of ability to regulate apoptosis can lead to disease. For example, many cancer cells have lost the ability to undergo apoptosis in response to normal signals or after damage from therapeutic interventions, whereas unrestrained apoptosis of neurons may contribute to Alzheimer's and other neurodegenerative diseases.

In contrast, necrosis results from high levels of cell damage, in which plasma membrane integrity is lost, cells lyses, and tissue inflammation is triggered. This type of killing occurs rapidly. Although PDT can produce apoptosis or necrosis, or a combination of the two mechanisms, in many cases PDT is highly efficient in inducing apoptosis. This property is of more than theoretical interest, because it implies that lower doses than those needed to produce necrosis are very effective in producing the desired cell killing result [53]

1.6.1.2 Apoptosis in PDT

Argawal et al. Showed that murine L5178Y lymphoma cells progressed to apoptosis in as little as 30 min after PDT treatment *in vitro* [54]. Generally apoptotic responses require several hours to days to complete. Argarwal suggested that PDT-induced cellular damage bypassed the normal apoptotic mechanisms and initiates late-stage processes directly [52]. Zaidi et all observed apoptotis *in vivo* (apoptotic bodies and DNA laddering) in RIF-1 tumors treated with Photofrin-PDT [55]. However Zaidi reported that the apoptotic bodies and digested DNA may have come from host cells infiltrating the tumor rather than the tumor cells. He *et al.* demonstrated that PDT does not induce apoptosis in all cell lines *in vitro* [56]. Despite having similar sensitivities to Photofrin-PDT, an LD_{85} dose of Photofrin-PDT induced apoptosis in rat MTF7 cells while an LD_{85} dose was required to induce apoptosis in PC3 human prostatic adenocarcinoma cells, and apoptosis could not be

induced in H322a non-small cell carcinoma cells. He *et al.* suggested that there are many different pathways through which PDT can induce apoptosis [57].

Kossel *et al.* [57] and Lou *et al.* [58] showed that different photosensitizers induce apoptosis to varying degrees. They treated cultured cells with SnET2 or tin octaethylpurpurin amidine (Scopa, a cationic variant of SnEt2)-PDT. Tin ethyl etiopurpurin induced apoptosis within 60 min of treatment while Scopa required 24 h or longer [57, 58]. Tin octaethylpurpurin amidine localized uniformly throughout the cell and its membranes while SnET2 localized to the lysosomes and mitochondria, thus Lou suggested that Scopa damaged cellular membranes, retarding the cell's ability to regulate apoptosis [58].

Argarwal *et al.* demonstrated that phospholipases C and A_2, which are involved in apoptosis, are activated after Photofrin-PDT [59]. When the actions of phospholipases C and A_2 were locked with inhibitors, the transient increases in intracellular calcium levels and DNA fragmentation commonly observed during apoptosis were eliminated [59]. Kick *et al.* reported that the proto-oncogenes *c-jun* and *c-fos,* which are commonly associated with apoptosis, were activated after treating cultured cells with Photofrin-PDT [60]. *C-jun* and *c-fos* may be turned on to transcribe apoptosis mediating factors. Fisher *et al,* showed that cultured HL-60 cells expressing higher levels of p53 were less sensitive to Photofrin-PDT than cells expressing normal levels of p53 [61]. The tumor suppressor gene p53 is known to arrest damaged cells in the S-phase of the cell cycle and force them into apoptosis if they cannot repair the damage [62].

In the last ten years there has been a shift away from thinking that the nucleus is the only organelle to control apoptosis. Guido Kroemer and other have established that the mitochondria can induce and control nuclear apoptosis. Kossel *et al.* hypothesized that PDT may kill cells by mitochondrially controlled apoptosis.

1.6.1.3. PDT and Apoptosis

There are many similarities between the mechanisms by which mitochondria regulate apoptosis and mechanisms by which PDT kills cells. Kessel *et al*. have proposed that mitochondrially controlled apoptosis, similar to the mechanisms described above, is occurring after PDT treatment [63, 64]. Active photosensitizers may localize to mitochondrial targets such as the membranes surrounding the PT pore or specific proteins in the PT pore. Hilf *et al.* and others have shown other important mitochondrial proteins may be involved as well. During PDT singlet oxygen attacks mitochondrial proteins and possibly alters their amino acid structures, thereby disrupting the protein's folding conformation. This may force them into other conformations that disrupt their normal functioning. Ruck *et al.* recently demonstrated that ANT, reconstituted into liposomes, could act normally as **an** ADP-ATP exchange carrier or it could form non-specific channels with conductance properties similar to the PT-pore [65]. The PT pores allow water molecules to flow into ions and antioxidants flow out as the system settles towards equilibrium. The membrane potential decreases and the electron transport chain uncouple spewing out detrimental ROS. The remaining antioxidants may scavenge some ROS but if PT is not reversed damage will accumulate and the electron transport chain will collapse. Petit *et al.* reported that bcl-2 decreases the likelihood of apoptosis by inhibiting PT-pore formation and He *et al.* have shown that cells overexpressing bcl-2 were more resistant to *in vitro* Photofrin^{B}-PDT than parental cells [66]. Kim *et al.* also demonstrated that bcl-2 mediates PDT-induced cell death, and that aluminum phthalocyanine-PDT selectively destroys bcl-2, enhancing the apoptotic response after PDT [66]. Both results imply that PT-pore formation is a component of PDT-mediated cell death [65, 66]

1.6.1.4 Measuring Apoptosis

Quantification of the precise extent of apoptosis vs. necrosis and total cell death in cultured cells is difficult and several issues need to be considered. Apoptosis is a biochemical process that passes through several stages each with its own hallmarks and timing. The kinetics of the process depend upon a variety of factors, including the dose of the inducing agent and the ability of different cell types to carry out steps in the process. Thus the percentage of cells in apoptosis will vary with time after initiation. Cells treated with doses higher than those needed to cause apoptosis may die without exhibiting the usual characteristics of apoptosis, and are generally regarded as undergoing necrosis. As noted above, during the later stages of apoptosis, cells disintegrate into membrane-enclosed apoptotic bodies that *in vivo* are phagocytosed by macrophages or adjacent tumor cells and further catabolised. Since phagocytic cells are not found in tissue cultures, apoptotic bodies may complete the breakdown of their cellular constituents or may simply become detached from the culture substrate. In addition, late apoptotic cells or bodies can eventually lose the ability to maintain their membrane pumps and as a result may be unable to exclude vital dyes, such as trypan blue. Such apoptotic cells or bodies would then appear as necrotic cells. Therefore, one cannot produce an apoptotic response without studying a range of doses of the initiating agent and assaying for apoptotic markers over a wide range of times.

There are numerous assays for apoptosis. The two most common endpoints of apoptosis are morphological changes (cell shrinkage, condensation of nuclear chromatin, formation of apoptotic bodies) and DNA fragmentation[to large 300 kbp and 50 kbp fragments and then to oligonucleosome-sized fragments (multiples of 200 bp that appear as a 'ladder' of DNA bands upon agarose gel electrophoresis)]. Although observation of these endpoints is an indicator of apoptosis, quantification of the percentage of cells in a population that are in apoptosis is difficult or imposible without more sophisticated methods. For this purpose, many investigators use the TUNEL assay (during which fluorescently tagged or biotinylated nucleotides are added to the ends of DNA fragments within fixed cells). The cells are then strained in their DNA with propidium iodide and can be viewed on a microscope stage, or

they can be quantified by flow cytometry to indicate the presence of viable, apoptotic, necrotic and late apoptotic cells. Apoptotic cells can also be detected with the protein Annexin V, which binds in a highly selective manner to phosphotidyl serine; this phospholipid flips from the inner to the outer leaflet of the plasma membrane during apoptosis. This assay is also adaptable to quantification by flow cytometry or to imaging.

Since many of the enzymatic steps in apoptosis are known, it is often desirable to follow the process by monitoring those steps. Antibodies are available commercially for all of the common caspases, so that procaspase levels and their proteolytic processing can be monitored by western blot analysis. In addition, model peptide substrates can also be purchased for many of the caspases in fluorogenic or chromogenic forms, permitting assay of cell extracts for the presence and level of individual active caspases. Inhibitors based on active site peptide motifs can be used to test the participation of suspected caspases. However, because caspases are not completely specific for the amino acid motifs, the model substrates and inhibitors cannot provide absolute identification of the involved caspase. Caspase action can also be monitored by assessing the cleavage of intracellular protein substrates; *e.g.* cleavage of PARP or lamin B is a common indicator of the action of caspase-3 or -7 in apoptosis. A listing of commercially available kits for these and other assays of apoptosis, including measurement of caspases, substrates, and inhibitors [67].

With any of these or other assays, it is advisable to study sufficient doses and post-treatment times so that the progress of cell death may be observed. In addition, it is necessary to use more than one assay to confirm results. Finally, if some or all of the cells do not undergo apoptosis, one cannot conclude that the cells remain alive, without conducting an assay for total cell death. The best assay for this purpose is a clonogenic assay, which measures the ability of each cell in a population to grow, replicate, and form a colony. Unlike assays for apoptosis or for viability, such as dye exclusion or tetrazolium reduction, clonogenic assays register all cell death events integrated over time.

1.6.1.5 Biological assays

The overall aim of photosensitizer bioassay in the present context is to arrive at a substance which is suitable for clinical PDT. This is a complex process, and there is no way of doing it. But it eventuall requires assays using a mamalian model, usually a rodent. It can be argued that such reslts on animal models do not apply closely to the human animal; this is true, but this approach is the closest we can get with the current state of knowledge. Certainly using a model with functioning organs and a vascular system is more likely to be succesful in its outcome than experiments in a cell culture, which has none of these things.

1.6.1.5.1 In Vitro Bioassays

This refers to assays with cells in culture, the cells usually being derived from a tumor source. Different workers adopt different cell lines and different procedures. It would be a valuable and progressive step if an agreed standard cell culture and irradiation protocol were adopted as a point of reference between laboratories, not to displace the variety of cell lines used (which is valuable, since cancer is not a single disease), but to allow a better correlation of results.

Prior to irradiation, two experiments are needed. First, a study of acute dark toxicity, for which cells can be used. If all the cells are killed in the dark, the photosensitizer is eliminated, at least for PDT applications. Second, a study of photosensitizer uptake the tumor cells, using extraction followed by fluorescence or absorption measurements

After irradiation, it is the photo chemically-induced cell death that is being determined against appropriate dark controls. Cell death that is being determined against dark controls. Cell death can be determined either by the staining of the cells with (eg with propidium iodide 200), and counting the dead cells under a light microscope; or by dilution and sub-culture, and counting the new colonies (colonies assay;)

To in vitro procedures deserve special mention.

(i) Multicellular Tumor Spheroids (MTS). This assay depends on measuring the ability of a photosensitizer to halt the rate of growth of a model microtone. Some tumor cell lines can be cultured as monolayers, and then induced to form small spheres (multicellular tumor spheroids) which continue to grow in a spherical shape. They develop a necrotic centre, and in this respect are thought to be good models for much larger tumors. Such spheroids are placed in growth medium in multi-well plates, and volume is measured with time in the presence and absence of photosensitizer and light. Activity is indicated by a diminution in the rate of growth of the spheroids compared with controls.

(ii) MTT assay. MTT stands for 3-(4,5-dimethylthiazol-2-yl)-2,5-diphenyl-2H-tetrazolium bromide: metabolically active mitochondria reduce MTT, which is yellowish, to the corresponding formazan, which blue.

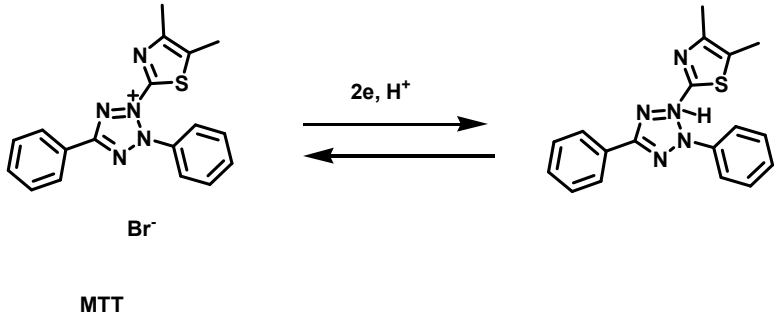

Figure 15. Structure of MTT

If it is accepted that metabolically active mitochondria signify a living cell, then this offers a convenient and rapid spectroscopic method for estimating cell death. A smore cells are photonecrosed, the amount of frozan decreases.

CHAPTER 2

EXPERIMENTAL

2.1. Instrumentation

^{1}H and ^{13}C NMR spectra were recorded on a Bruker Instruments Avance Series-Spectrospin DPX-400 Ultra shield (400 MHz) High Performance digital FT-NMR spectrometer (METU, NMR Laboratory). All chemical shifts are referenced to residual signals previously refenced to TMS and splitting patterns are designated as s (singlet), d (doublet), t (triplet), q (quartet), m (multiplet), p (pentet), dt (doublet of triplet) and br (broad).

Electronic absorbtion spectra were recorded on a **Shimadzu UV-1601** spectrophotometer. **A Perkin-Elmer LS 50 B luminescence spectrometer was used for recording the fluorescence emission spectra.** All instrumental parameters were controlled by Fluorescence Data Manager Software (FLDM). Measurements were conducted at 25°C using a 1x 0.5 cm rectengular quartz cuvette.

ESI-MS analysis were recorded on a Agilent 1100 MSD spectrometer (TUBITAK-ATAL analysis laboratory)

Chemicals and solvents were purchased from Aldrich and used without further purification. Column chromatography of all the products were performed using Merck Silica Gel 60 (particle size: 0.040- 0.063 mm, 230-400 mesh ASTM) pretreated with eluent. Reactions were monitored by thin layer chromatography using Merck Silica Gel 60 Kiesegel F_{254} TLC Aluminum Sheets 20x20 cm.

K-362 cell lines were purchased from American Tissue Cell Culture and frozen. They were taken from the bone marrow organ of homo sapiens (human) organism. Their diseases were the chronic myelogenous leukemia (CML).

2.1.1 MTT assay

K562 human erythroleukemia cells (ATCC) were cultured in 25 cm^2 culture flasks containing RPMI 1640 supplemented with heat inactivated 10 % fetal bovine serum, 2 mM L-glutamine, 100 units.mL^{-1} penicillin G and 100 μg.mL^{-1}streptomycin at 37^0C in a humidified incubator containing 5% CO_2. Dye was dissolved in RPMI 1640 and test concentrations were prepared daily.

The methlythiazolyltetrazolium (MTT) assay was used to evaluate cell viability. Briefly, 50 μl cell suspensions containing 4 x 10^4 K562 cells were seeded in 96-well round-bottom plates (Costar, Cambridge, MA) and varying concentrations of dye (25 nM-500nM) were added in 50 μl into each well. All concentrations were studied in quadriplicate.

Then, cells were kept either in dark or under illumination with a red (625 nm) LED array at 3.0 mW/cm^2 fluence rate for a period of 4 h at 37^0C in a humidified incubator containing 5% CO_2. After 4 h of incubation, 25 μl of MTT solution (1mg/ml final concentration) (Sigma Chemical Co., St. Louis, MO) were added to each well, and the plates were incubated for a further 4 h. The formazan precipitate was solubilized by adding 80 μl lysing buffer (pH=4.7) composed of 23% SDS (sodium dodecyl sulfate) dissolved in a solution of 45% N,N-dimethylformamide. After an overnight incubation at 37^0 C, the optical densities (OD) were read at 570 nm using a microplate reader (Spectramax Plus, Molecular Devices, Sunnyvale,

California, USA). Cells incubated in culture medium alone served as a control for cell viability (nontreated wells) either in irradiated plate or in plate that was kept in dark. Cell viability (%) was calculated as (OD of treated wells/OD of nontreated cells) x 100. In order to evaluate the cytotoxicity of dye after 24 h incubation, 4 h irradiated plates were kept in dark for a further 20 h and then MTT solution was added for measuring cell viability. In addition, plates kept in dark for 4 h were also incubated for a further 20 h for control.

2.1.2 Cell Culture

K562 cells (human chronic myelogenous leukemia cell line, ATCC) were maintained in RPMI-1640 culture medium supplemented with 10% heat-inactivated fetal bovine serum, 2 mM L-glutamine, 100 IU/ml penicillin and 100 μg/ml streptomycin at 37^0 C in a humidified incubator containing 5% CO_2 . *2.1.3*

2.1.3Preparation of stock solutions

A stock solution of propidium iodide (PI) (Sigma P-4170) was prepared in distilled water, and used at a concentration of 0.5 mg/ml. Acridine orange (AO) was dissolved in phosphate buffered saline at a concentration of 100 μg/mL. One tablet of phosphate buffered saline (PBS) (Amresco) was dissolved in the distilled water to yield a pH=7.4 buffered solution.

2.1.4 Flow Cytometry

Dead cells were identified as propidium iodide (PI) permeable percentage of cells and the counts were measured by flow cytometry (Epics XL MCL, Beckman Coulter). Samples were analyzed immediately after each illumination. Cells which were incubated with photosensitizer at dark for 4 hours served as control [68].

2.2 Synthesis of ethyl 3,4,5-trihydroxybenzoate (16)

3, 4, 5- trihydroxy benzoic acid (5.00 g, 29.4 mmol) was dissolved in 30 mL EtOH. 1 mL of H_2SO_4 was carefully added as a catalyst in 10 min. and the reaction mixture was refluxed overnight. The crude product was chromatographed on silica gel and eluted with chloroform-isopropanol 7:3(v/v) to yield 3.20 g solid compound **16.** Yield 55%.Without further purification **16** was used through next step.^{1}H NMR ($CDCl_3$): δ (ppm) 6.95 (s, 2H ar-H), 4.20 (t, 2H, -CH_2), 1.25 (q, 3H, CH_3), ^{13}C NMR (100 MHz, $CDCl_3$, D-DMSO) δ 144.4, 136.9, 125.7, 120.8, 108.9, 59.9, 13.8.

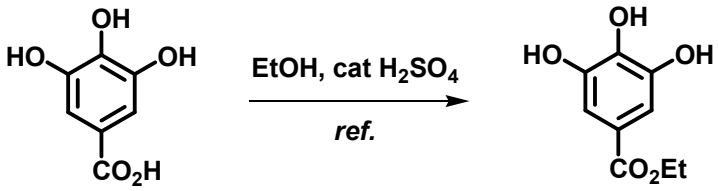

16

Figure 16 Esterification 3, 4, 5- trihydroxybenzoic acid

2.3 Synthesis of triehylene glycol methyl ether tosylate (17)

Compund **16** (3.00g, 15. 0 mmol) and 5 mL of Et_3N was dissolved in 150 mL of CH_2Cl_2.In a dropwise manner TosCl (3.20g, 15. 0 mmol) was added to the mixture. The reaction was over after mixing one day at room temperature. The desired product was then collected with column chromatography in which the eluent was $CHCl_3$. to yield 3.32g **17 in a liquid form .**Yield 81%

^{1}H NMR ($CDCl_3$): δ (ppm) 7.55 (d, 2H, ar-H), 7.15 (d, 2H, ar-H), 4.00 (m, 2H, -CH_2), 3.60-3.30 (m, 10H), 3.20 (s, 3H, CH_3), 2.30 (s, 3H, CH_3). ^{13}C NMR (100 MHz, $CDCl_3$) δ 144.7, 132.9, 129.8, 127.8, 71.8, 70.5, 70.4, 69.3, 68.5, 58.8, 21.4

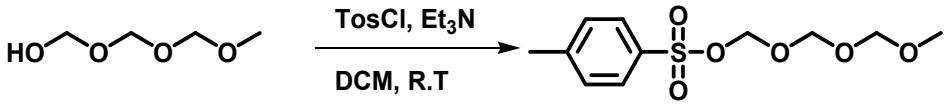

17

Figure 17 Tosylation of triehylene glycol methyl ester

2.4 Synthesis of compound 18

A suspension of **16** (3.00g, 15. 0 mmol), **17** (12.4g, 45.0 mmol), K_2CO_3 (8.10g, 45.0mmol) and catalyt amount of 18-crown-6 in 200 ml acetone was refluxed overnight. Acetone was removed by evaporation, and the residue was redissolved in $CHCl_3$ and extracted with distilled water three times. The organic phase was taken and solvent was removed by evaporation. The expected product was taken without any further purification as a brown oil.(8.50 g, 92%). ^{1}H NMR ($CDCl_3$): δ (ppm) 7.20 (s, 2H, ar-H), 4.40- 3.10 (m, 45 H), 2.30 (t, 3H, -CH_2), 1.30 (q, 3H, CH_3).

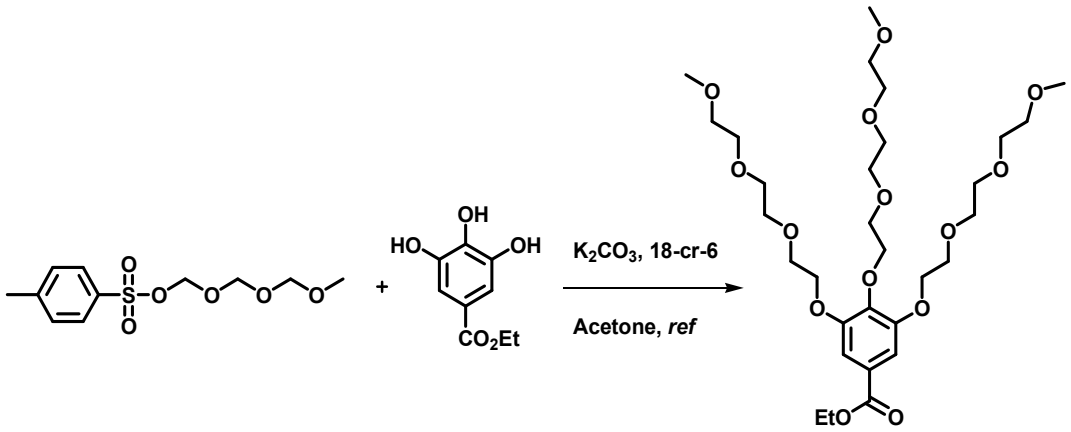

18

Figure 18 Substitution reaction of **18** with **17**

2.5 Synthesis of compound 19

An excess amount of 2.0 g $LiAlH_4$ was dissolved in dry 20 ml of THF and **18** (8.00 g, 12.5 mmol) was added to the reaction mixture in a dropwise manner in 30 min. After reaction was completed which was monitered with TLC the excess amount of $LiAlH_4$ was killed with a cold water. The crude reaction was filtered and washed with methanol. The solvent then was removed by evaporation and **19** was taken as an only product.(7.40 g, 100%)^{1}H NMR ($CDCl_3$): δ (ppm) 7.30 (s, 1H,-OH), 6.60 (s, 2H, -ar-H), 4.55(s, 2H, -CH_2), 4.30- 3.30 (m, 45H)

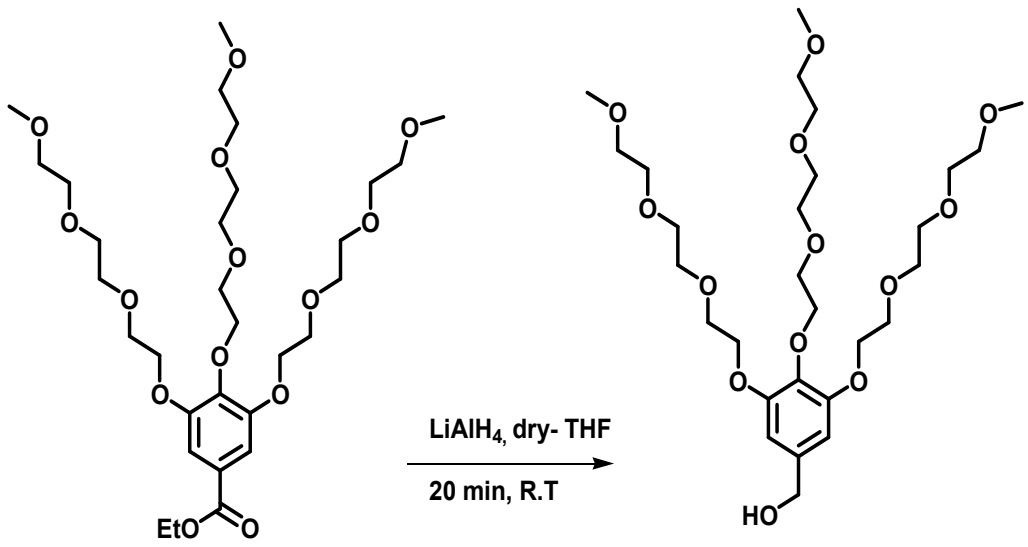

19

Figure 19 Reduction reaction of **18** with $LiAlH_4$

2.6 Synthesis of compound 20

Compound **19** (7.00 g, 11.8 mmol) and excess amount of pyridinium chloro chromate (PCC) (5.00 g) was dissolved in CH_2Cl_2. The reaction was monitered by TLC and when complete consumption of **19** was seen the reaction was completed. Crude reaction was extracted with basic aqueous solution one times, then three times with acidic aqueous solution. The organic phase was collected and solvent removed by evaporation. **20** was taken as only product after workup steps (6.90g, 100%) ^{1}H NMR ($CDCl_3$): δ (ppm) 9.80 (s, 1H), 7.10 (s, 2H, ar-H), 4.30- 3.30 (m, 45H), ^{13}C NMR (100 MHz, $CDCl_3$) δ 190.9, 153.0, 144.1, 131.6, 109.0, 72.5, 71.9, 70.8, 70.6, 70.5, 69.6, 69.0, 58.9.

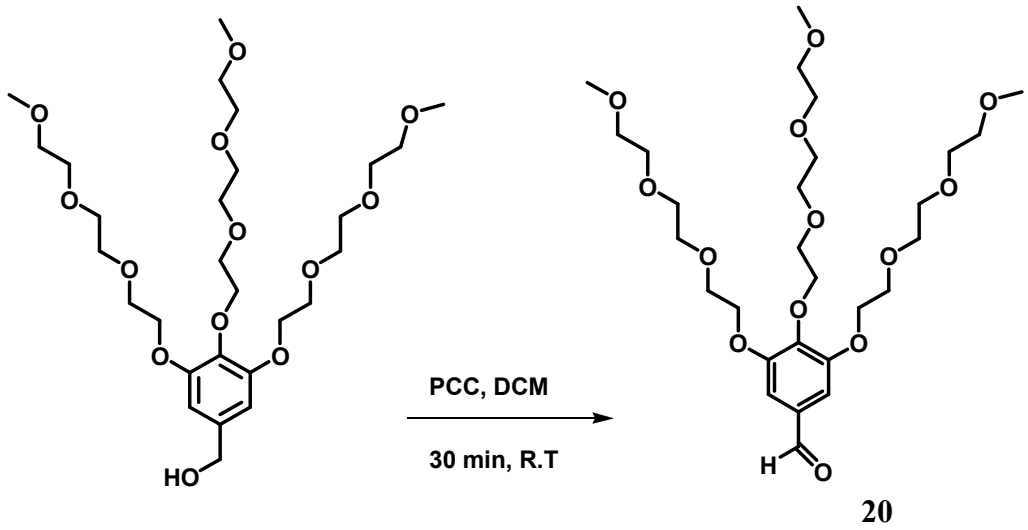

Figure 20 Oxidation reaction of **19** with PCC

2.7 Synthesis of compound 22.

3,4,5-tris(2-(2-(2-methoxyethoxy)ethoxy)ethoxy)benzaldehyde (20) (0.34 mmol, 200 mg) and 2,4-dimethyl pyrrole (21) (0.68 mmol, 84mg) were dissolved in CH_2Cl_2 (250 mL) purged with argon in a 100 mL flask. 1 drop of TFA was added and the mixture was stirred at room temperature for 3 hrs. When TLC showed consumption of the aldehyde was complete, a solution of 166 mg (0.68 mmol) of DDQ (Tetrachloro- 1,4-benzoquinone) in CH_2Cl_2 was added. After 3 h, Et_3N (3 ml) and $BF_3.OEt_2$ (3 ml) were added. Immediately after the addition of $BF_3.OEt_2$ bright green fluorescence was observed. Crude product washed three times with water, dried over Na_2SO_4 and concentrated in vacuo. Then crude product purified by silica gel column chromatography using $CHCl_3/CH_3OH$ (99/1, v/v). The orange fraction which has bright green fluorescence was collected. Orange solid (0.147 mmol, 120 mg, 43 %).^{1}H NMR (400 MHz, CDCl3) δ 6.48 (s, 2H), 5.91 (s, 2H), 4.15 (t, *J*= 5. 0 Hz, 2H), 4.06 (t, *J*= 5.0 Hz, 4H), 3.76 (t, *J*= 4.9 Hz, 4H), 3.42- 3.70 (m, 26H), 3.30 (s, 3H), 3.27 (s, 6H), 2.48 (s, 6H), 1.46 (s, 6H); ^{13}C NMR (100 MHz, CDCl3) δ 155.6, 153.7, 143.0, 141.2, 139.2, 131.3, 129.9, 121.1, 107.8, 72.7, 72.0, 71.9, 70.9, 70.7, 70.6, 70.5, 69.8, 69.3, 59.0, 14.5, 14.3.

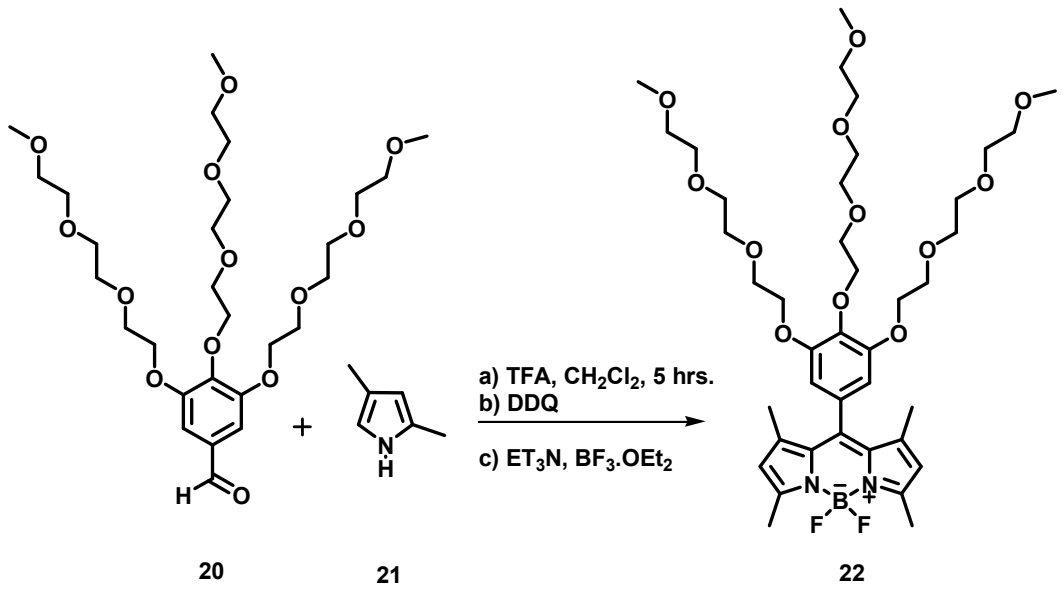

20 21 22

Figure 21 Reaction scheme for compound **22**

2.8 Synthesis of compound 23.

Compound **22** (0.123 mmol, 100 mg), α, α'-Azoisobutyronitrile (AlBN) (0.0123 mmol, 2.0 mg) and N-Bromosuccinimide (NBS) (0.246 mmol, 43.78 mg) were refluxed in CCl_4 (20 ml). After 30 min, crude product concentrated under vacuo, then purified by sillica gel column chromatography using $CHCl_3$. The red colored fraction was collected then the solvent was removed under reduced pressure to yield the desired compound **23** (0.0984 mmol, 95.28 mg, 81%).^{1}H NMR (400 MHz, $CDCl_3$) δ 6.30 (s, 2H), 4.00 (t, *J*= 4.9 Hz, 2H), 3.90 (t, *J*= 4.9 Hz, 4H), 3.24-3.64 (m, 30H), 3.14 (s, 3H), 3.12 (s, 6H), 2.34 (s, 6H), 1.28 (s, 6H);
^{13}C NMR (100 MHz, $CDCl_3$) δ 154.0, 141.6, 140.5, 139.6, 130.3, 129.1, 111.7, 107.5, 107.3, 72.8, 72.5, 72.0, 71.9, 71.8, 71.2, 70.8, 70.7, 70.6, 70.5, 70.5, 70.4, 69.7, 69.3, 61.7, 58.9, 58.7, 13.9, 13.6;

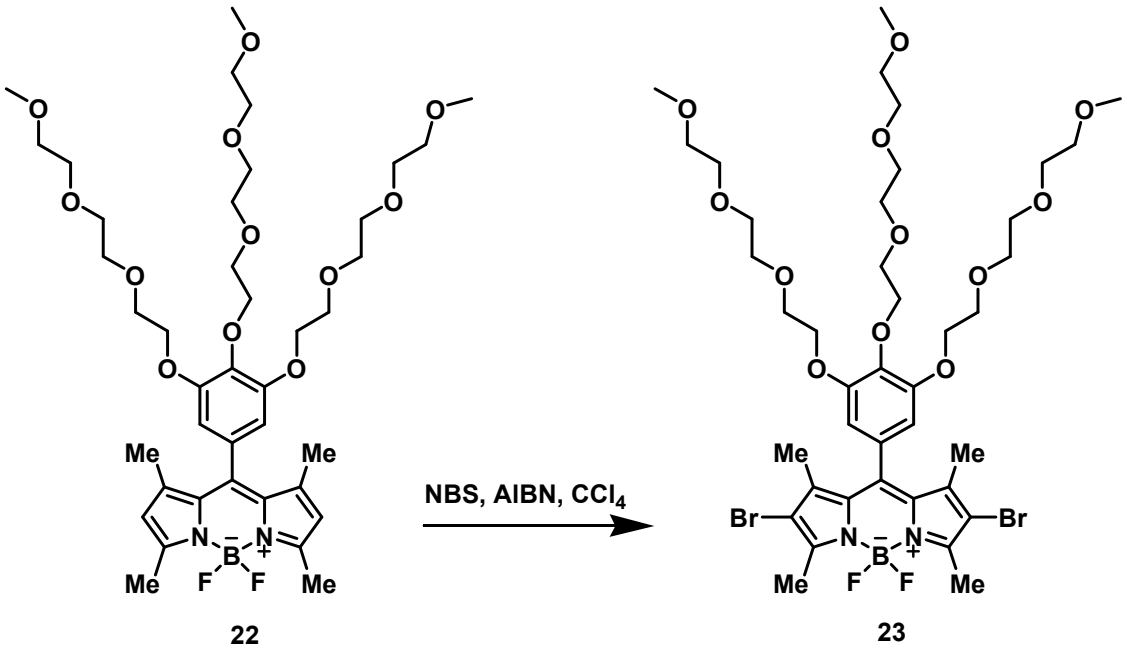

Figure 22 Bromination reaction of compound **22** with NBS

2.9 Synthesis of compound 24

Compound **23** (0.093 mmol, 90 mg) and **20** (0.186 mmol, 110.2 mg) were refluxed in a mixture of toluene (20 ml), glacial acetic acid (1.5 mL), and piperidine (2 mL). Any water formed during the reaction, was removed azeotropically by heating overnight in a Dean-Stark apparatus. Solvents were removed under reduced pressure, and the crude product was then purified by silica gel column chromatography using $CHCl_3/CH_3OH$ (95/5, v/v). The green colored fraction was collected then the solvent was removed under reduced pressure to yield compound **24** (0.0186 mmol, 39.5 mg, 21%). ^{1}H NMR (400 MHz, $CDCl_3$) δ 7.91- 7.86 (d, *J*= 16 Hz, 2H) 7.44- 7.39 (d, *J*= 16 Hz, 2H), 6.78 (s, 4H), 6.50 (s, 2H), 4.22- 3.22 (m, 135H), 1.50 (s, 6H); ^{13}C NMR (100 MHz, $CDCl_3$) δ 154.0, 153.0, 148.5, 141.1, 140.4, 139.7, 139.5, 139.0, 132.3, 132.2 129.5, 117.2, 110.7, 108.0, 107.9, 72.8, 72.5, 72.0, 71.9, 70.9, 70.8, 70.7, 70.6, 70.5, 69.7, 69.4, 69.2, 59.0, 53.4, 13.8,

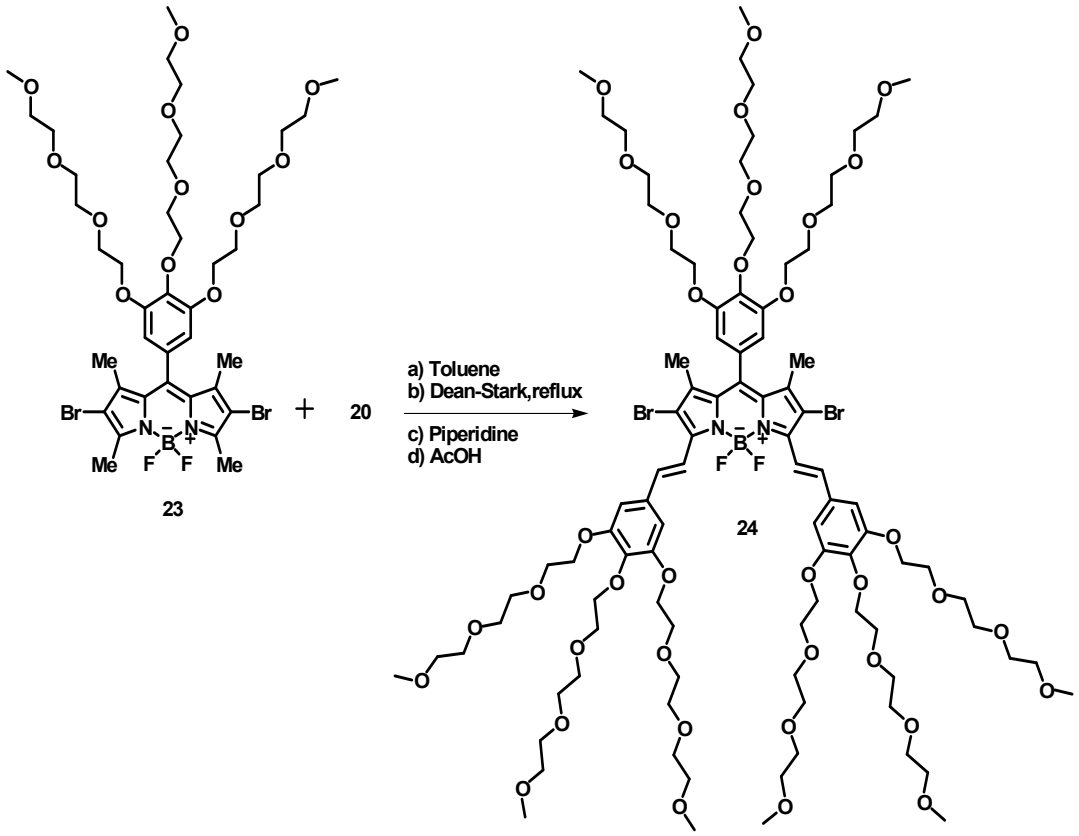

Figure 23 Synthesis of di-styryl BODIPY derivative, **24**

2.10 Synthesis of compound 26

Compound **23** (0.103 mmol, 100 mg) and 4-bromobenzaldehyde, **25**, (0.206 mmol, 38.0 mg) were refluxed in a mixture of toluene (20 ml), glacial acetic acid (1.5 mL), and piperidine (2.0 mL). Any water formed during the reaction, was removed azeotropically by heating overnight in a Dean-Stark apparatus. Solvents were removed under reduced pressure, and the crude product was then purified by silica gel column chromatography using $CHCl_3$/Hexane (75/25, v/v). The green colored fraction was collected then the solvent was removed under reduced pressure to yield compound **26** (0.021 mmol, 27.0 mg, 20%). ^{1}H NMR (400 MHz, were removed under reduced pressure, and the crude product was then purified by silica gel column chromatography using $CHCl_3$/Hexane (75/25, v/v). The green colored fraction was collected then the solvent was removed under reduced pressure to yield compound **26** (0.021 mmol, 27.0 mg, 20%). ^{1}H NMR (400 MHz, $CDCl_3$) δ 8.04-7.95 (d, *J*= 16Hz, 2H), 7.57- 7.66 (d, *J*= 16 Hz, 2H), 7.44 (q, *J*= 8 Hz, 8H), 6.49 (s, 2H), 4.20 (t, *J*= 4.9 Hz, 2H), 4.08 (t, *J*= 4.9 Hz, 4H), 3.82- 3.41 (m, 30H), 3.32 (s, 3H), 3.27 (s, 6H), 1.50 (s, 6H);^{13}C NMR (100 MHz, $CDCl_3$) δ 154.1, 148.3, 141.6, 139.8, 139.7, 138.0, 135.7, 132.3, 132.0, 129.3, 129.1, 123.5, 118.7, 110.6, 107.9, 72.8, 72.0, 71.9, 70.9, 70.7, 70.6, 70.5, 69.8, 69.4, 59.0, 13.8

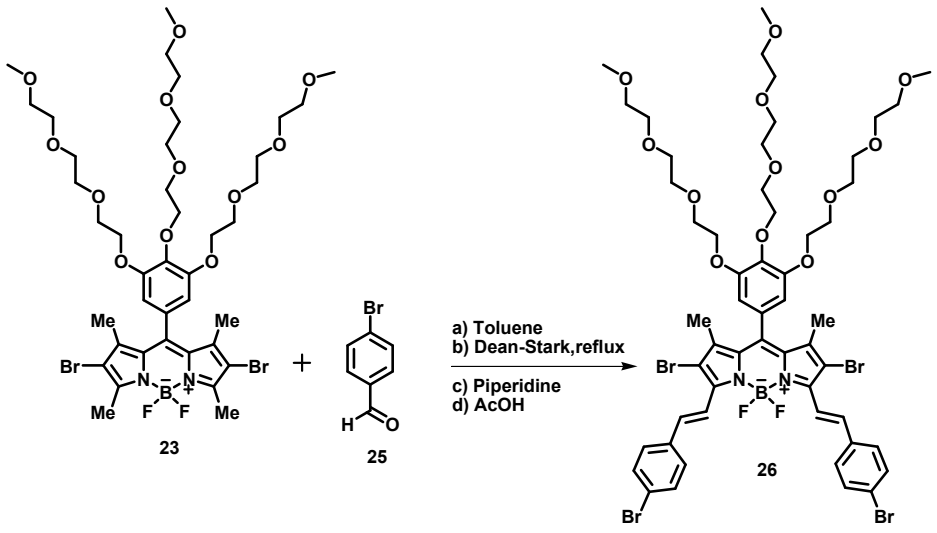

Figure 24 Reaction scheme for compound 26

2.11 Synthesis of compound 27

4-Bromo benzaldeyhde, **25**, (1.08 mmol, 200 mg) and 2,4-dimethyl pyrrole, **21**, (2.16 mmol, 205.0 mg) were dissolved in CH_2Cl_2 (250 mL) purged with argon in a 100 mL flask under argon atmosphere. 1 drop of TFA was added and the mixture was stirred at room temperature for 3 hrs. When TLC showed consumption of the aldehyde was complete, a solution of DDQ (1.08 mmol, 177.5 mg) in CH_2Cl_2 (20 mL) was added. After 3 h, Et_3N (3 ml) and $BF_3.OEt_2$ (3 ml) were added. Immediately after the addition of $BF_3.OEt_2$ bright green fluorescence was observed. Crude product washed three times with water, dried over Na_2SO_4 and concentrated in vacuo. Then crude product purified by silica gel column chromatography using $CHCl_3$. The orange fraction which has bright green fluorescence was collected. Orange solid (0.46 mmol, 187 mg, 45%).^{1}H NMR ($CDCl_3$): δ (ppm) 7.51 (d, *J*= 8.2 Hz, 2H, ar-H), 7.10 (d, *J*= 8.2 Hz, 2H, ar-H), 5.90 (s, 2H), 2.50 (s, 6H), 1.20 (s, 6H). ^{13}C NMR (100 MHz, CDCl3) δ 159.7, 155.2, 143.2, 142.0, 131.9, 129.2, 126.9, 121.1, 115.1, 26.6, 25.7.

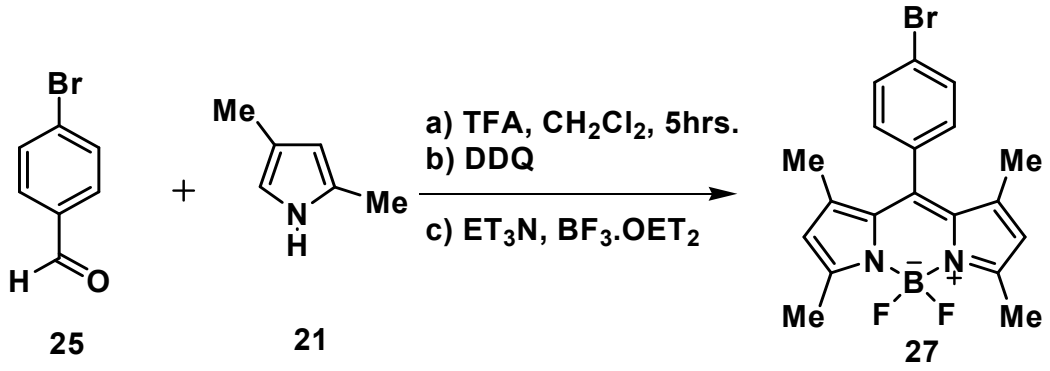

Figure 25 Synthesis of BODIPY derivative, **27**

2.12 Synthesis of compound 28

Compound **27** (0.37 mmol, 150 mg), NBS (0.74 mmol, 132.0 mg), AlBN (0.037 mmol, 6.0 mg) were refluxed in CCl_4 (20 ml). After 30 min, crude product concentrated under vacuum, then purified by sillica gel column chromatography using $CHCl_3$. The red colored fraction was collected then the solvent was removed under reduced pressure to yield the desired compound **9** (0.29 mmol, 162 mg, 78%) .^{1}H NMR (400 MHz, $CDCl_3$) δ 7.60 (d, *J*= 8.2 Hz, 2H), 7.08 (d, *J*=8.2 Hz, 2H), 2.53 (s, 6H), 1.34 (s, 6H) ^{13}C NMR (100 MHz, $CDCl_3$) δ 154.5, 140.4, 133.3, 132.8, 130.2, 129.7, 124.0, 112.0, 14.0, 13.7

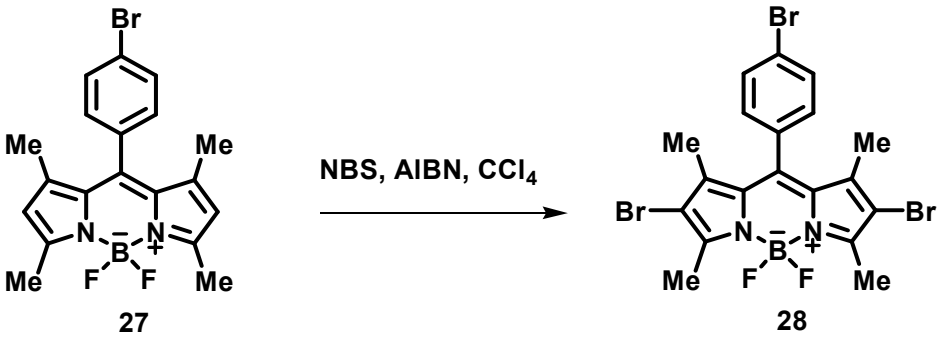

Figure 26 Bromination reaction of compound **27** with NBS

2.13 Synthesis of compound 29

Compound **28** (0.178 mmol, 100.0 mg) and **20** (0.356 mmol, 211.0 mg) were refluxed in a mixture of toluene (20 ml), glacial acetic acid (1.5 mL), and piperidine (2.0 mL). Any water formed during the reaction, was removed azeotropically by heating overnight in a Dean-Stark apparatus. Solvents were removed under reduced pressure, and the crude product was then purified by silica gel column chromatography using $CHCl_3/CH_3OH$ (97/3, v/v). The green colored fraction was collected then the solvent was removed under reduced pressure to yield compound **29** (0.043 mmol, 74 mg, 24%). ^{1}H NMR (400 MHz, $CDCl_3$) δ 7.92- 7.85 (d, *J*= 16.5

Hz, 2H), 7.65-7.60 (d, *J*= 8.3 Hz, 2H), 7.47-7.38 (d, *J*= 16.5 Hz, 2H), 7.15-7.11 (d, *J*= 8.3 Hz, 2H), 6.77 (s, 4H), 4.19-4.11 (m, 12H), 3.82-3.41(m, 60 H), 3.31 (s, 6H), 3.28 (s, 12 H), 1.41 (s, 6H); ^{13}C NMR (100 MHz, $CDCl_3$) δ 152.9, 148.8, 140.5, 139.8, 132.7, 132.2, 132.0, 130.5, 130.2, 129.0, 128.4, 125.5, 124.0, 117.2, 111.0, 107.9, 77.3, 77.0, 76.7, 72.5, 71.9, 70.8, 70.7, 70.5, 69.7, 69.2, 61.8, 59.0, 14.1

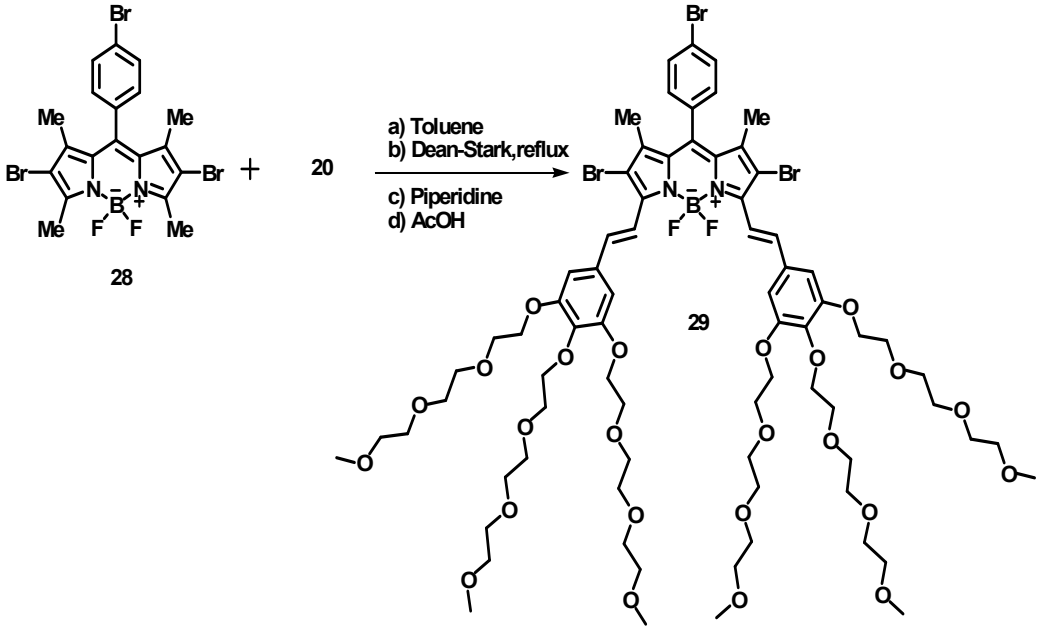

Figure 27 Reaction scheme for the compund **29**

CHAPTER 3

RESULTS AND DISCUSSION

3.1 Generation of a novel photosensitizer: Di-styrl Boradiazaindacenes

Boradiazaindacenes (BODIPY dyes or difluoroboradipyrrines) are well known fluorescent dyes with emerging applications in light harvesting systems and chemosensors. In recent years, there have been exciting reports demonstrating their versatile chemistry. Boradiazaindacenes with methyl substituents on 3 (or 5) positions were shown to undergo condensation reactions with aldehydes previously to yield longer wavelength absorbing dyes (100 nm red shifted) of internal charge transfer (ICT) characteristics. The extended conjugation in these dyes moves the absorption peak to 590-600 nm. Recently, we discovered that very efficient removal of water from the reaction mixture resulted in a double condensation yielding a distyryl-derivatized boradiazaindacene. These dyes have strong absorptions in the 650-680 nm region. In order to transform these novel dyes into potential PDT reagents, we wanted to incorporate two structural modifications. First, to facilitate the intersytem crossing via the heavy atom effect, bromine substituents were placed. Secondly, to improve water solubility, without compromising organic solubility which is essential for chromatographic manipulations, we introduced a number of amphiphilic tetraethyleneglycol moieties on the parent structure. It is also known that oligoethylene glycol moieties confer cell permeability and targeting of the dyes *in vivo* through favorable interactions with lipoproteins. Thus, three dyes shown in Figure 28 were targeted.

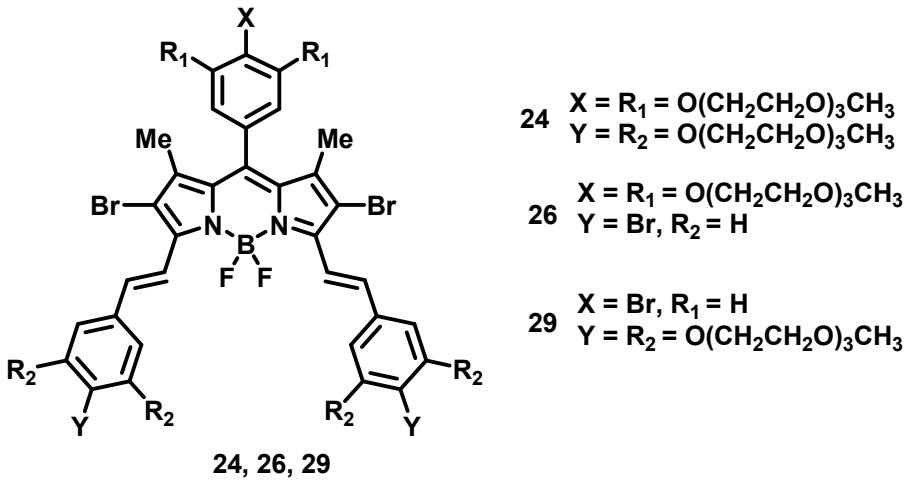

Figure 28 Chemical structure of the compound **24, 26, 29**

The syntheses are straight-forward, starting with known 3,4,5-trihydroxybenzaldehyde derivative. The key steps are the final double condensation steps leading to the target molecules. The absorption and emission characteristics of the dyes were studied. Alkoxystyryl-substituents introduced larger red shifts in both absorption and emission spectra compared to the 4-bromostyryl substituent (Figure 28). The effect of concentration on the absorbance spectra was studied. The dye **24** with 9 tetraethyleneethylglycol arms, showed no signs of aggregation in buffered aqueous solutions even at mM concentrations.

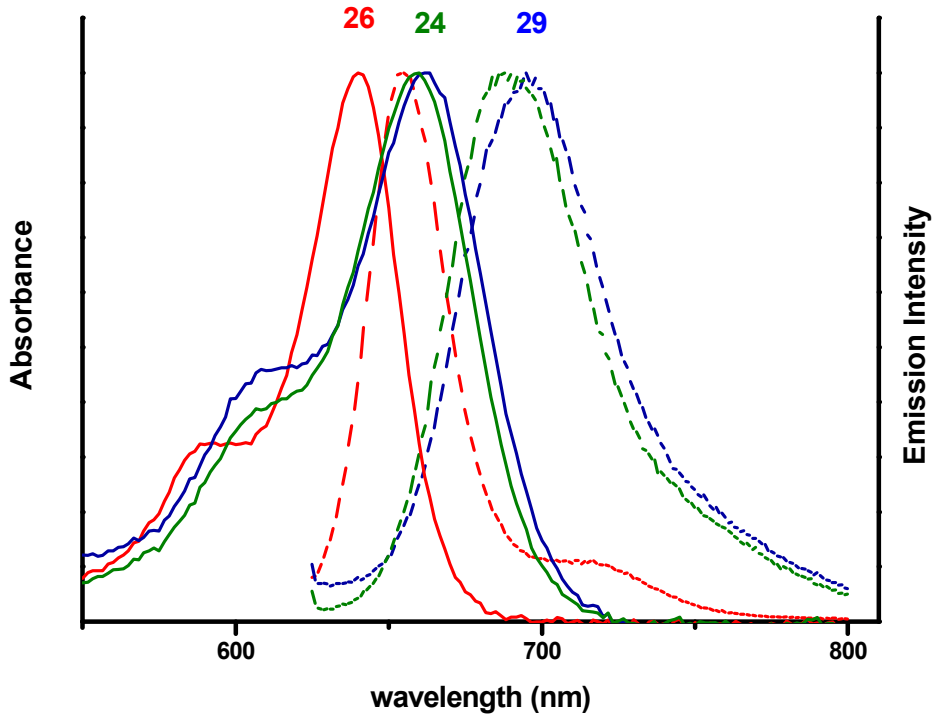

Figure 29 Absorbance (solid line) and Emission (dashed line) spectrum of di-styrl BODIPY dyes (**24, 26, 29).**

3.2 Degradation of distyrl BODIPY's and 1,3-diphenyl-isobenzofuran under red light

The singlet oxygen generation efficiency of these novel water soluble di-styrl BODIPY's were studied with the singlet oxygen trap 1,3-diphenylisobenzofuran (DPBF).

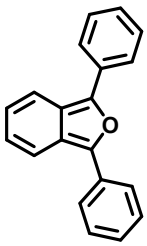

Figure 30 Structure of the singlet oxygen trap 1,3-diphenylisobenzofuran (DPBF).

In order to facilitate comparison to previously reported sensitizers, the activity was studied in isopropanol. Even at very low concentrations levels of 9 nM dyes (**24, 26, 29**) and under relatively weak red LED irradiation at 625 nm, remarkable efficiency was observed. The light intensity was determined to be 2 mW/ cm^2.

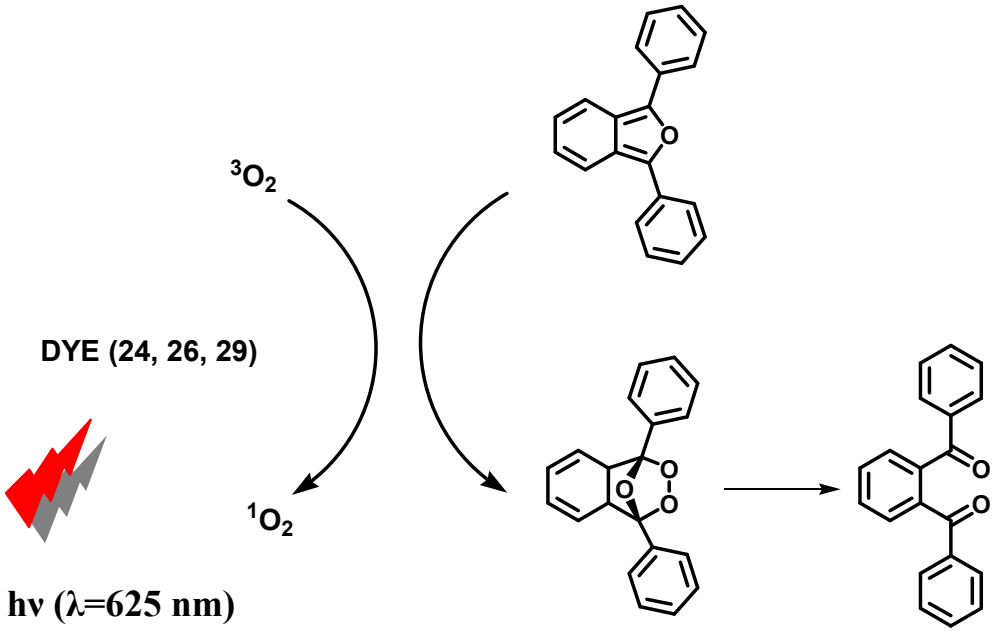

Figure 31 Excitation of water souble di-stryl BODIPY dyes with LED light in air-saturated solution causes a remarkable degradation of the selective singlet oxygen trap 1, 3-diphenyl-iso-benzofuran.

No degradation of the trap was observed either in dark or under rigorously deaerated solutions. Thus, Figure 32 shows the change in the absorption spectrum of the selective singlet oxygen trap 1,3-diphenyl-iso-benzofuran (5x 10^{-5} mM) absorbance in the aerated for 5 minutes before the irradiation started. During irradiation, the absorbance measured in every 5 minutes in dark and also under red light. Under these experimental conditions, the absorbance at the peak absorbance

wavelength of 1,3-diphenyl-iso-benzofuran did not change whereas, the solutions containing BODIPY dyes showed significant decreases in absorbance. In order to eliminate any contribution to the absorbance changes from dark reactions, we also recorded absorbance under the same conditions for 30 minutes in dark, followed by a 30 minutes period of irradiatin with red light. None of the compounds studied resulted in any absorbance changes in the reaction mixture. Only when the light was turned on, the degradation of the singlet oxygen trap started.

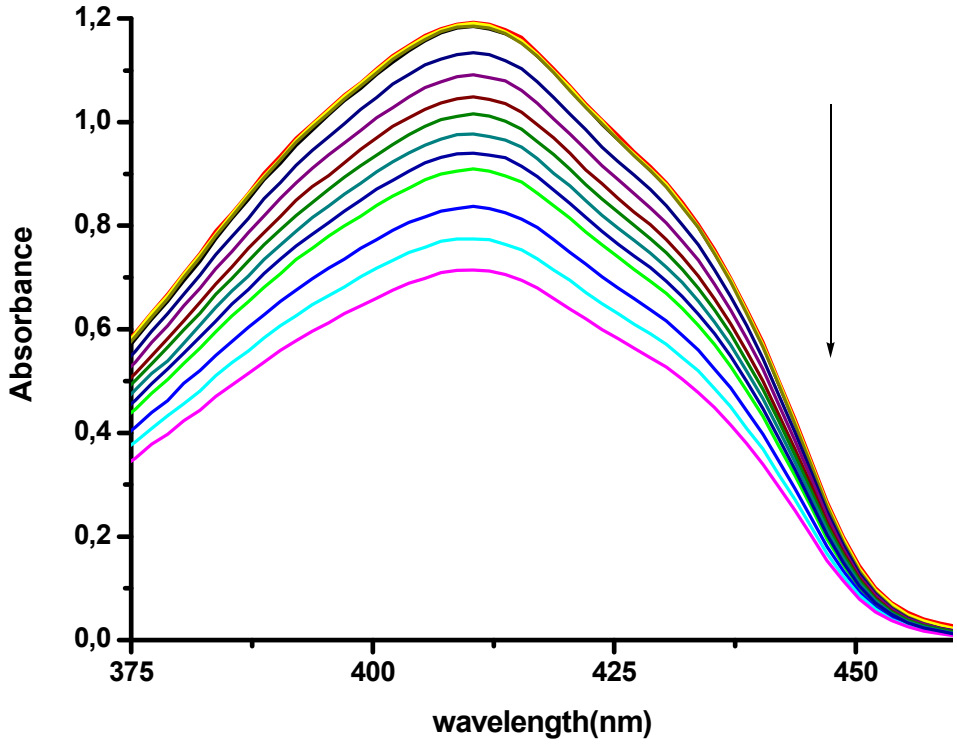

Figure 32 The change in the absorbance spectrum of 1,3-diphenyl-iso-benzofuran and dye (**24**) mixture on irradiation with LED light source (λ= 625 nm).

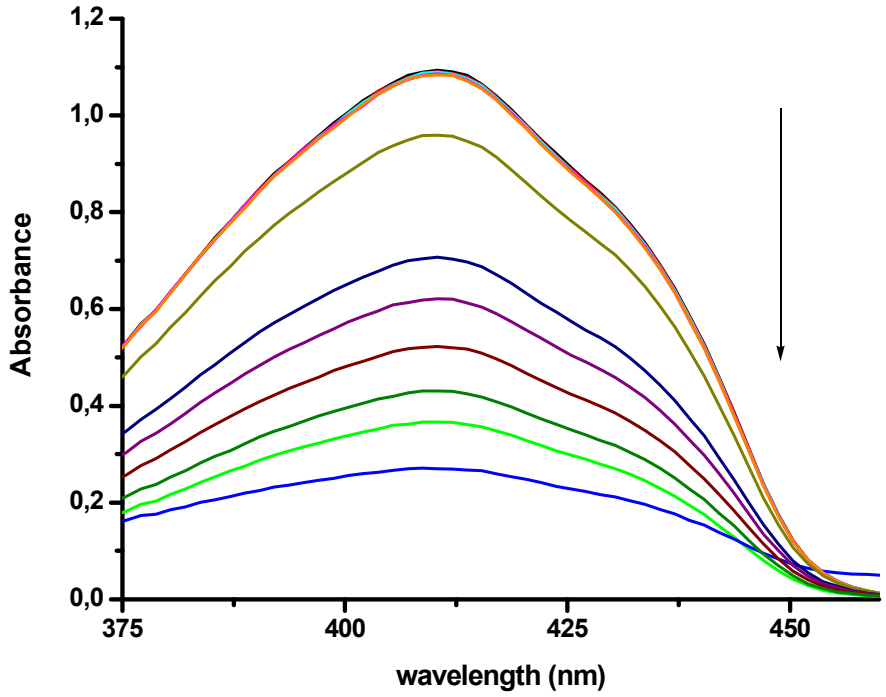

Figure 33 The change in the absorbance spectrum of 1,3-diphenyl-iso-benzofuran and dye (26) mixture on irradiation with LED light source (λ= 625 nm).

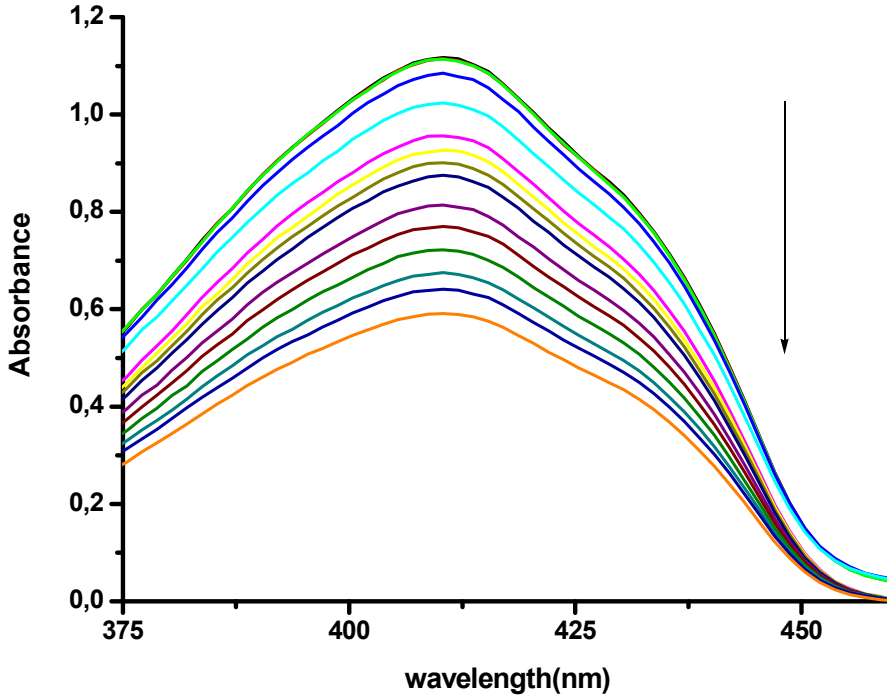

Figure 34 The change in the absorbance spectrum of 1, 3- diphenyl-iso-benzofuran and dye (**29**) mixture on irradiation with LED light source (λ= 625 nm).

3.3 Cytotoxixity

Encouraged by observations, we tested the most promising sensitizer **24** on K-562 human erythroleukemia cells. Standard MTT assay was used to quantify cytotoxicity. Cells which were kept in dark either with or without the sensitizer showed no decrease in viability.

However, in the presence of the sensitizer **3** under red LED irradiation at 625 nm at 2.0 mW/cm^2 fluence rate for 4 hours, followed by an incubation period of an additional 20 hr, very large decreases in cell viability were observed (Figure 35).

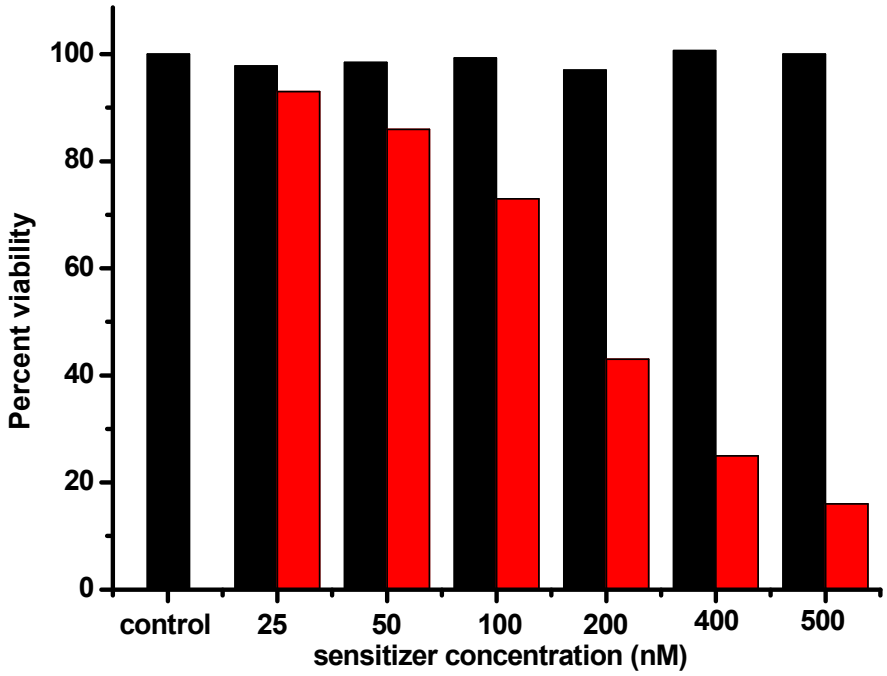

Figure 35. Percent viability as determined by a standard MTT assay. "Control" corresponds to assay data obtained with K562 cells kept in full medium in dark at 37 ^{o}C in an incubator. The other black bars show cell viability at different sensitizer (**24**) concentrations in dark. Red bars show percent viability at the indicated concentrations under 4 hr irradiation with red LED at 2.0 mW/cm^2 fluence rate,

followed by 20 hr incubation in dark at 37^{o}C. Percent viability values shown here are the averages of 4 runs

3.4 Viability studies of di-styrl-BODIPY's in the presence of red LED illumination in dark

K-362 cells (human chronic myelogenous leukemia cell line) were seeded on tissue culture dish at a density of 1x106 cells/dish. BODIPY (24) was dissolved in water. BODIPY'S was diluted in RPMI 1640 at a concentarion of 6 μg/ mL. During incubation, the light intensity was determined 2.0 mW/cm^2. EC_{50} value under these conditions was less than 200 nM. Even longer incubation periods following irradiation is known to further decrease tumor cell viability. After incubation, the dead cells appeared in red color due to propidium iodide (PI) and acridine orange (AO) staining under fluorescence microscope. The living cells appeared in green color due to the acridine orange (AO) and propidium iodide (PI) under fluorescence microscope. Two color staining experiment with acridine orange and propidium iodide under fluorescence microscope reveals that only under LED irradiation and in the presence of the sensitizer, the membrane integrity is compromised and preferential staining with propidium iodide (PI) takes place resulting in red fluorescence Figure 36

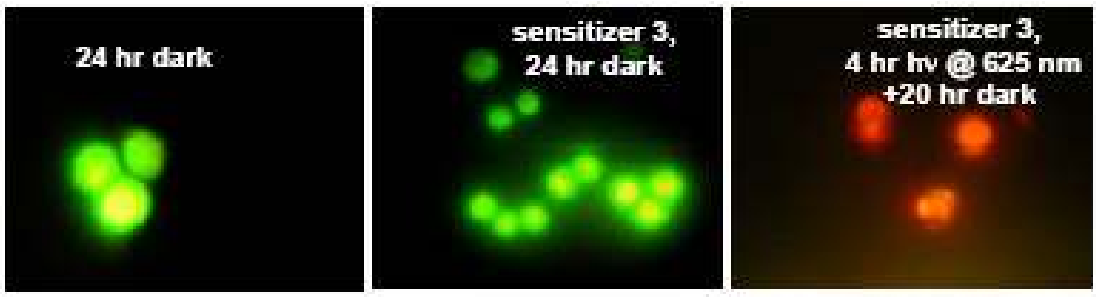

Figure 36. Fluorescence microscope images of acridine orange (AO) and propidium iodide (PI) stained K562 cells, incubated in full medium with 500 nM sensitizer **24** in dark (the middle panel); irradiated with red LED at 625 for 4 hours followed by 20 hr incubation in dark at 37 ^{o}C in the presence of 500 nM sensitizer **24** (right panel); and

incubated in dark for 24 hr (left panel). Live cells were preferentially stained with AO (green) and dead cells with PI (red) due to increased cellular permeability.

CONCLUSION

In this study novel distyryl derivatives of BODIPY dyes were synthesized. These novel distyrylborodiazaindacene dyes with bromo substituents on the fluorochrome π-system are very efficient singlet oxygen generators. In addition, these water soluble photosensitizers were shown to have spectacular photoinduced cytotoxicity at very low concentrations and even under low fluence rate LED irradiation. Dark toxicity was nil at the concentration range studied. Structure-activity fine tuning of the sensitizer with further in vitro and in vivo studies is likely to result in highly promising reagents for use in PDT.

By using these modified dyes we satisfied all the requirements for an ideal photosensitizer. Results showed that these dyes are very efficient photosensitizer for PDT. Cell culture studies also support our conclusions.

REFERENCES

[1]. Steed, J. W. , Atwood, J. L., Supramolecular Chemistry ,**2000,** p.2- 3,

[2]. Lehn, J. M., Encyclopedia of Supramolecular Chemistry, Strasbourg, France, September, **2003.**

[3]. Dolmans, D. E. J. G. J.; Fukumura, D.; Jain, R. K. *Nature Reviews Cancer* **2003**, *3*, 380.

[4]. Detty, M.R., Gibson, S.L., and Stephen J. Wagner Journal of Medicinal Chemistry**, 2004**, Vol. 47, No. 16.

[5]. Capella, M. A. M., Capella, L. S., J.Biomed. Sci **2003**; 10: 361- 366

[6]. Bonnett R., Martinez G., Tetrahedron 57, **2001**: 9513-9547

[7]. Gorman A.., Killoran J., O'Shea C., Kenna T., Gallagher W. M., O'Shea, D. F., J. Am Chem. Soc. **2004**, 126, 10619- 10631.

[8]. MacDonald, I. J.;Dougherty, T. J. Porphyrins Phthalocyanines **2001**, 5, 105.

[9]. Sharman, W.M.; Allen, C. M.; van Lier, J. E. Drug Discovery Today **1999**, 4, 507- 517

[10]. Wilkinson, F.; Helman, W. P.; Ross, A. B. J. Phys. Chem. Ref. Data **1993**, 22, 113- 262.

[11]. Kessel, D.; Thompson, P.; Saatio, K.; Nantwi, K. D. Photochem. Photobiol. **1987**, 45, 787- 790.

[12]. Sema, A. A. F.; Kennedy, J. C.; Blakeslee, D.; Robertson, D. M. Can. J. Neurol. Sci. **1981**, 8, 105- 114.

[13]. Latos-Grazynski, L.; Lisowski, J.; Olmstead, M. M.; Balch, A. L. Inorg. Chem. **1989**, 28, 1183- 1188.

[14]. Ziolkowski, P.; Milach, J.; Symonowicz, K.; Chmielewski, P.; Latos-Grazynski, L.; Marcinkowska, E. Tumori **1995**, 81, 364- 369

[15]. Marcinkowska, E.; Ziolkowski, P.; Pacholska, E.; Latos-Grazynski, L.; Chmielewski, P.; Radzikowski, C. Z. Anticancer Res. **1997**, 17, 3313- 3320

[16]. Paquette, B.; Boyle, R. W.; Ali, H.; MacLennan, A. H.; Truscott, T. G.; van Lier, J. E. Sulfonated phthalimidomethyl aluminum phthalocyanine: The effect of hydrophobic substituents on the in vitro phototoxicity of phthalocyanines

[17]. Margarone, P.; Gre´goire, M.-J.; Scasna´ rt, V.; Ali, H.; van Lier, J. E. Photochem. Photobiol. **1996**, 63, 217- 223.

[18]. Berg, K.; Bommer, J. C.; Moan, J.Photochem. Photobiol. **1989**, 49, 587- 594.

[19]. Colussi, V. C.; Feyes, D. K.; Mulvihill, J. W.; Li, Y.-S.; Kenney, M. E.; Elmets, C. A.; Oleinick, N. L.; Mukhtar, H. Photobiol. **1999**, 69, 236- 241.

[20]. Boyle, R. W.; Paquette, B.; van Lier, J. E. Br. J. Cancer **1992**, 65, 813- 817.

[21]. Wyss, P.; Schwarz, V.; Dobler-Girdziunaite, D.; Hornung, R.; Walt, H.; Degen, A.; Fehr, M. K. Int. J. Cancer **2001**, 93, 720- 724.

[22]. Friberg, E. G.; Cunderlikova, B.; Pettersen, E. O.; Moan, J.Cancer Lett. **2003**, 195, 73-80.
[23]. Funda Yükrük, PhD thesis, METU, **2005**
[24]. Killoran J., Allen L., Gallapher J. F., Gallapher W. M., O'Shea D. F., Chem.Commun., **2002**,1862-1863
[25]. Karolin, J.; Johansson, L. B. A.; Strandberg, L.; Ny, T. J. Am. Chem. Soc. **1994**, 116, 7801- 7806.
[26]. Wittmershaus, B. P.; Skibicki, J. J.; McLafferty, J. B.; Zhang, Y. Z.; Swan, S. J. Fluoresc. **2001**, 11, 119- 128.
[27]. Yogo T., Urano Y., Ishitsuka Y., Maniwa F., and Nagano T., J. Am. Chem. Soc. **2005**, 127, 12162- 12163.
[28]. Weishaupt KR.,Gomer CJ., Dougherty TJ., Cancer Res.,**1976** ,2326-2329.
[29]. Gilbert, A., Baggott, J., Essentials of Molecular Photochemistry, **1991**, 501-525.
[30]. Dye D., Watkins J., *Br. Med. J*. **1980**, *280*, 1353─1353
[31]. Turro, NJ., Modern Molecular Photochemistry, **1991**, 583-593.
[32]. Pass, HI., J.Natl.Cancer Inst., **1993**, 86, 443-456
[33]. Hendreson, BW., Fingar, VH., Cancer Res., **1987**, 47, 3110-3114
[34]. Dubbelman, TMAR, Prinsze, C., Penning, LC., Van Steveninck, J., In Photodynamic Therapy:Basic Principles and Clinical Applications, **1992**, 37-46.
[35]. Forbes KL., , Betts IJ., Photochem. Photobiol., **1984,** 39, 631- 634.
[36]. Henderson, BW., Dougherty, TJ., Photochem Photobiol **1992**, 55, 145-157.
[37]. Moan, J., Sommer, S. Cancer Res **1985,** 45:1608-1610;
[38]. Tromberg, BJ., Orenstein, A., Kimel, S.., Brker, S.J.., Hyatt, J., Nelson, J.S., Berns, M.W., Photochem Photobiol **1990**, 52: 375-385.
[39]. Lower, S. K.; El-Sayed, M. A. *Chem. Re*V. **1966**, *66*, 199
[40]. Yuster, P.; Weissman, S. I. *J. Chem. Phys.* **1949**, *17*, 1182.
[41]. Koziar, J. C.; Cowan, D. O. *Acc. Chem. Res*. **1978**, 334.
[42]. Turro, N. J. In *Modern Molecular Photochemistry*; University Science Books: Sausalito, CA, **1991**; pp 191- 195
[43]. Chandra, A. K.; Turro, N. J.; Lyons, A. L., Jr.; Stone, P. J. Am. Chem. Soc. **1978**, 100, 4964.
[44]. Valeur B., Molecular fluorescence principles and applications,Wiley, **2001**, p.34-47
[45]. Jesionek, A.; von Tappeiner, H. Arch. Klin. Med. **1905**, 82, 223- 227.
[46]. Schwartz, S. K.; Abolon, K.; Vermund, H. Univ. Minn. Med. Bull. **1955**, 27, 7- 8.
[47]. Fingar, V. H.; Mang, T. S.; Henderson, B. W. Cancer Res. **1988**, 48, 3350- 3354.
[48]. Peng, Q., Moan, J., Neslan, J.M. Correlation of subcellular and intratumoral photosensitizer localization with ultrastructural features after photodynamic therapy

[49]. Kessel, D, LuoY., Deng Y, Cang CK.. Photochem Photobiol. **1992,** 65:422- 426.
[50]. Zaidi, SIA, Oleinick, N.I., Zaim, M.T., Mukhtar, H. Photocehm Photobiol **1993,** 58: 771- 776;
[51]. Moan, J., Cancer Res., **1995,** 55, 2620-2626
[52]. Figge, F.H.J.., AAAS Research Conf.on Cancer, 1**945**, 117-128.
[53]. Oleinick, N.L., Moms, R.L., Belichenko, I., Photochem. Photobiol. Sc., **2002**, 1, 1-21.
[54]. Agarwal, M. L., Clay, ME., Harvey, H.E., Cancer Res., **1991,** 51, 5993- 5996.
[55]. Zaidi, S.I.A., Oleinick, ML,, Zaim, MT., Mukhtar, H., Photochem. Photobiol. **1993**, 58, 771-776.
[56]. He, X., Sikes, RA., Thomsen, S., Photochem. Photobiol., **1994,** 59, 468-473
[57]. Kessel, D., Lou, Y., Deng, Y., Chang, CK., Photochem. Photobiol., **1997,** 65, 422-426.
[58]. Lou, Y., Kessel, D., Photochem. Photobiol. **1997,** 66, 479-483.
[59]. Agarwal, M. L., Larkin H. E., Zaidi S.I.A. et al., Cancer Res. **1993,** 53, 5897- 5902.
[60]. Kick, G., Messer, G., Plewig, G. et al., Br. J. Cancer **1996,** 74, 30-36.
[61]. Fisher, A.M.R., Danenberg. K., Nanerjee D. et al., Photochem. Photobiol. **1997,** 66, 265-270.
[62]. Apoptosis 1996, publication of Oncogene Research Products, **1996**. Calbiochem.Ref Type: Pamphlet.
[63]. Kessel, D., Luo Y., Cell Death Diff. **1999,** 6, 28-35.
[64]. Kessel, D., Luo, Y., J. Photochem. Photobiol. B: Biol, **1998,** 42, 89-95.
[65]. Ruck, A., Dolder, M., Wallimann, T., Brdiczka, D., FEBS Lett. **1998**, 426, 97-101.
[66]. Petit, P.X., Susin, S.A., Zamzami, N. et al., FEBS Lett., **1996,** 396, 7-13.
[67]. Kim, HR., Luo, Y., Li, G., Kessel, D., Cancer Res., **1999,** 59, 3429-3432.
[68]. Hansen, M.B. Nielsen, S.E. Berg K., **1989**, J. Immunol Methods,119(2): 203-210.

APPENDIX

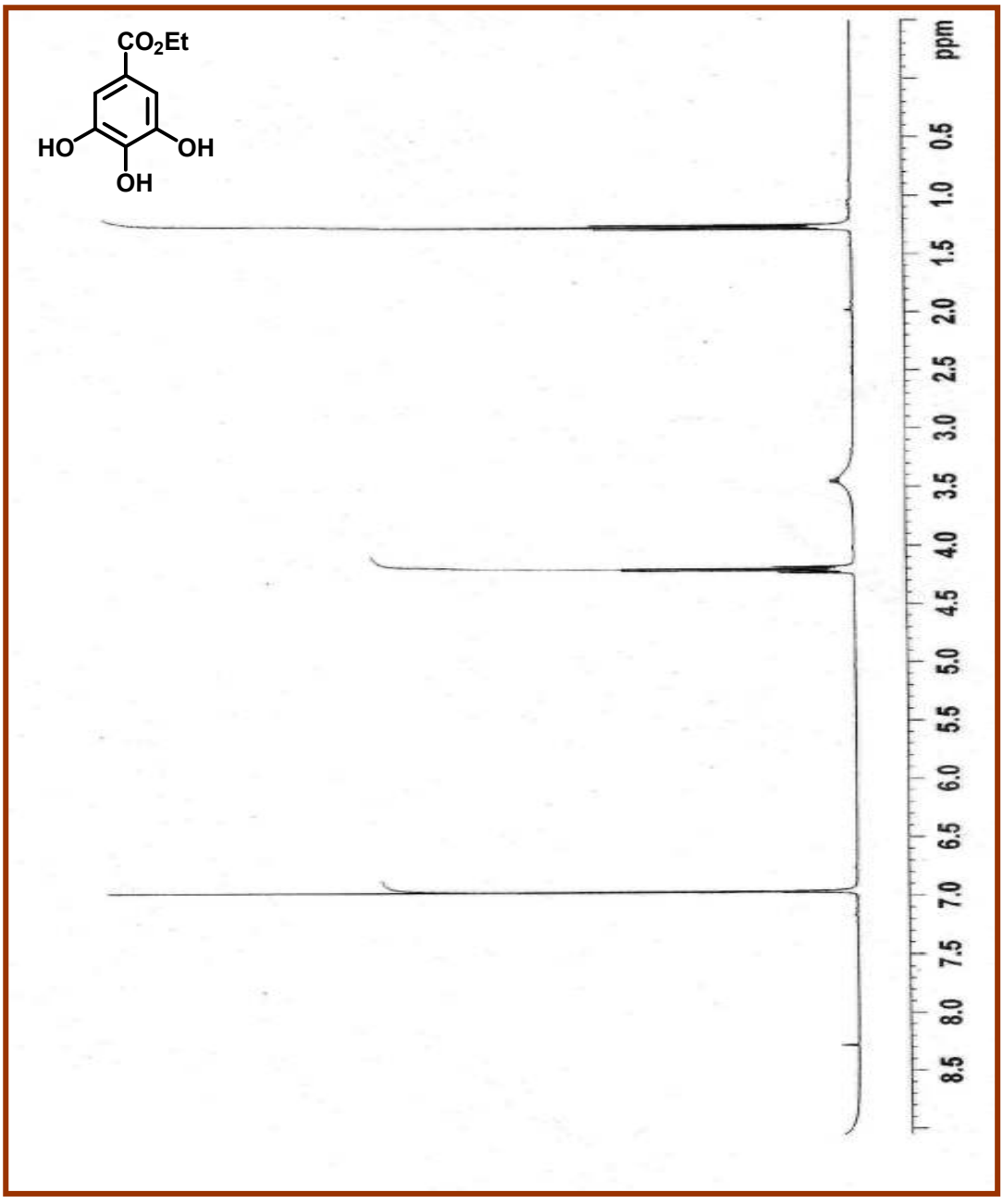

Figure 37 ^{1}H NMR Spectra of compound **16**

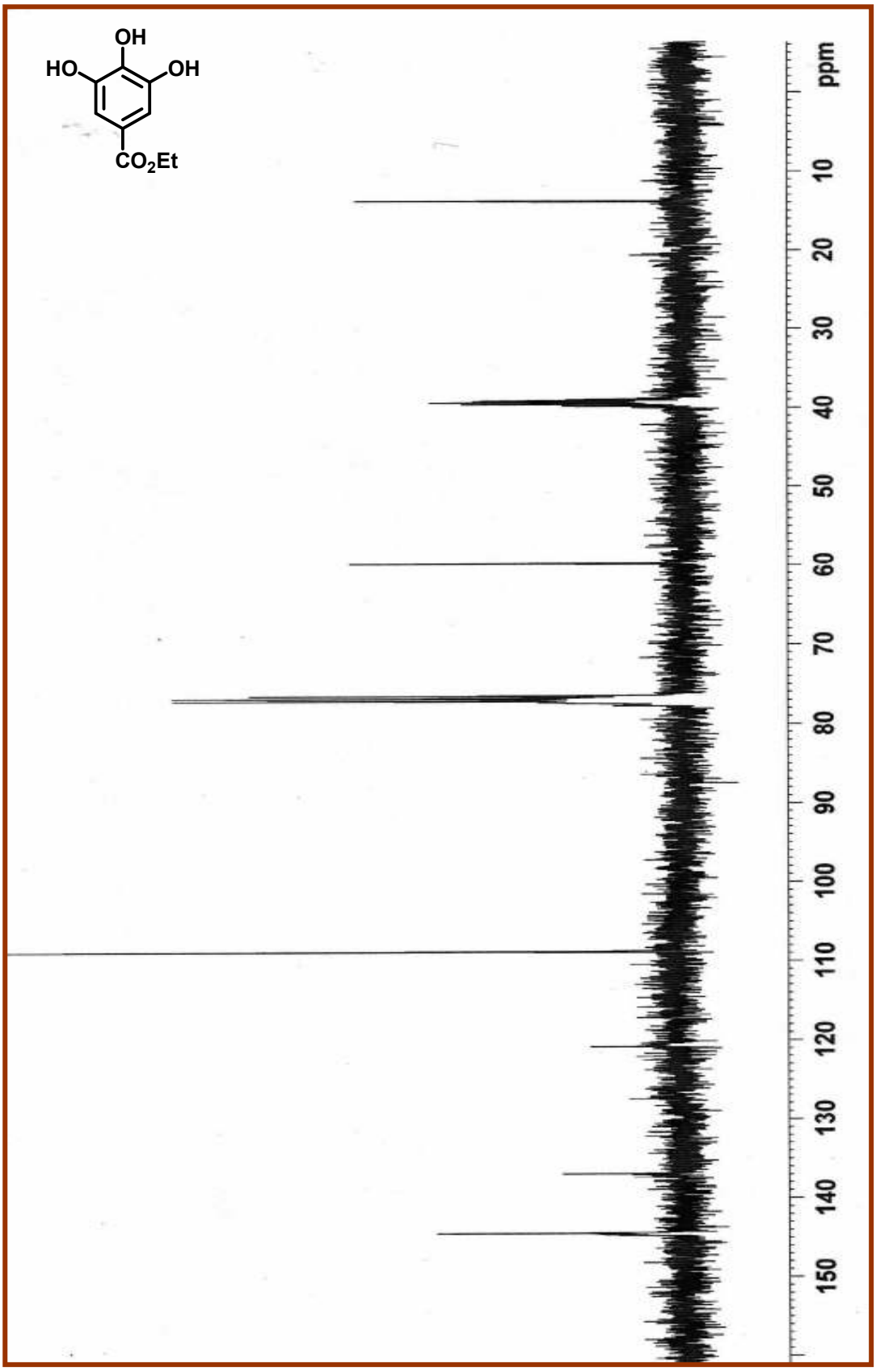

Figure 38 ^{13}C NMR Spectra of compound **16**

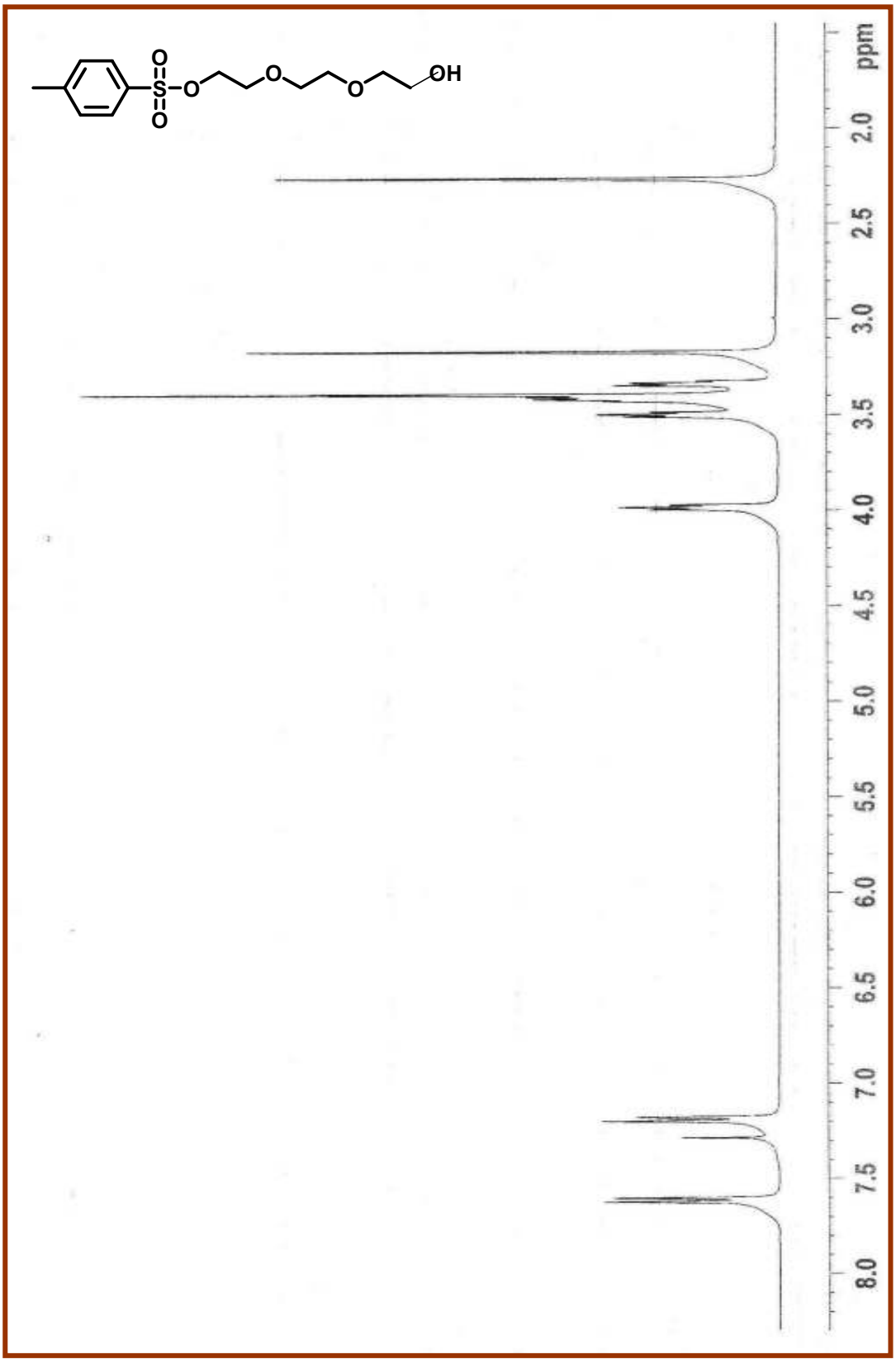

Figure 39 ^{1}H NMR Spectra of compound **17**

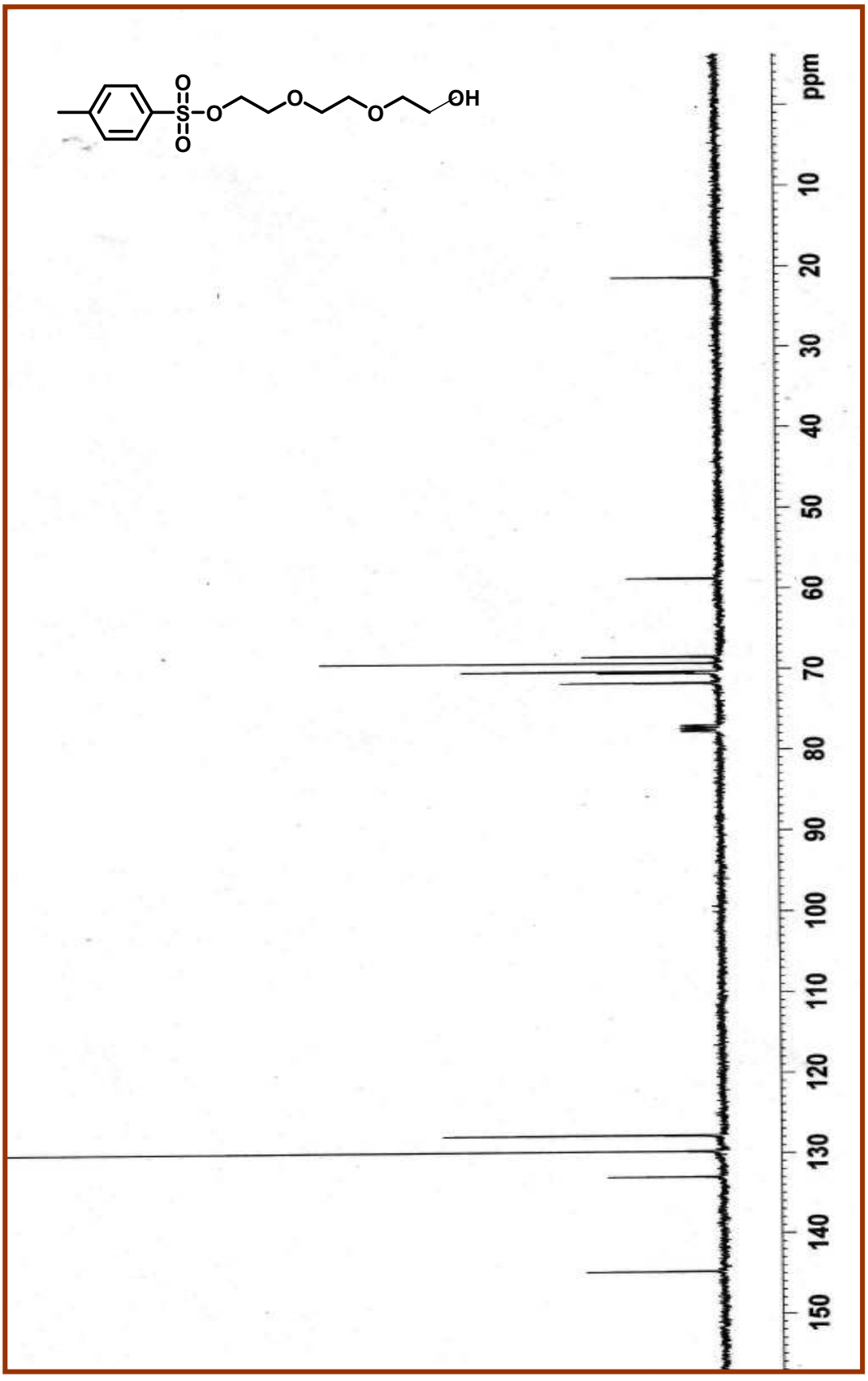

Figure 40 ^{13}C NMR Spectra of compound **17**

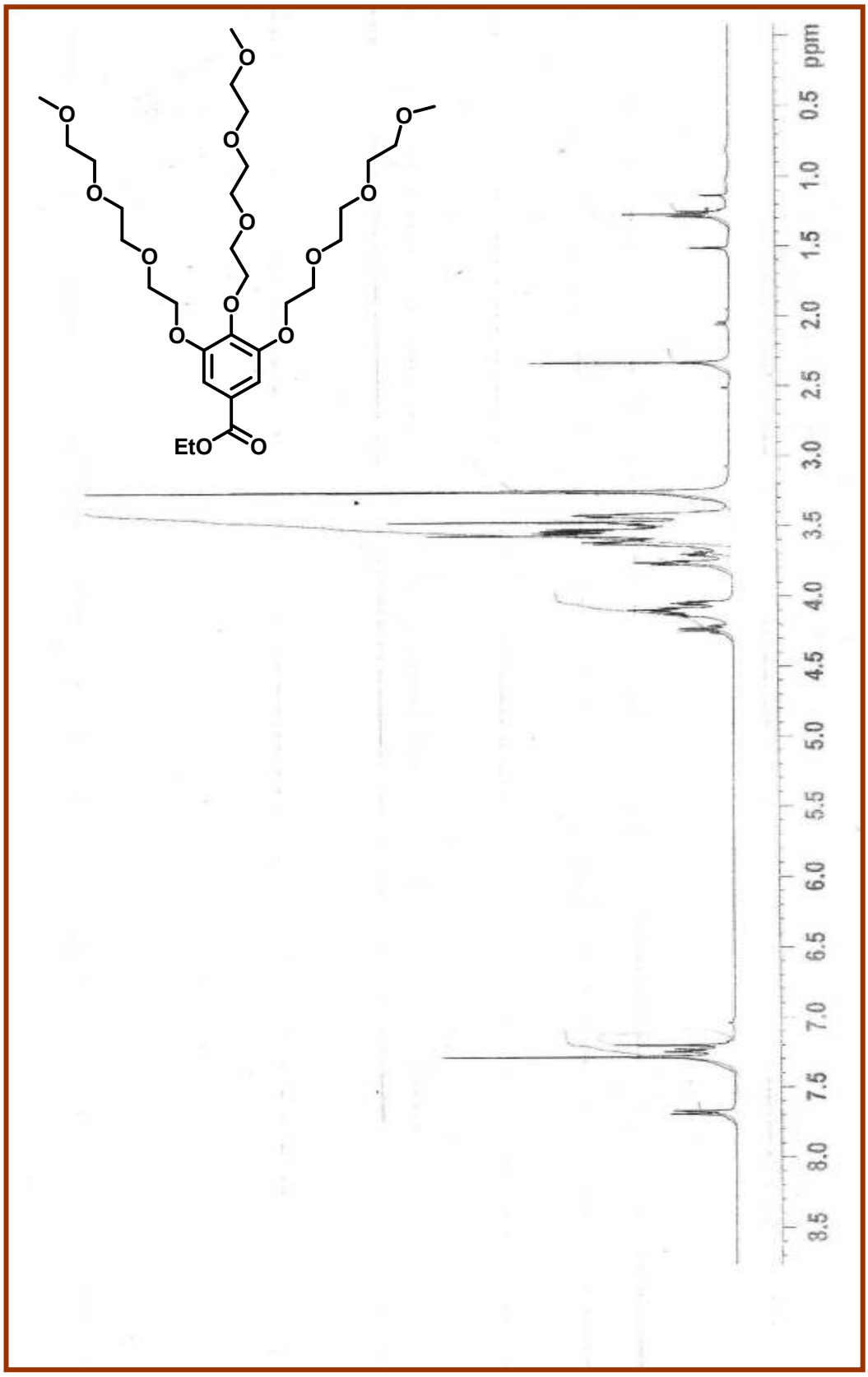

Figure 41 ^{1}H NMR Spectra of compound **18**

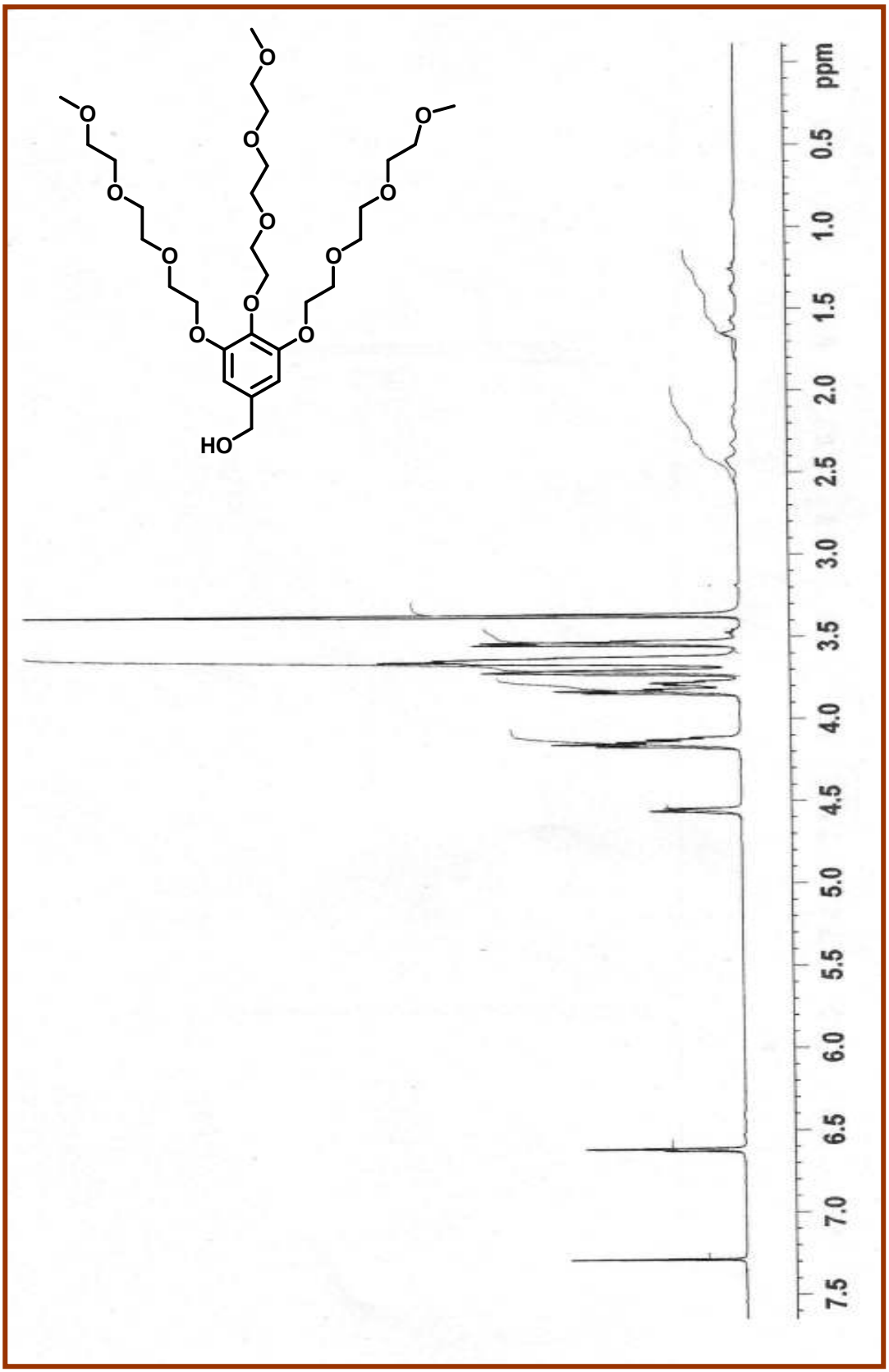

Figure 42 ^{1}H NMR Spectra of compound **19**

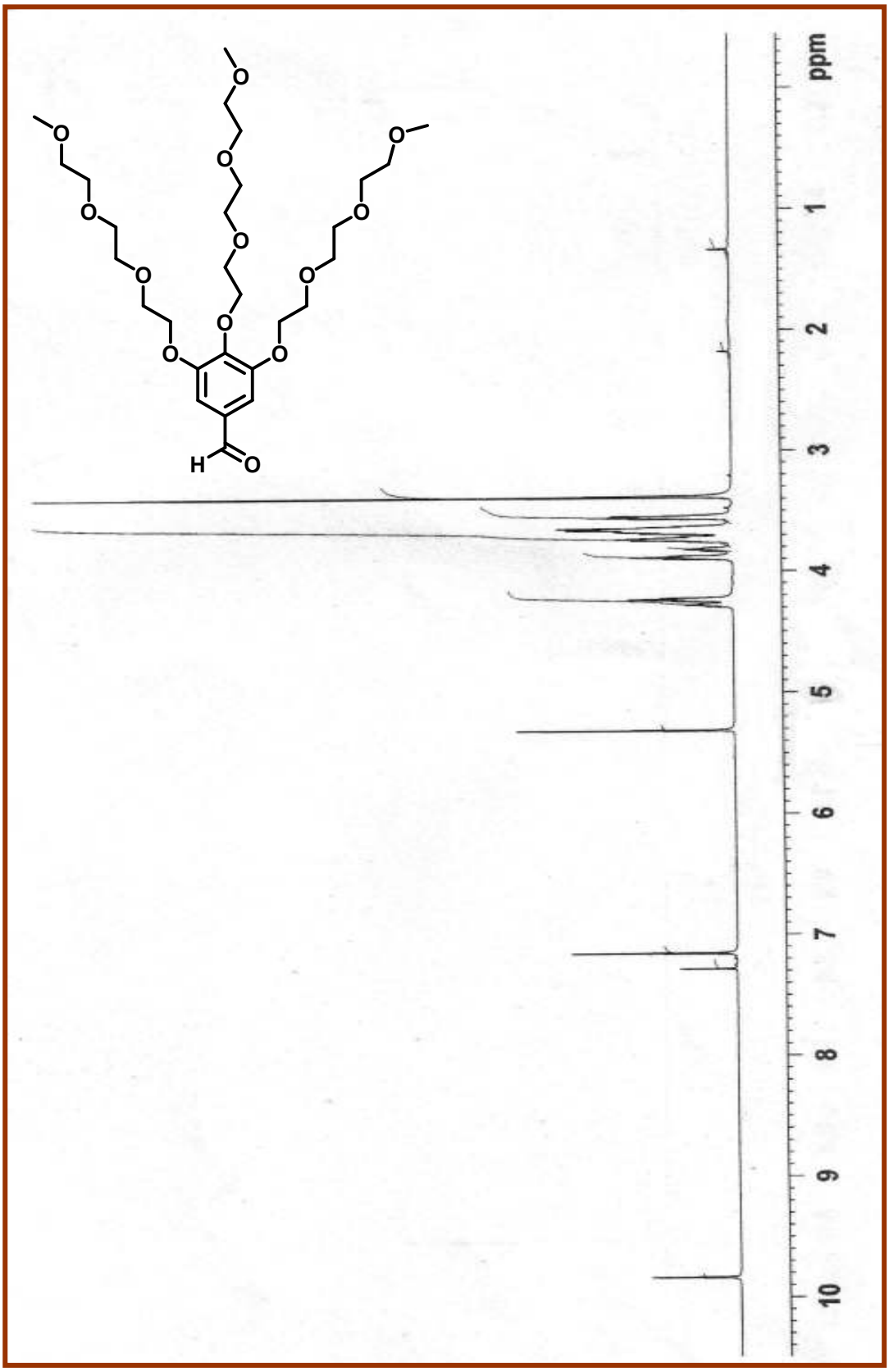

Figure 43 ^{1}H NMR Spectra of compound **20**

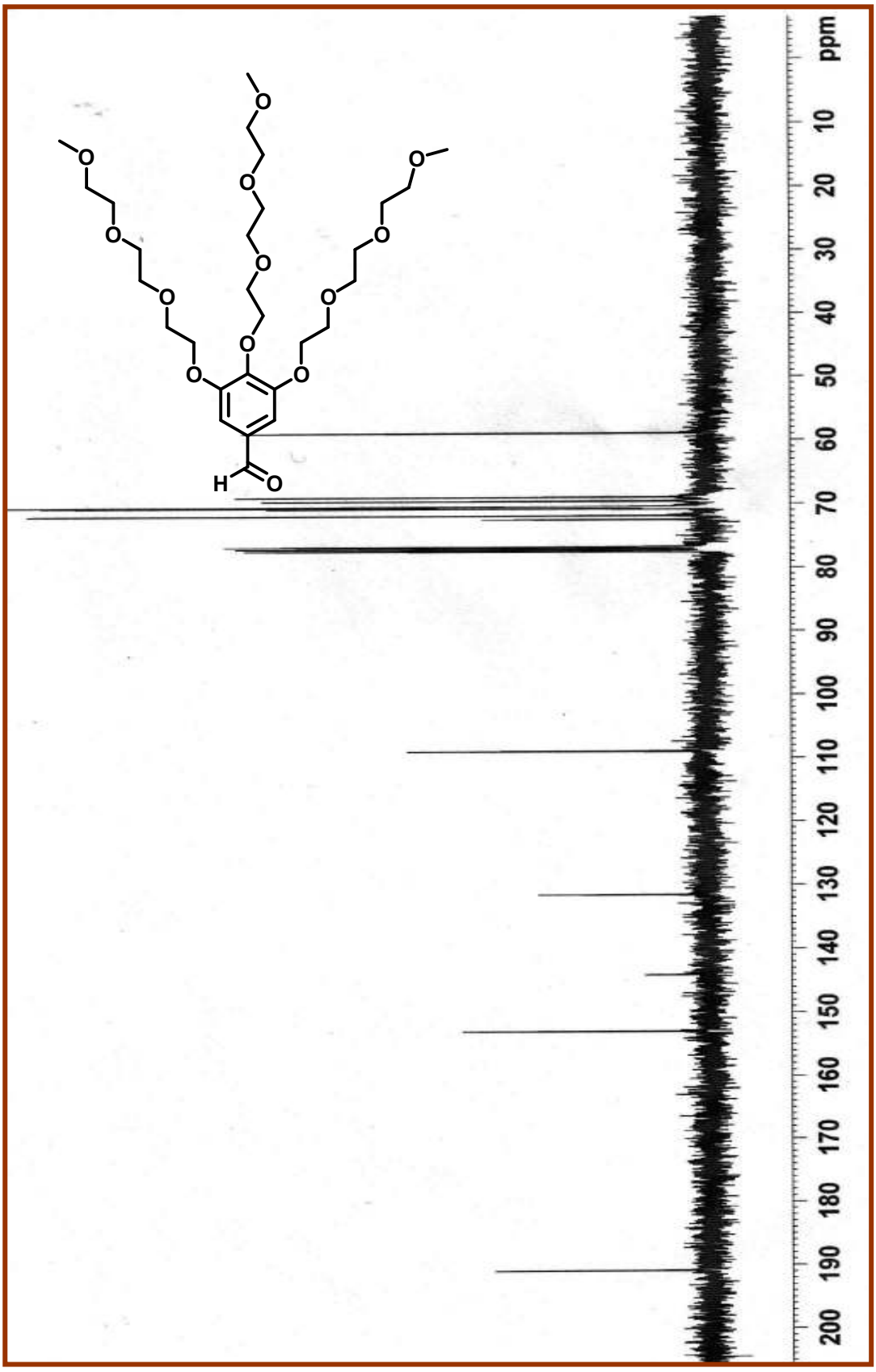

Figure 44 ^{13}C NMR Spectra of compound **20**

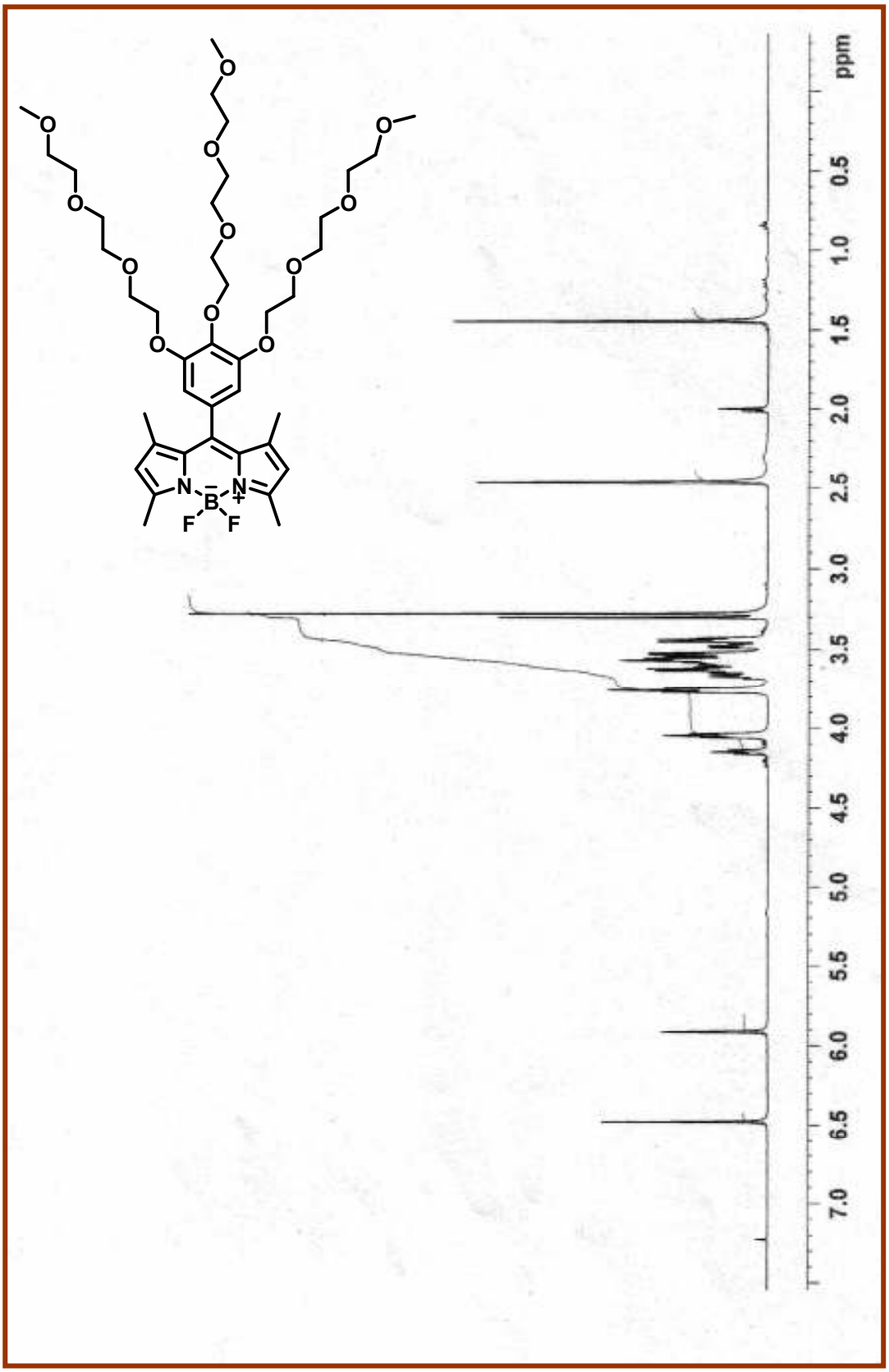

Figure 45 ^{1}H NMR Spectra of compound **22**

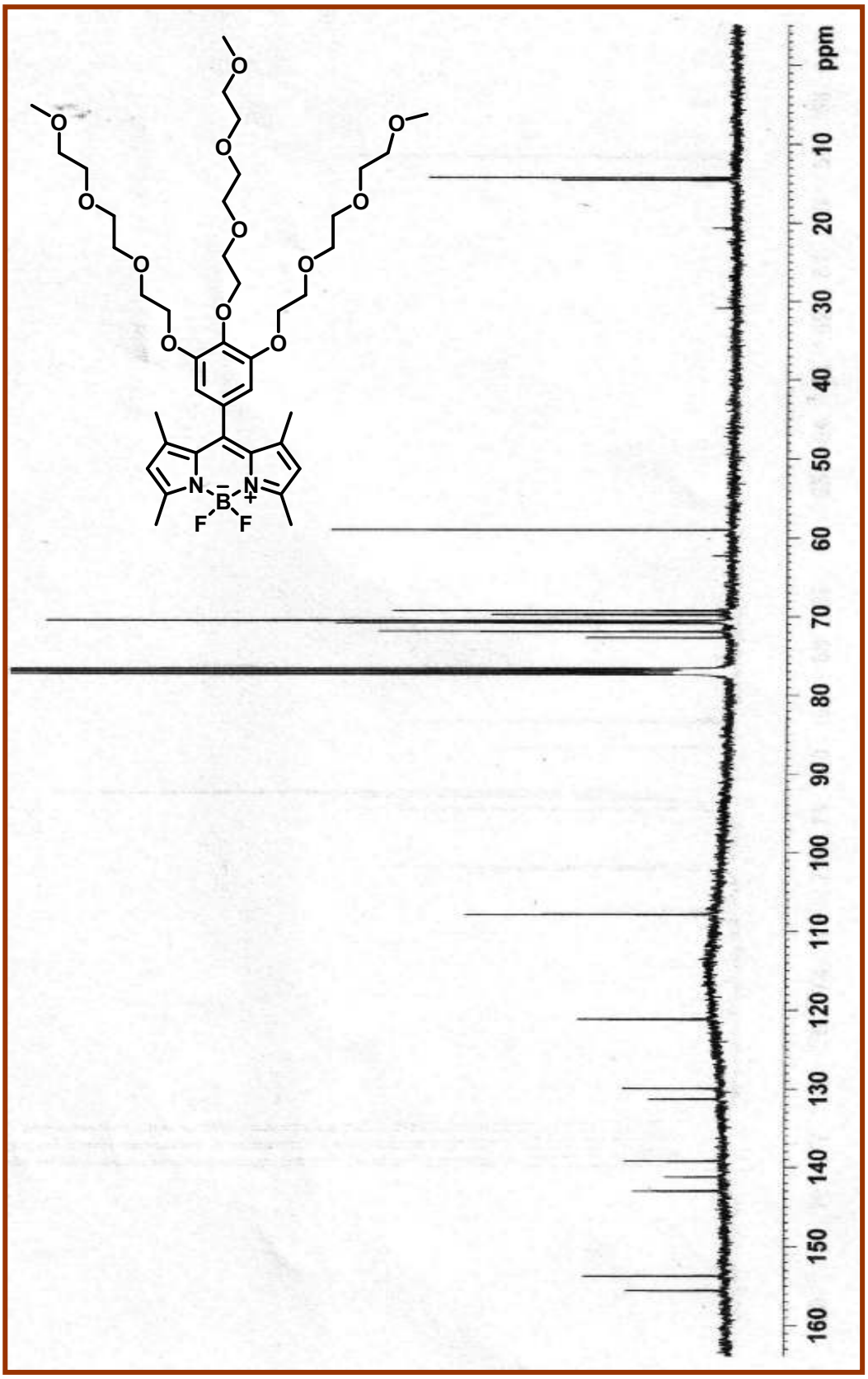

Figure 46 ^{13}C NMR Spectra of compound **22**

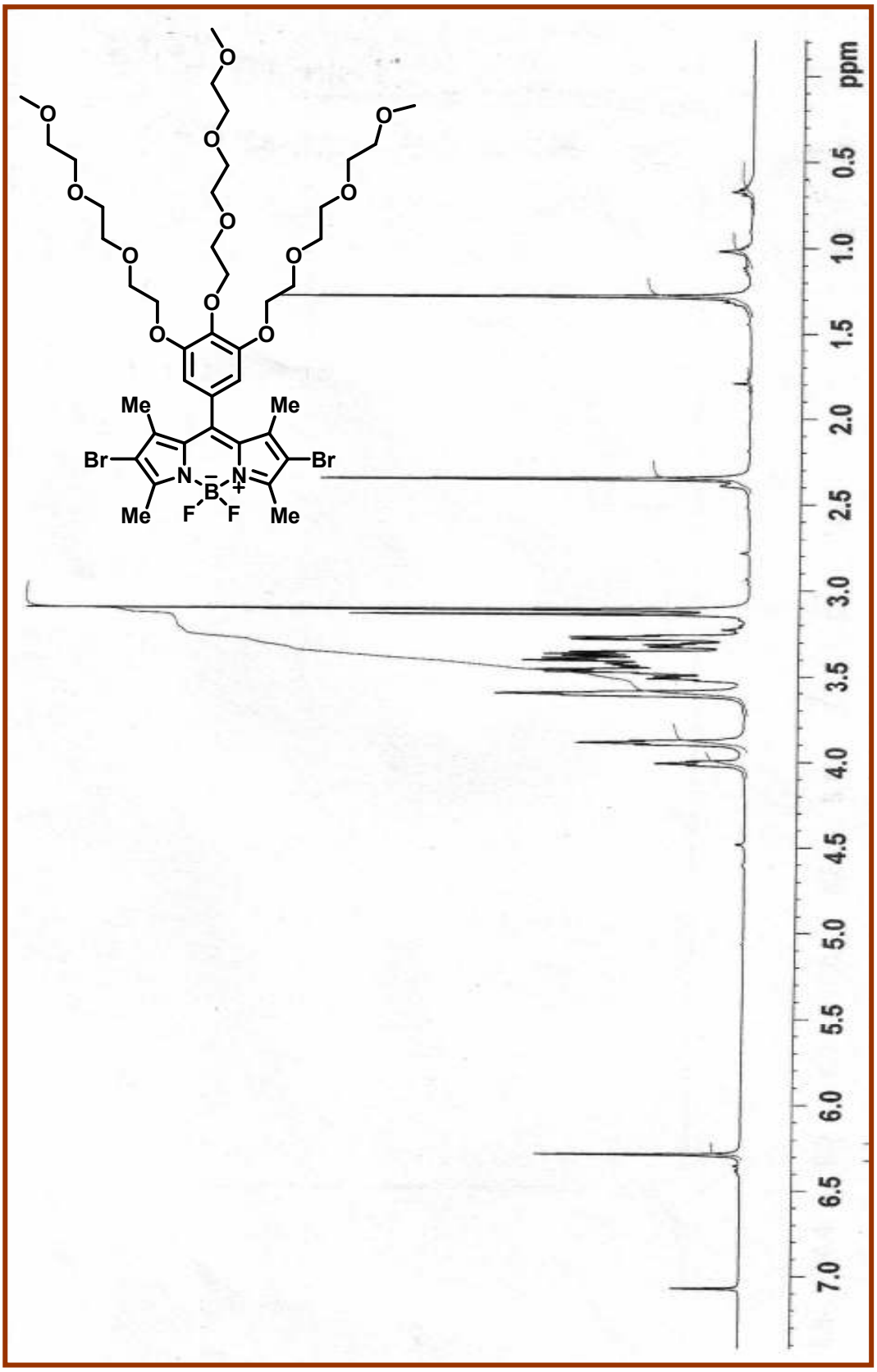

Figure 47 ^{1}H NMR Spectra of compound **23**

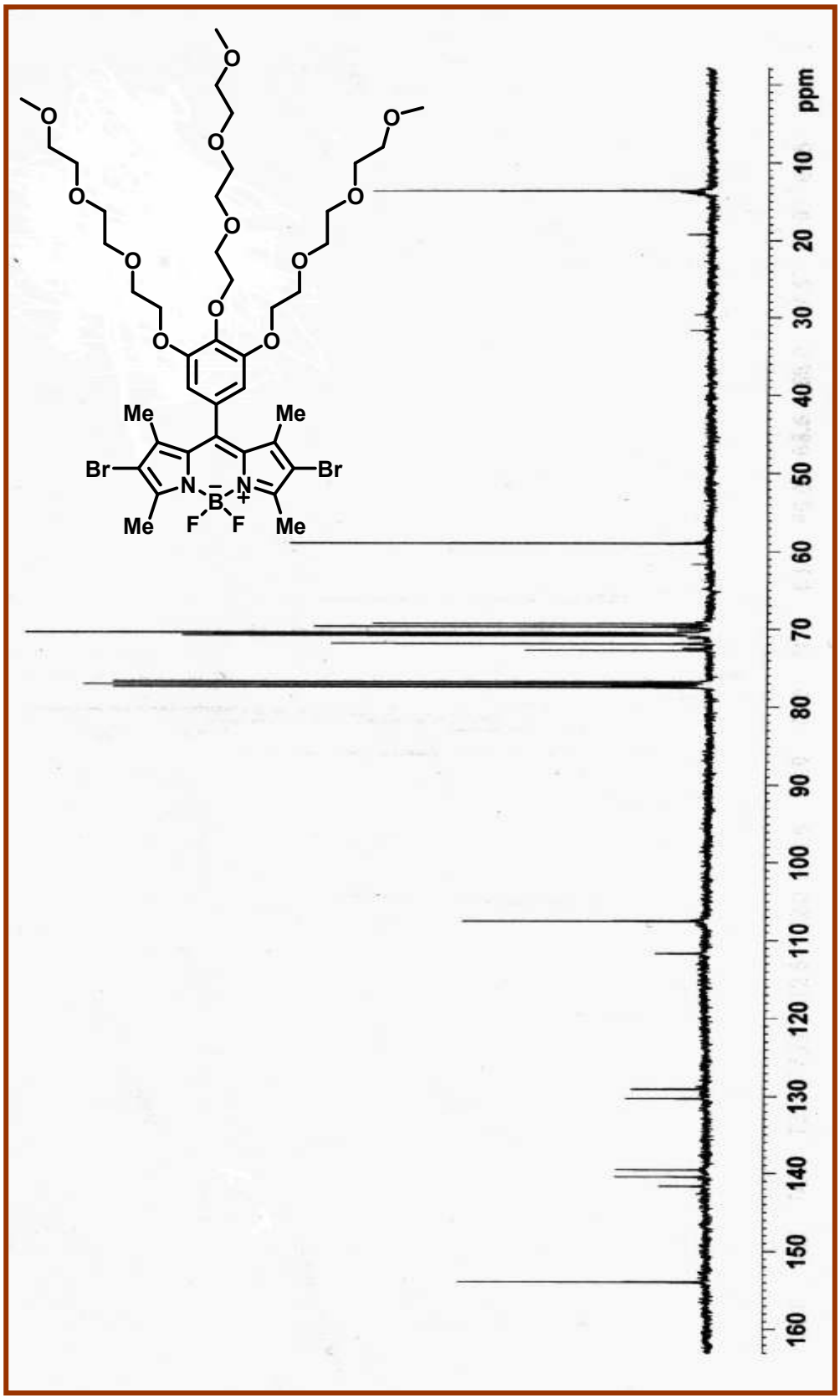

Figure 48 ^{13}C NMR Spectra of compound **23**

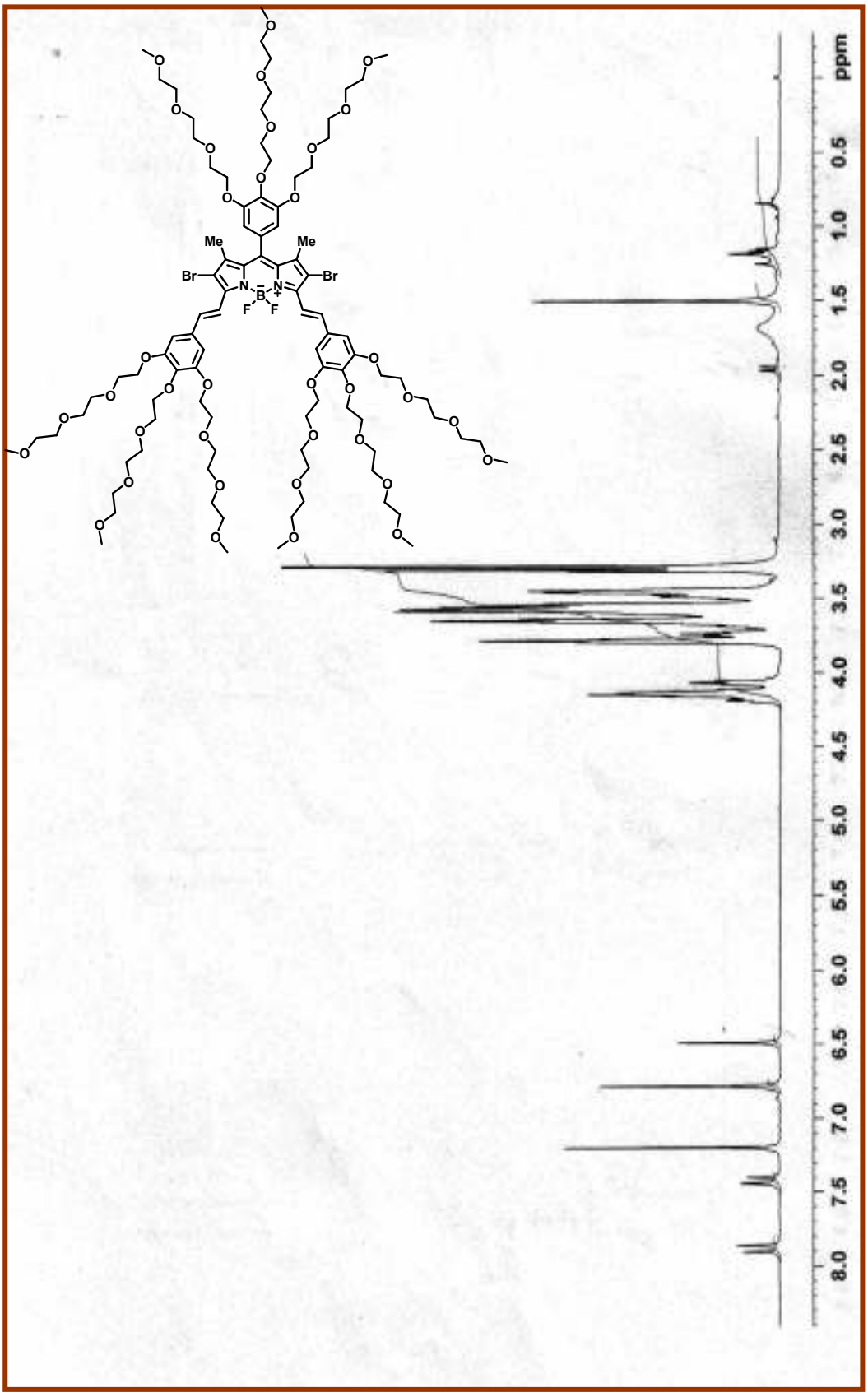

Figure 49 ^{1}H NMR Spectra of compound **24**

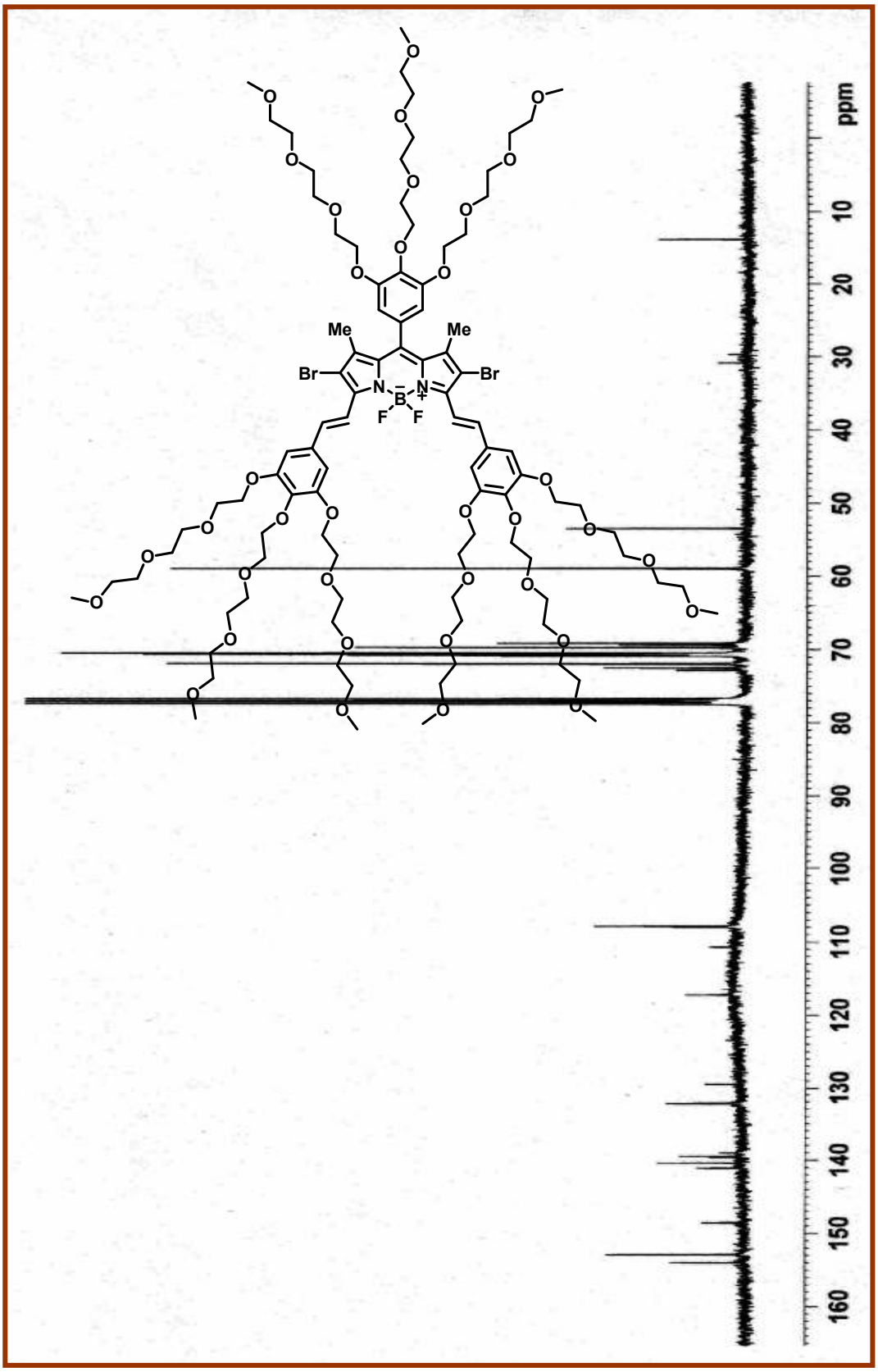

Figure 50 ^{13}C NMR Spectra of compound **24**

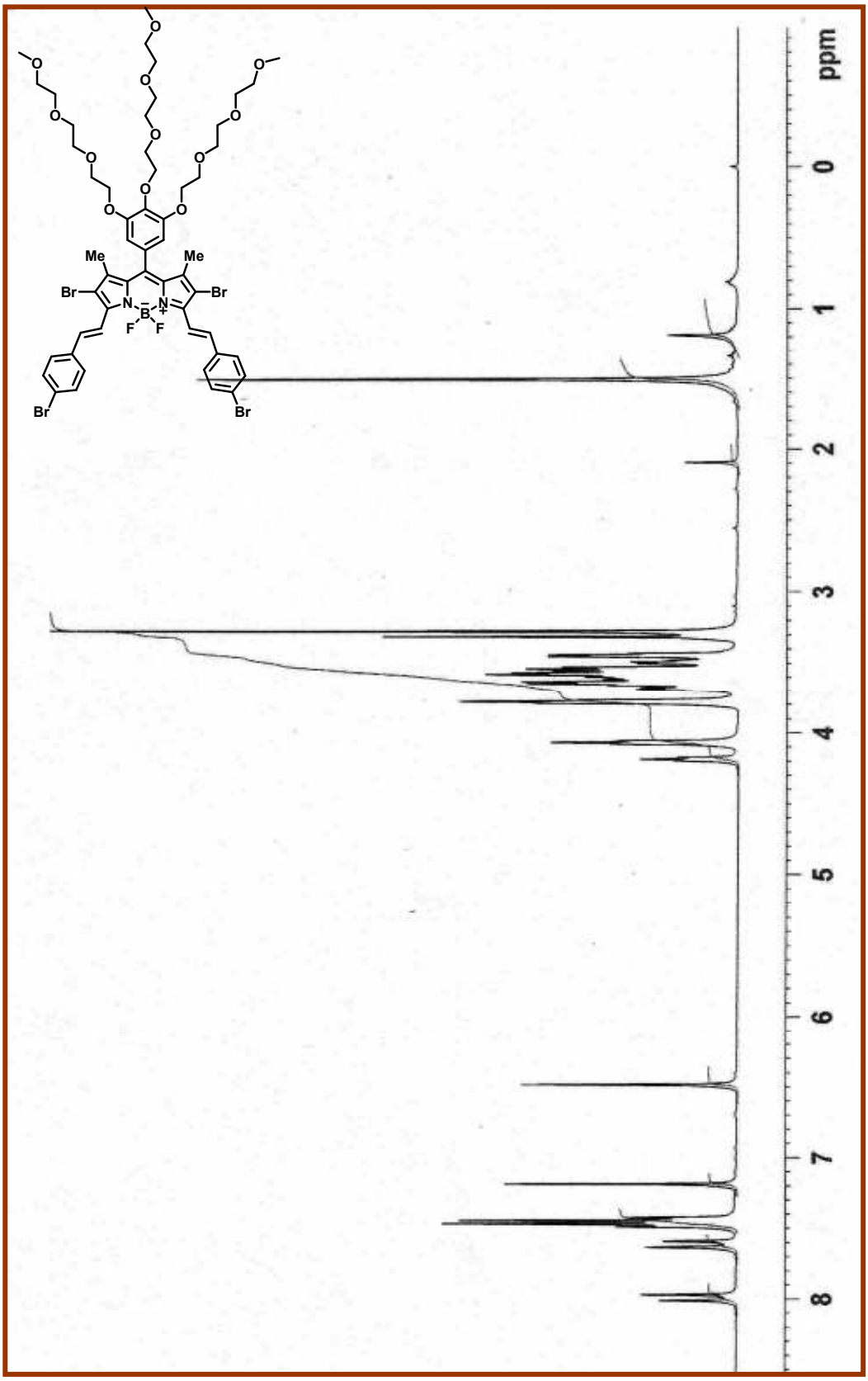

Figure 51 ^{1}H NMR Spectra of compound **26**

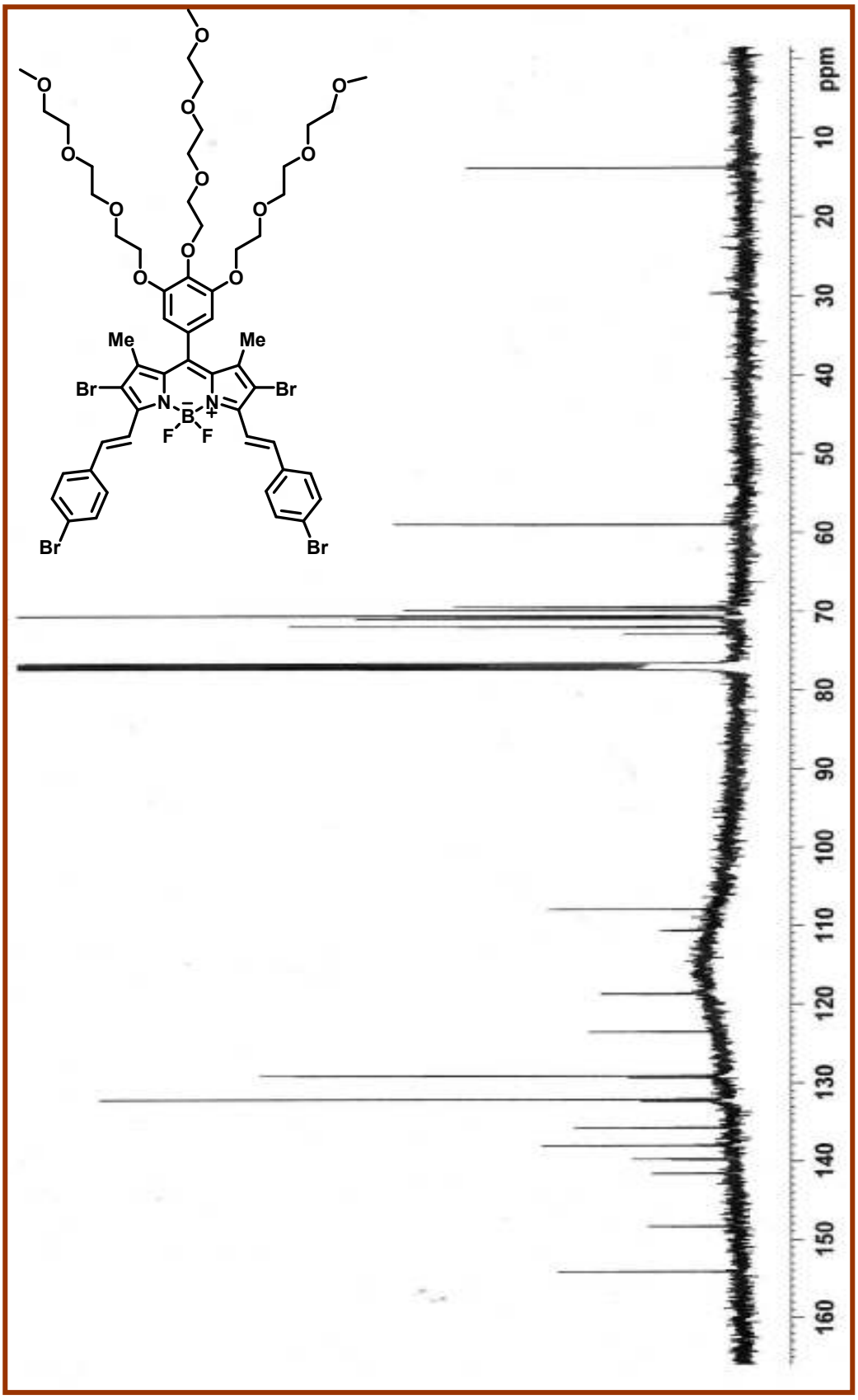

Figure 52 ^{13}C NMR Spectra of compound **26**

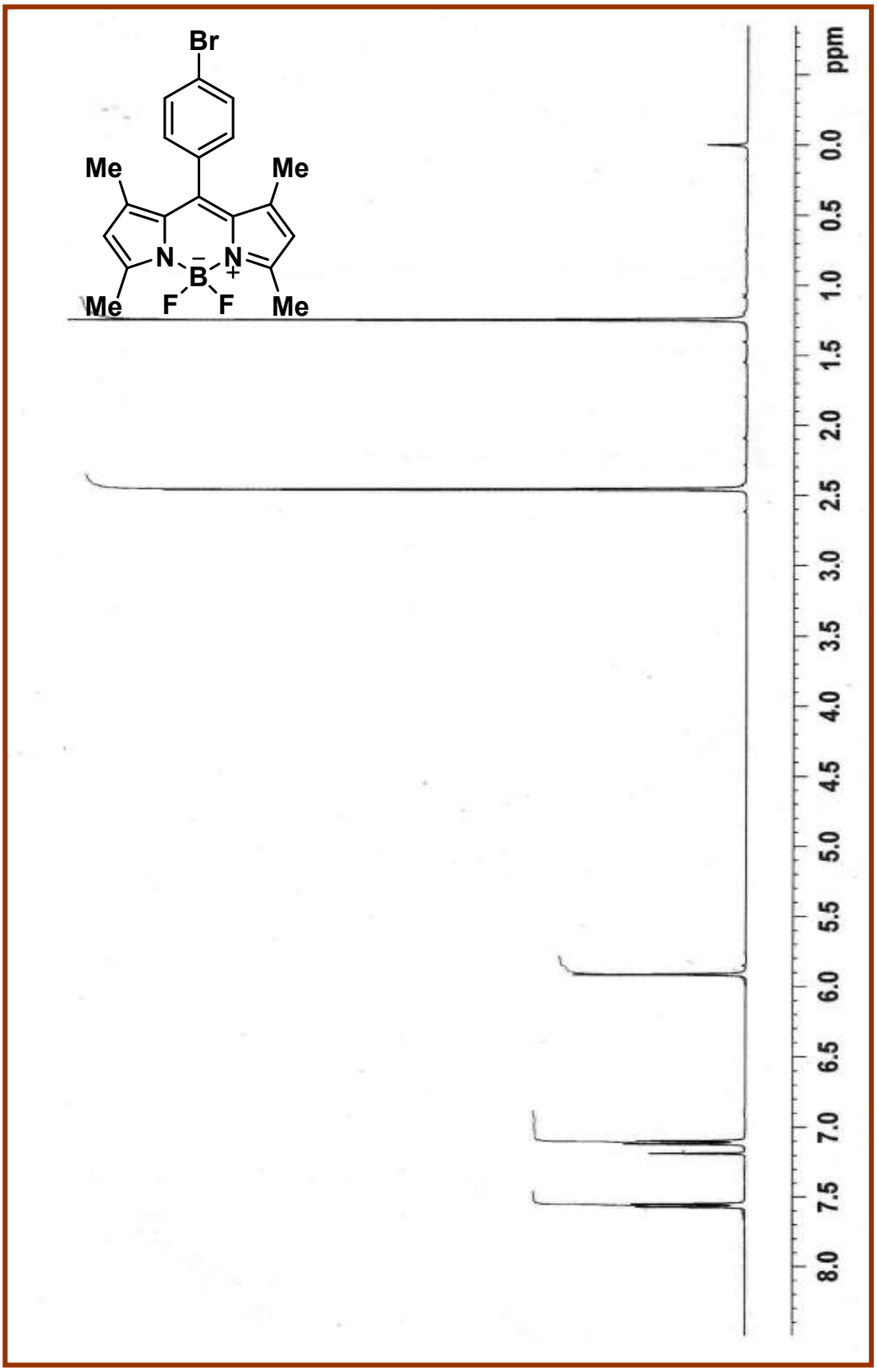

Figure 53 ^{1}H NMR Spectra of compound **27**

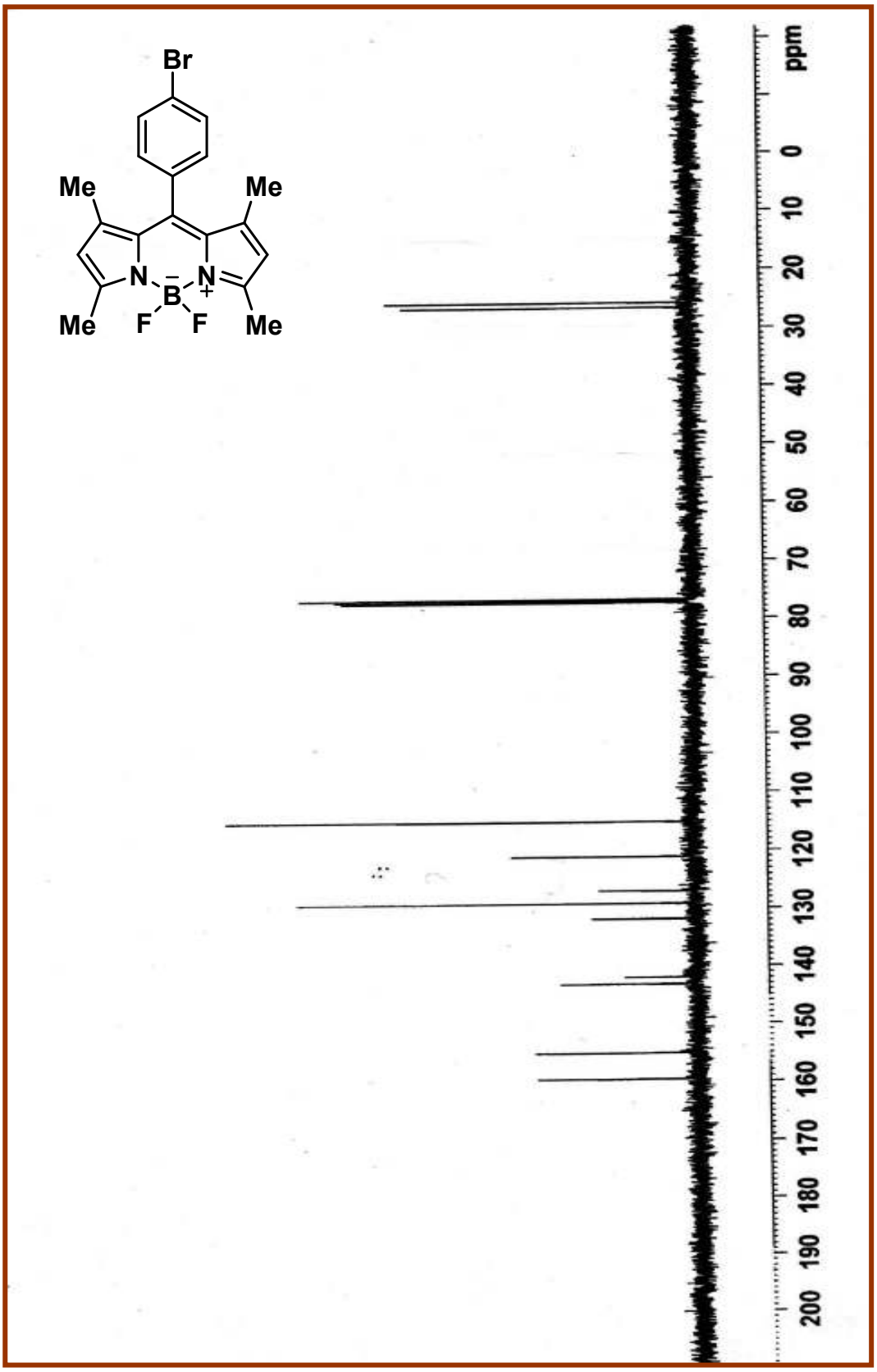

Figure 54 ^{13}C NMR Spectra of compound **27**

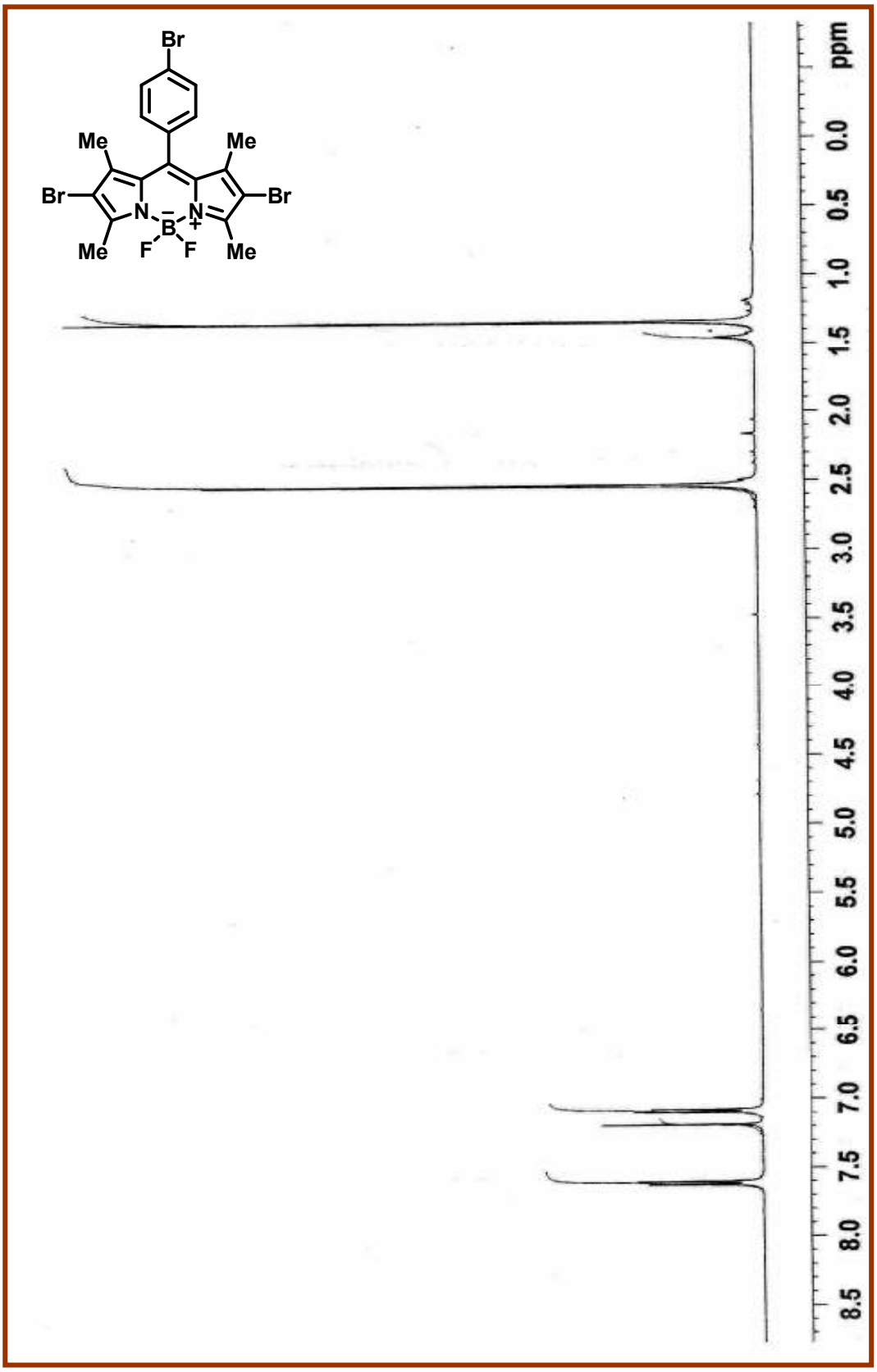

Figure 55 ^{1}H NMR Spectra of compound **28**

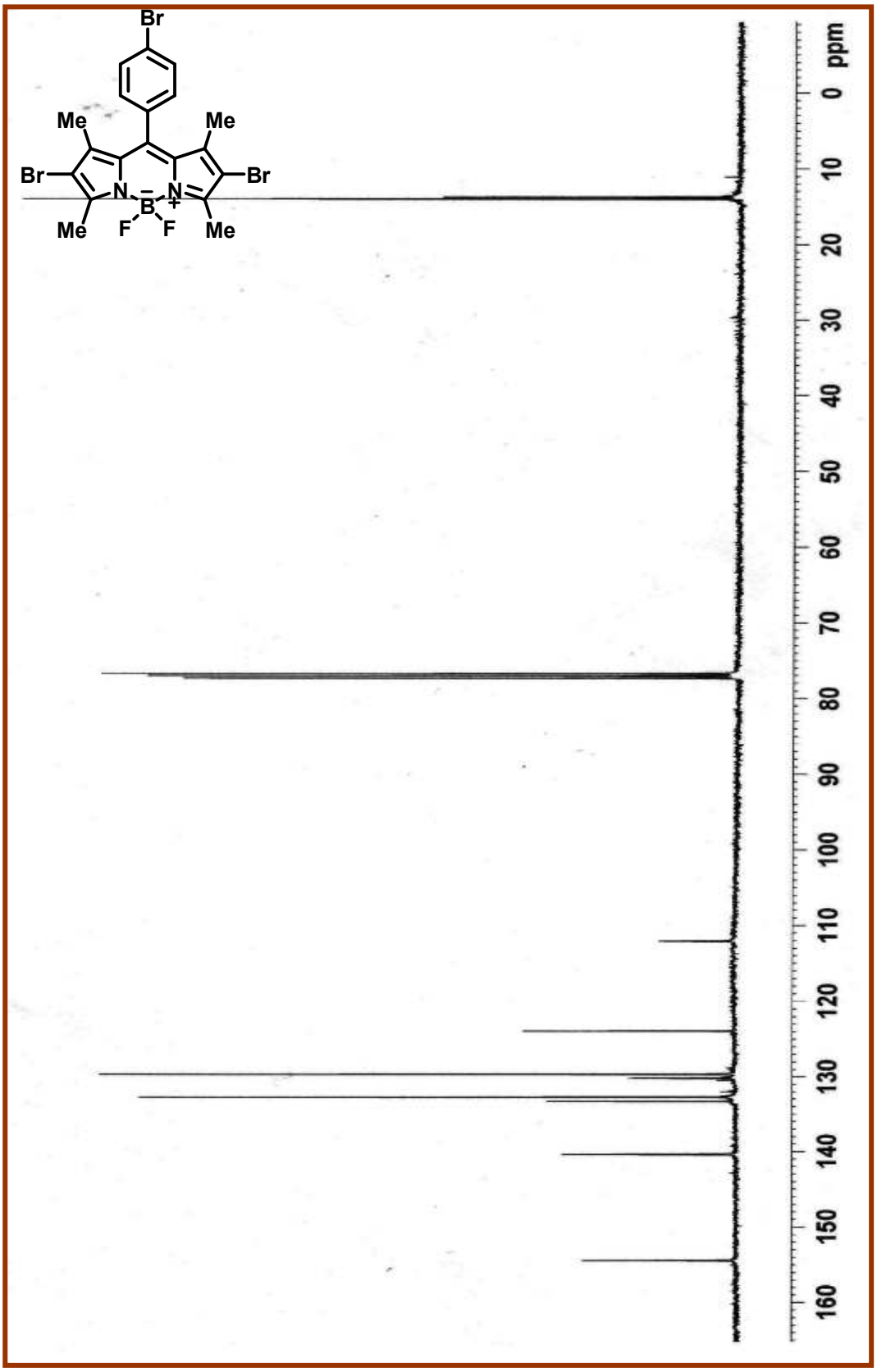

Figure 56 ^{13}C NMR Spectra of compound **28**

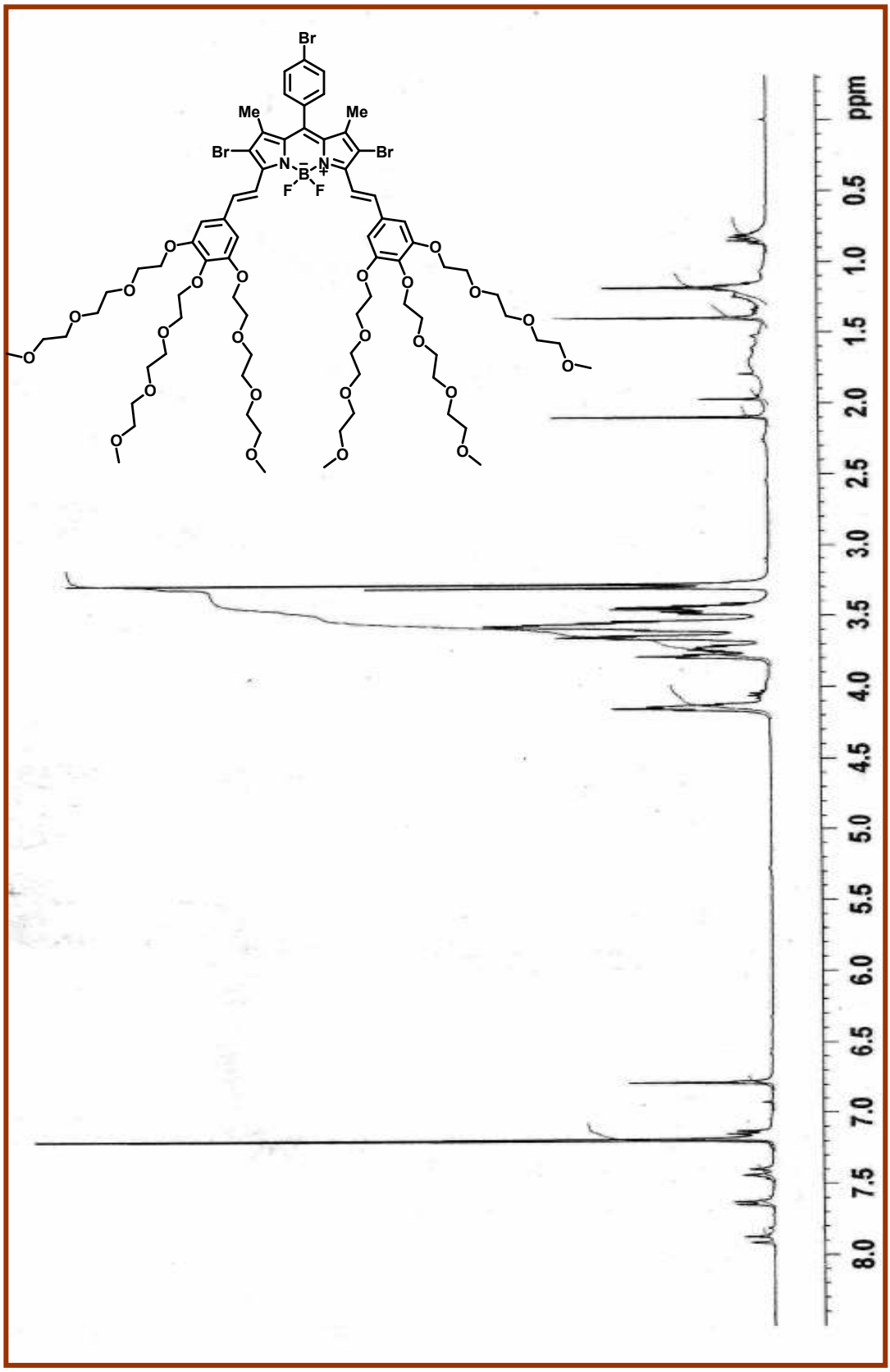

Figure 57 ^{1}H NMR Spectra of compound **2**

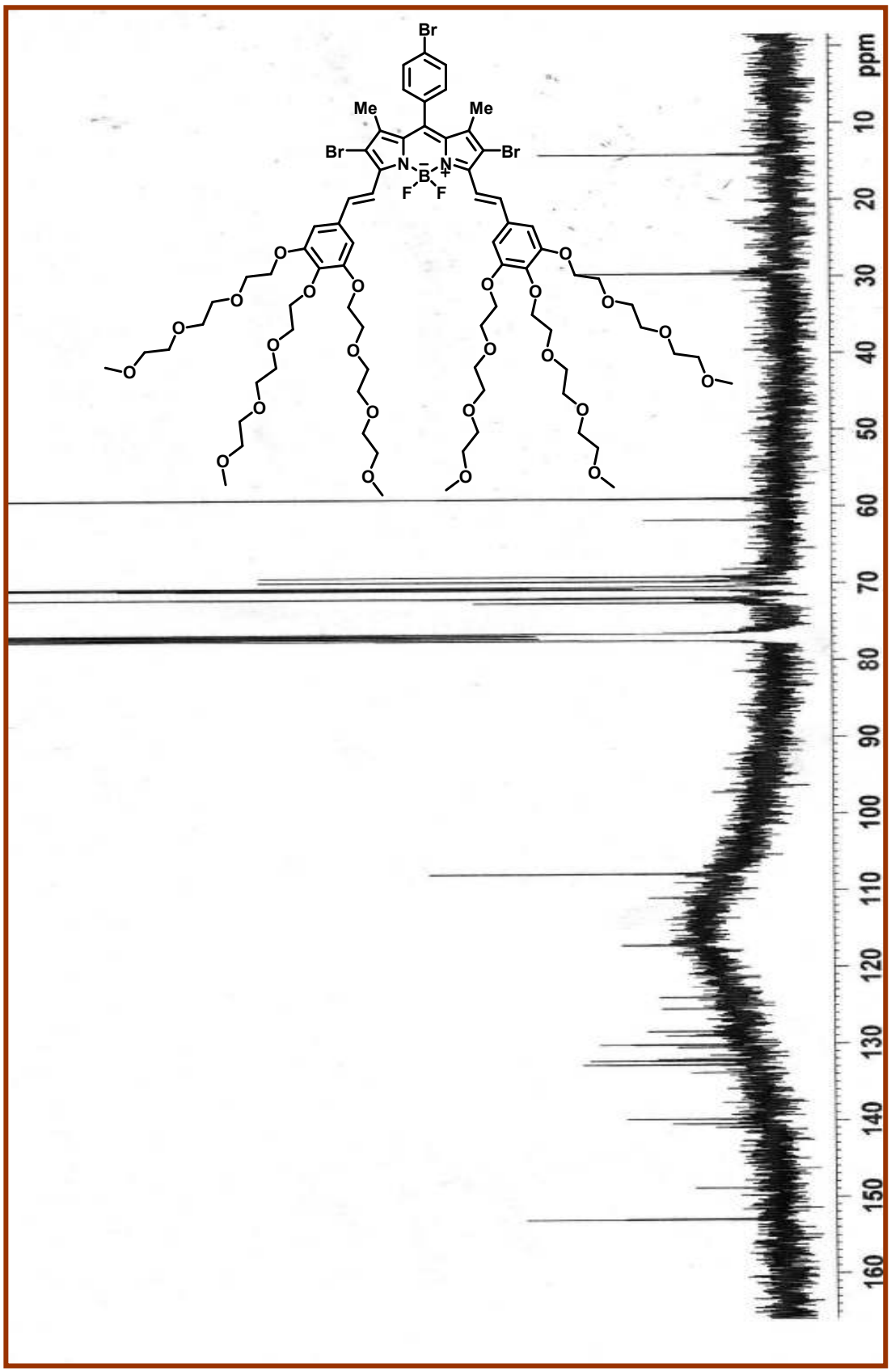

Figure 58 ^{13}C NMR Spectra of compound **29**

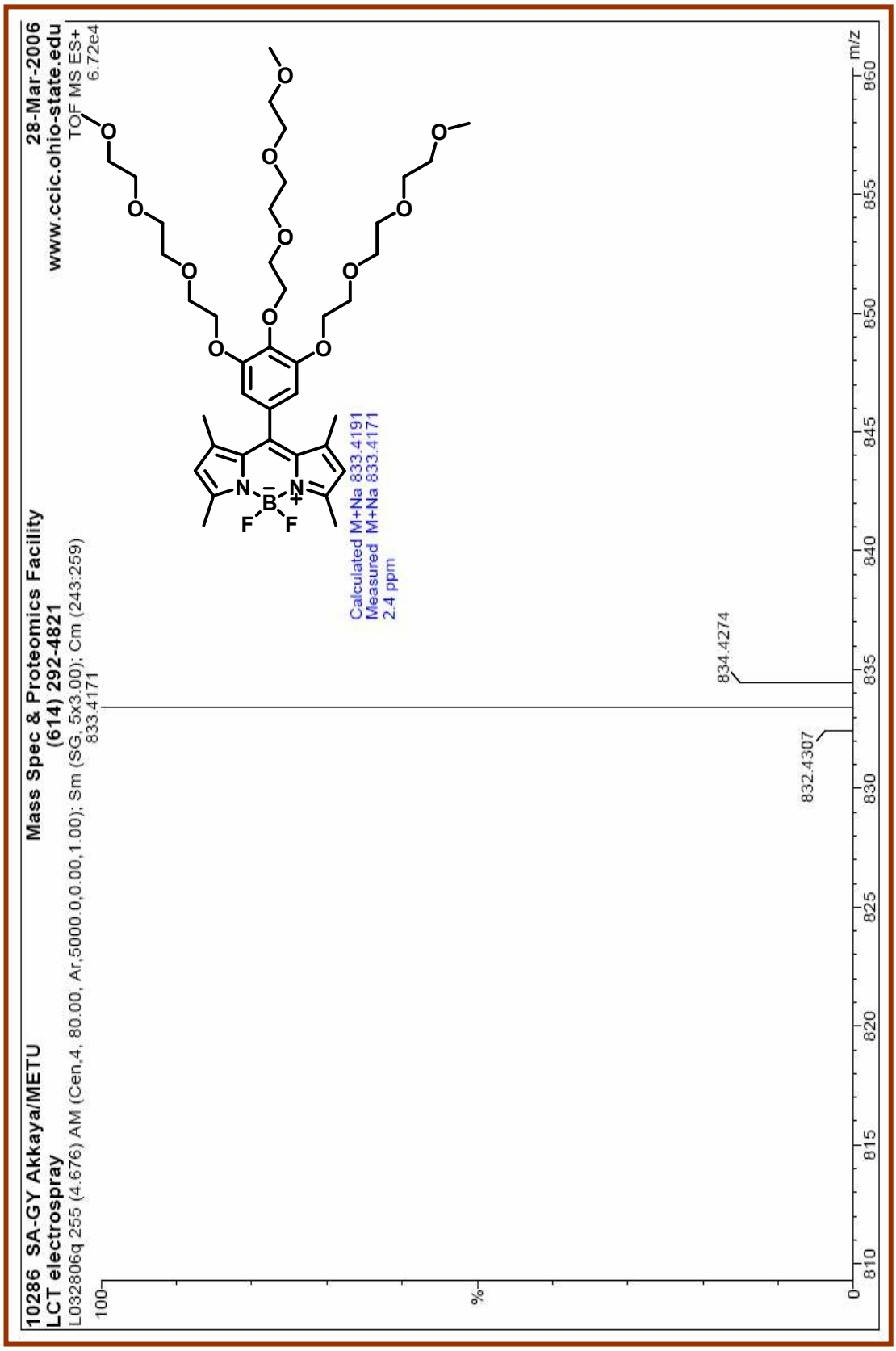

Figure 59 MALDI-TOF mass spectra of the compound **22**

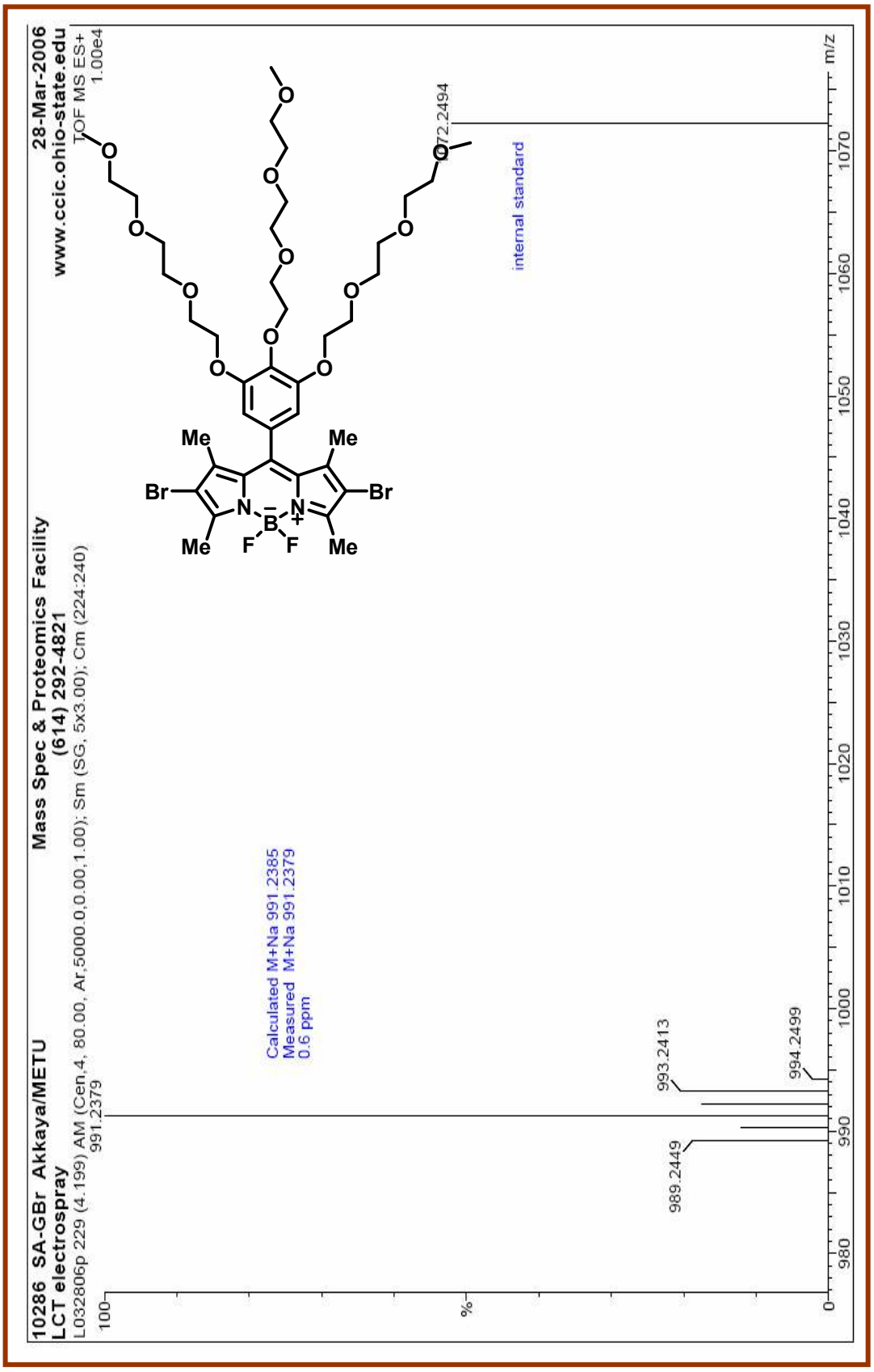

Figure 60 MALDI-TOF mass spectra of the compound **23**

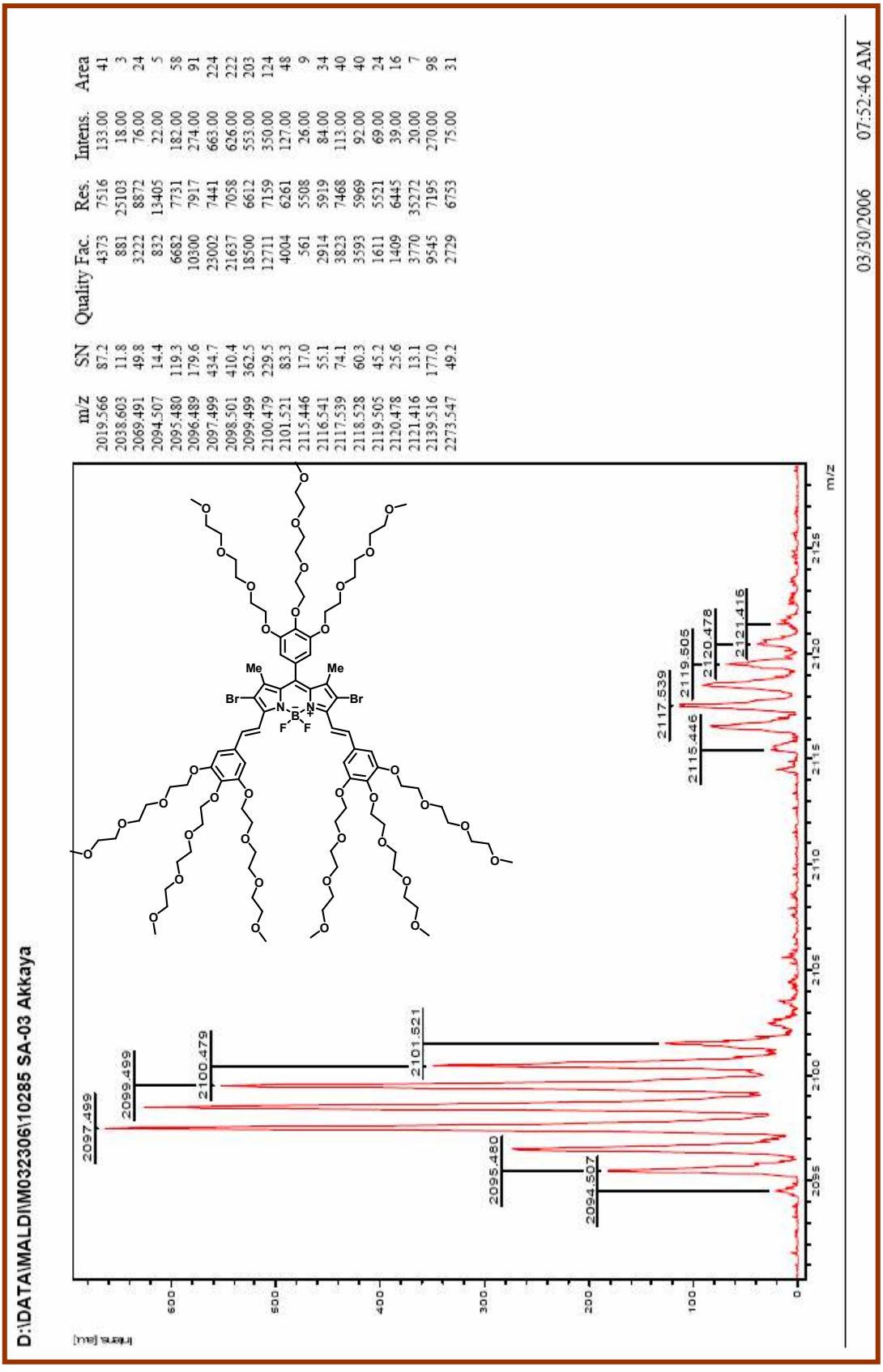

m/z	SN	Quality Fac.	Res.	Intens.	Area
2019.566	87.2	4373	7516	133.00	41
2038.603	11.8	881	25103	18.00	3
2069.491	49.8	3222	8872	76.00	24
2094.507	14.4	832	13405	22.00	5
2095.480	119.3	6682	7731	182.00	58
2096.489	179.6	10300	7917	274.00	91
2097.499	434.7	23002	7441	663.00	224
2098.501	410.4	21637	7058	626.00	222
2099.499	362.5	18500	6612	553.00	203
2100.479	229.5	12711	7159	350.00	124
2101.521	83.3	4004	6261	127.00	48
2115.446	17.0	561	5508	26.00	9
2116.541	55.1	2914	5919	84.00	34
2117.539	74.1	3823	7468	113.00	40
2118.528	60.3	3593	5969	92.00	40
2119.505	45.2	1611	5521	69.00	24
2120.478	25.6	1409	6445	39.00	16
2121.416	13.1	3770	35272	20.00	7
2139.516	177.0	9545	7195	270.00	98
2273.547	49.2	2729	6753	75.00	31

Figure 61 MALDI-TOF mass spectra of the compound **24**

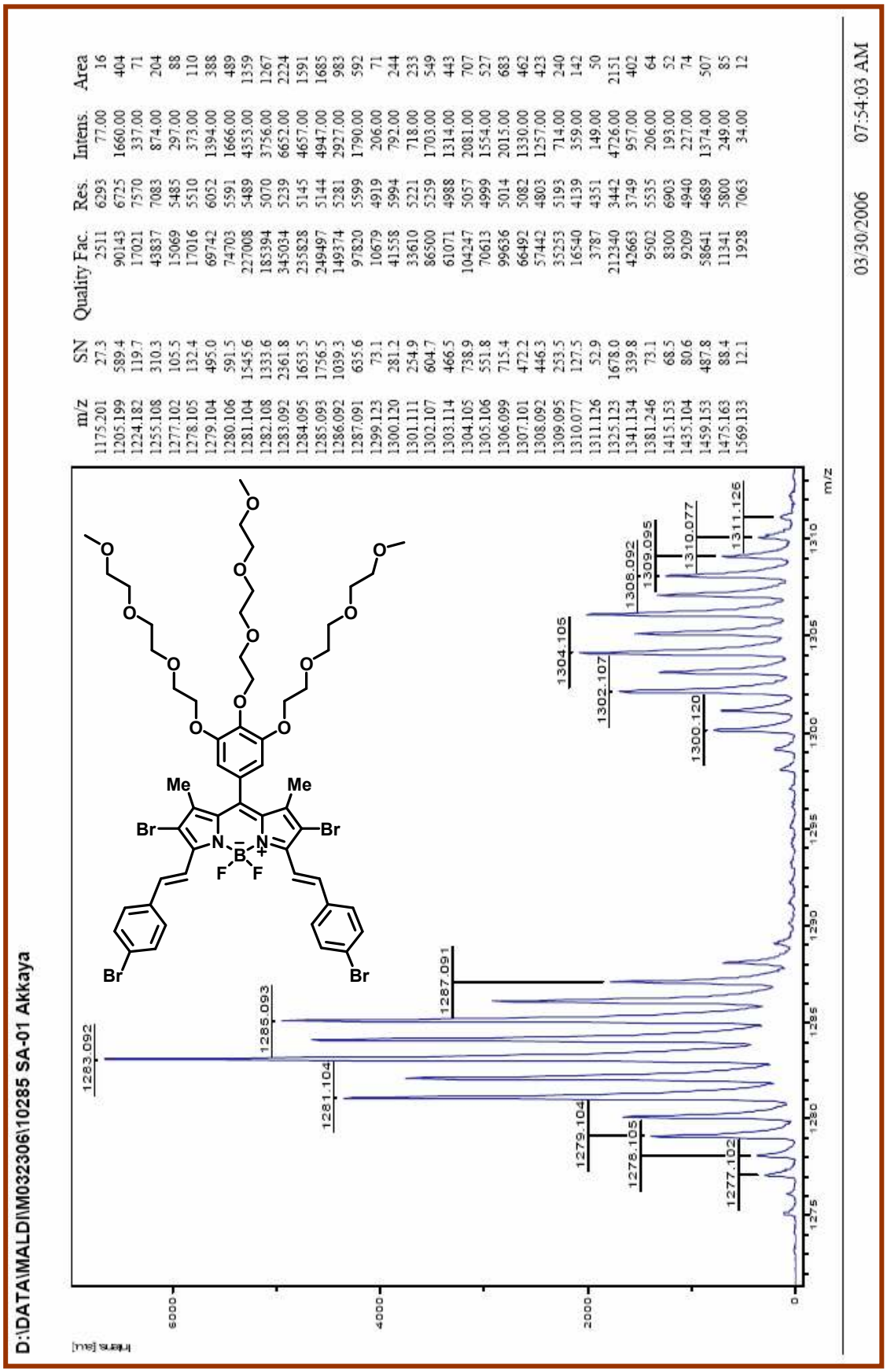

m/z	SN	Quality Fac.	Res.	Intens.	Area
1175.201	27.3	2511	6293	77.00	16
1205.199	589.4	90143	6725	1660.00	404
1224.182	119.7	17021	7570	337.00	71
1255.108	310.3	43837	7083	874.00	204
1277.102	105.5	15069	5485	297.00	88
1278.105	132.4	17016	5510	373.00	110
1279.104	495.0	69742	6052	1394.00	388
1280.106	591.5	74703	5591	1666.00	489
1281.104	1545.6	227008	5489	4353.00	1359
1282.108	1333.6	185394	5070	3756.00	1267
1283.092	2361.8	345034	5239	6652.00	2224
1284.095	1633.5	235828	5145	4657.00	1591
1285.093	1756.5	249497	5144	4947.00	1685
1286.092	1039.3	149374	5281	2927.00	983
1287.091	635.6	97820	5599	1790.00	592
1299.123	73.1	10679	4919	206.00	71
1300.120	281.2	41558	5994	792.00	244
1301.111	254.9	33610	5221	718.00	233
1302.107	604.7	86500	5259	1703.00	549
1303.114	466.5	61071	4988	1314.00	443
1304.105	738.9	104247	5057	2081.00	707
1305.106	551.8	70613	4999	1554.00	527
1306.099	715.4	99636	5014	2015.00	683
1307.101	472.2	66492	5082	1330.00	462
1308.092	446.3	57442	4803	1257.00	423
1309.095	253.5	35253	5193	714.00	240
1310.077	127.5	16540	4139	359.00	142
1311.126	52.9	3787	4351	149.00	50
1325.123	1678.0	212340	3442	4726.00	2151
1341.134	339.8	42663	3749	957.00	402
1381.246	73.1	9502	5535	206.00	64
1415.153	68.5	8300	6903	193.00	52
1435.104	80.6	9209	4940	227.00	74
1459.153	487.8	58641	4689	1374.00	507
1475.163	88.4	11341	5800	249.00	85
1569.133	12.1	1928	7063	34.00	12

Figure 62 MALDI-TOF mass spectra of the compound **26**

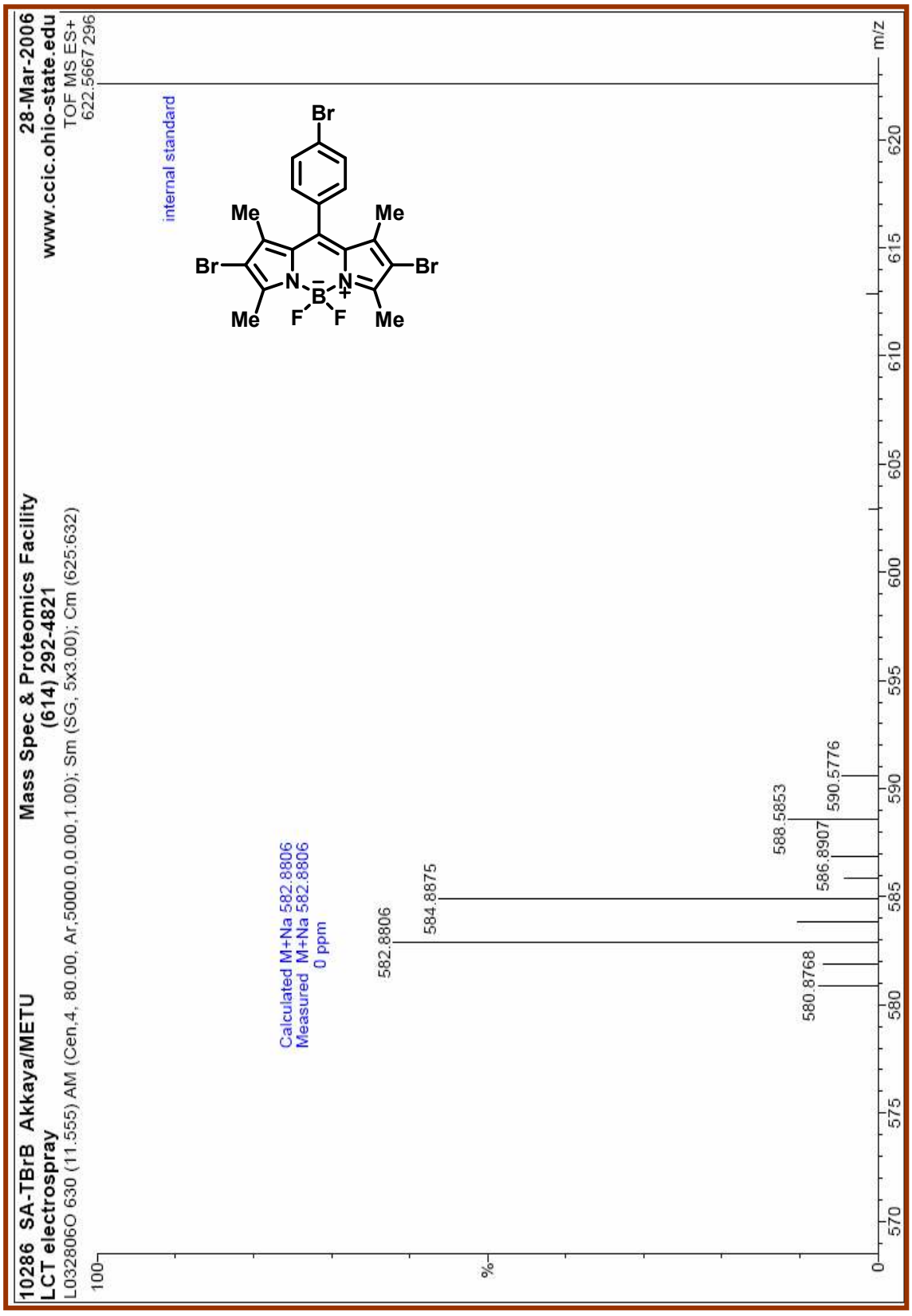

Figure 63 MALDI-TOF mass spectra of the compound **28**

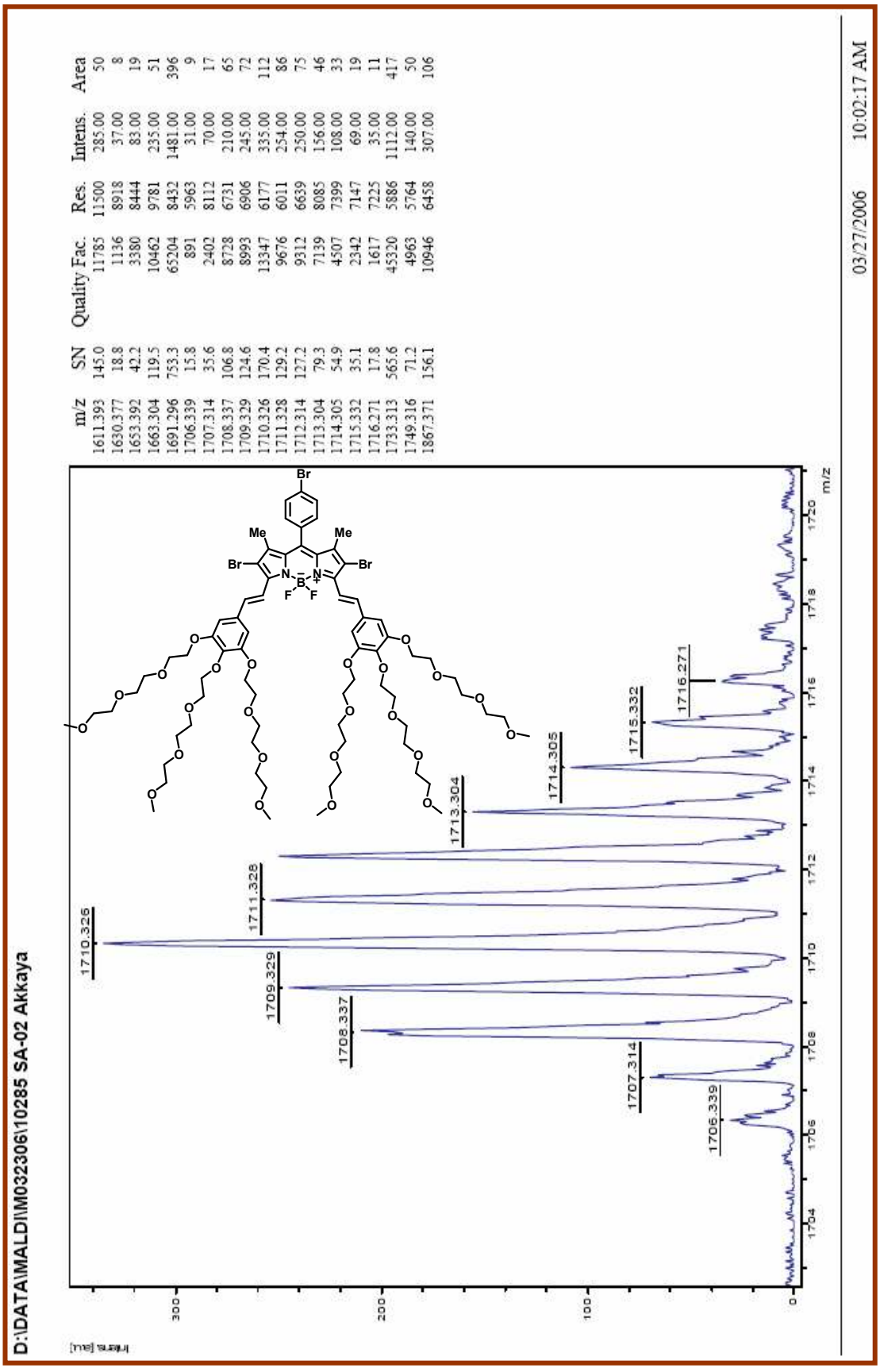

m/z	SN	Quality Fac.	Res.	Intens.	Area
1611.393	145.0	11785	11500	285.00	50
1630.377	18.8	1136	8918	37.00	8
1653.392	42.2	3380	8444	83.00	19
1663.304	119.5	10462	9781	235.00	51
1691.296	753.3	65204	8432	1481.00	396
1706.339	15.8	891	5963	31.00	9
1707.314	35.6	2402	8112	70.00	17
1708.337	106.8	8728	6731	210.00	65
1709.329	124.6	8993	6906	245.00	72
1710.326	170.4	13347	6177	335.00	112
1711.328	129.2	9676	6011	254.00	86
1712.314	127.2	9312	6639	250.00	75
1713.304	79.3	7139	8085	156.00	46
1714.305	54.9	4507	7399	108.00	33
1715.332	35.1	2342	7147	69.00	19
1716.271	17.8	1617	7225	35.00	11
1733.313	565.6	45320	5886	1112.00	417
1749.316	71.2	4963	5764	140.00	50
1867.371	156.1	10946	6458	307.00	106

Figure 64 MALDI-TOF mass spectra of the compound **29**

P